POLITECNICO DI MILANO
Doctoral Programme in Electrical Engineering
Department of Energy

Holistic MILP microgrid planning for rural electrification

Doctoral Dissertation of:
Marina Petrelli

Supervisor:
Prof. Alberto Berizzi

Tutor:
Prof. Marco Merlo

The Chair of the Doctoral Program:
Gabriele D'Antona

2021-XXXIV Cycle

Ringraziamenti

Questo dottorato, le cui aspirazioni di apertura ed esplorazione sono state fisicamente ostacolate dalla pandemia, è stato un viaggio con il pensiero fatto da seduta alla scrivania, alla ricerca di soluzioni e stimoli a cui molte persone hanno contribuito e alle quali vorrei esprimere gratitudine.

Il primo pensiero va al Prof. Berizzi, sempre diretto e deciso nel guidare il mio percorso, disponibile a sopportare infinite domande e accogliente nel venire incontro ai miei bisogni e nello scherzare insieme.

Grazie al Prof. Bovo, per l'essenziale supporto fornito in alcune fasi della ricerca. Grazie al Prof. Merlo, per avermi inclusa con entusiasmo e costanza in attività che davano un senso pratico alle nostre elucubrazioni accademiche.

Un enorme grazie a Davide Fioriti, che ha contribuito in maniera essenziale allo sviluppo di questo lavoro, grazie a uno scambio di idee sempre interessante e fruttuoso e a una gentilezza rara.

Grazie a tutti i colleghi che in questi tre anni hanno reso l'ufficio una casa accogliente, in cui lavorare, distrarsi, fare infinite e bellissime pause the e trovare stimoli sempre nuovi.

Voglio anche ringraziare tutte le persone a me vicine, spesso essenziali nel rassicurarmi e nel regalarmi nuove prospettive che mi hanno guidata in questo percorso e che sicuramente mi guideranno anche nei prossimi.

E grazie a Milano, contenitore di musica, lotte e persone che mi hanno reso una persona che qualche anno fa non avrei neanche potuto immaginare. Con oggi si chiude, almeno per ora, la mia vita qui.

Abstract

An extensive adoption of isolated microgrids is crucial to reach universal access to electricity by 2030, complying with the Sustainable Development Goals set by the United Nations. Effective rural electrification programs require the use of comprehensive computer tools, able to capture the complexity and the dynamics involved in such projects.

Standard microgrid planning optimization algorithms identify the least-cost solution and its corresponding optimal design and operation of the plant. These tools are extremely important in supporting decision makers and in overcoming traditional sizing methods, which fail to provide accurate and efficient indications. However, the state of the art does not fulfil the need of a thorough and exhaustive analysis and often neglects crucial aspects that significantly impact the outcome of the project in the long run.

This thesis develops a holistic MILP microgrid planning tool that allows decision makers to accurately evaluate the different options and to select the most suitable and long-lasting solution for the specific application.

In particular, the multi-year characteristics of the system are modelled, namely assets degradation and demand growth. An iterative procedure is adopted to effectively describe the non-linear phenomenon of storage capacity reduction, related to the hourly scheduling of resources, within the MILP framework.

The outcome of a project is closely linked to the socio-economic dynamics that are triggered after the first installation; these can lead to very different overall behaviours and considerably impact the effectiveness of the system. This long-term uncertainty is tackled by means of a stochastic optimization evaluating different load scenarios and identifying the best compromise solution, ensuring feasibility and reliability of the service under any realization of the inputs. In order to reduce risks and adapt the configuration of the microgrid to the actual load trends in time, the installation of components is not limited to the outset of the project: it can be integrated through subsequent capacity expansions, tailored on the pertaining scenario.

Rural electrification studies are often focused on the identification of the least-cost solution; hence, cost is usually the only decision criterion adopted. Recent attention to environmental issues and sustainability has pushed some researchers to also include environmental indicators. Social impacts are rarely assessed, although they strongly contribute to determining the effectiveness of rural electrification actions. In this work, a multi-objective optimization is used to extend the decision-making process and evaluate the trade-offs between economic, environmental and social objective functions. A novel algorithm is proposed to reduce the computational burden and significantly improve traditional multi-objective methods.

Therefore, this work presents a comprehensive model for rural microgrid planning, whose performances are tested on the case study of an isolated community in Uganda. In order to include all the aforementioned features without hindering the tractability of the problem, novel computationally-efficient algorithms are developed; they allow to dramatically reduce the simulation time while preserving the quality of the results. The proposed methods have general value and they can therefore contribute transversally to any sector that uses mathematical programming and optimization to solve complex problems.

Contents

IV Appendices 99

List of Figures

List of Tables

Acronyms

A-AUGMECON2 Advanced AUGMECON2

AUGMECON2 Improved Augmented ε-constraint Method

BESS Battery Energy Storage System

CAPEX Capital Expenditure

CO$_2$ CO_2 emissions

CON Converter

DG Diesel Generator

ENS Energy Not Served

GA Genetic Algorithm

HDI Human Development Index

IMY Iterative Multi-Year

IMYrd Iterative Multi-Year using representative days

JC Job Creation

LCA Life Cycle Assessment

LCOE Levelized Cost of Electricity

LU Land Use

MCDA Multi-Criteria Decision Analysis

MILP Mixed Integer Linear Programming

NPC Net Present Cost

O&M Operation and Maintenance

OPEX Operating Expense

OSMY One-Shot Multi-Year

OSMYrd One-Shot Multi-Year using representative days

PL Public Lighting

PV Photovoltaic

RES Renewable Energy Source

SDG Sustainable Development Goal

SHS Solar Home System

SOC State Of Charge

SSA Sub-Saharan Africa

WT Wind Turbine

Part I

Background and motivation

Chapter 1

Access to electricity in the Global South

1.1 Introduction

This first chapter introduces the scope of the problem investigated in this research, providing a general overview of on the topic of access to electricity and rural electrification. In particular, Section 1.2 summarizes the main trends on access to electricity worldwide; Section 1.3 discusses the role of energy as an essential driver for socio-economic development and the complexity of measuring access levels; Section 1.4 reviews the main electrification strategies, identifying microgrids as an indispensable technology in the struggle towards universal access to electricity; finally, details about this electrification approach are provided in Section 1.5.

1.2 Problem statement

The 2030 Agenda for Sustainable Development was ratified in 2015 by all the United Nations Member States, with the aim of pursuing peace and prosperity for all humankind. It is composed of 17 Sustainable Development Goals (SDGs) targeting specific scopes; in particular, SDG7 is devoted to "ensure access to affordable, reliable, sustainable and modern energy for all" by 2030 [1].

Since the adoption of the Agenda, many efforts have been made by public institutions and third sector, with the growing support of private companies, to reach such target by 2030, with a particular attention to access to electricity. In recent years, a dramatic improvement was seen in Latin America and the Caribbean and Eastern and South-Eastern Asia, where the access rates exceed 98%, while in Sub-Saharan Africa (SSA) about 53% of the people does not benefit from this service [3]. Figure 1.1 shows the access rates worldwide in 2019, highlighting the serious lag of SSA with respect to the rest of the world.

The COVID 19 pandemic is leading to a significant setback of the recent progress, as
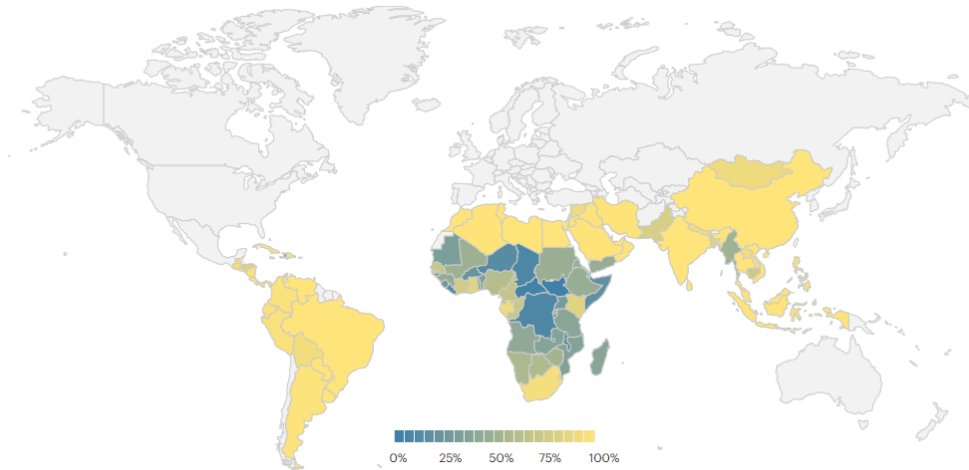
Figure 1.1: Proportion of population with access to electricity, 2019 [2].

governments redirect funds and delay programs that are not considered strategic for the post-COVID recovery. The first evaluations of the International Energy Agency estimate 2% more people lacking access to electricity in 2020 with respect to 2019: it would be the first time in recent years that the growth of access to electricity is slower than the growth of population. Without any further boost in national electrification plans, the goal of the Agenda 2030 would not be reached and around 660 million people would be lacking access to electricity in 2030, 50% of which would be concentrated in only 7 countries, namely Democratic Republic of the Congo (Congo DRC), Nigeria, Uganda, Pakistan, Tanzania, Niger and Sudan (see Figure 1.2) [2].

The unserved population is not evenly distributed in the areas of interest: a wide majority is concentrated in rural areas, where the access rate hardly reaches 80%, in contrast with 97% of the urban population accessing electricity. Still, Figure 1.3 shows that this is the result of a strong imbalance of electrification actions in favour of rural areas, that witnessed a significant increase in population accessing the service, far outpacing the population growth, while the access rates of urban areas remained quite steady [4].

1.3 SDG7 as enabler of development

Numerous analyses from international organizations confirmed the strict relationship between energy consumption and Human Development Index (HDI), as shown in Figure 1.4. On one hand, increased electricity consumption does not seem to have a significant influence on well-being if the HDI is above 0.8. On the other hand, electricity is an essential driver for a sharp improvement in living conditions in the early stages of human development.

Access to energy can impact on several pivotal aspects for the empowerment of disadvantaged communities. In particular, the Inter-American Development Bank examined 50
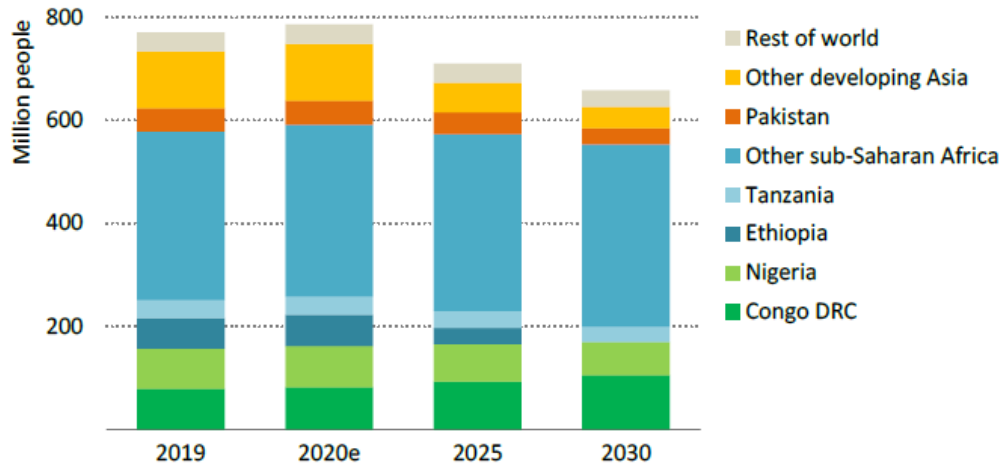
Figure 1.2: IEA estimates on population without access to electricity by main countries and regions, 2019-2030 [2].
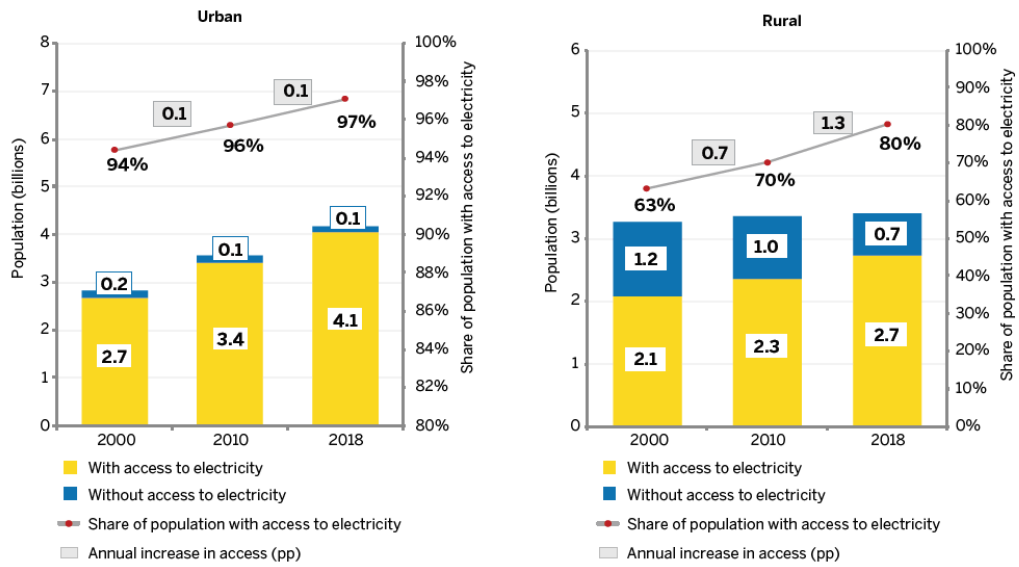
Figure 1.3: Gains in electricity access in urban and rural areas [4].

impact evaluation studies, to assess the effect of electrification on education, labour, and income: on average, the brief found a 7% increase in school enrolment, 25% in employment and 30% in incomes with respect to pre-electrification levels. Moreover, women and small enterprises benefited the most from access to power, suggesting that electrification may also contribute to reduce the gender gap. However, some of the studies under analysis

could not find any link between energy and economic development of the community [5]. In [6], the results of on-field surveys are described, highlighting that, thanks to access to electricity, the villagers could benefit from more security, better health, more resilience to climate change and better-quality leisure time. Also in this case, these considerations prevailed but they were not shared by the whole community, as different villagers had different means to exploit the new opportunities given by electrification.
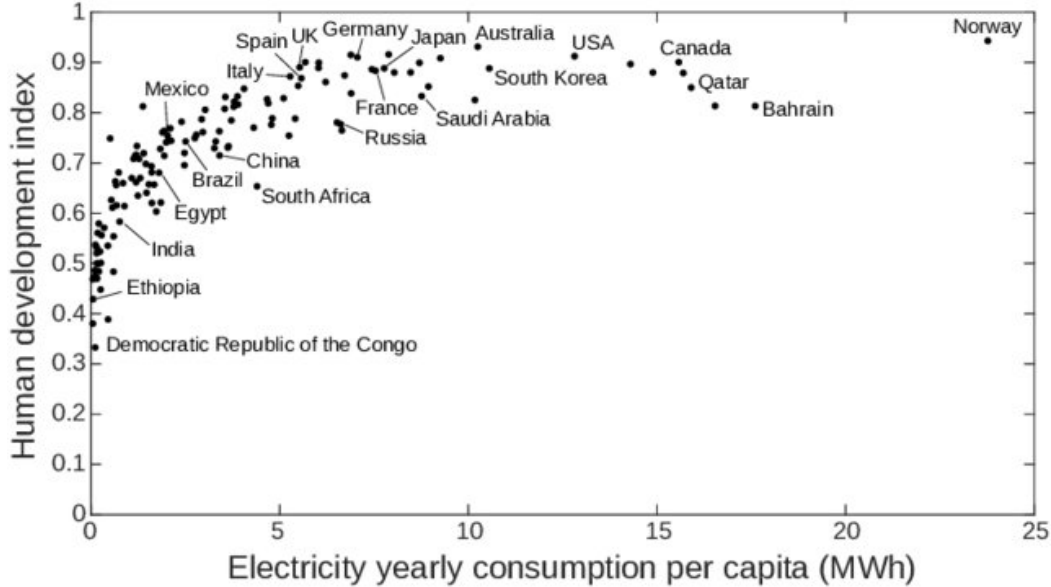
Figure 1.4: Relation between HDI and per capita energy consumption [7].

Therefore, practitioners have become more and more aware that electricity alone may not trigger the desired positive impact on the community, and that electrification plans should not look at access to electricity as a binary issue (connected/not connected): there are manifold access levels that would have completely different repercussions on the beneficiaries. Moreover, policy and business decision makers should not limit their evaluations to the technological perspective alone, but they should entail a holistic analysis [8, 9], solidly grounded on local social and political structures, gender roles and labour absorptive capacity [10].

For these reasons, the World Bank's Energy Sector Management Assistance Program (ESMAP) developed the Multi-tier Framework for electricity access, which defines six tiers of access, each one characterized by a progressively better service. Its aim is to highlight that access to electricity is multifaceted and could be described by several indicators, whose combination determines a wide variety of development potentials. As shown in Figure 1.5, seven attributes are used to distinguish the different access levels (some of which are only defined for high tiers, because hardly measurable in case of limited access):

(i) *Peak capacity.* The available capacity determines the limit in terms of usable appliances and can be measured in watts for grid connection and generators and in

watt-hours for rechargeable batteries, solar lanterns, and solar home systems. Alternatively, it can be assessed according to the available services.

(ii) *Availability.* Some electricity needs (e.g. lighting, refrigeration) require appliances to be active for a consistent amount of time. The number of hours of availability measures the ability of the system to support such requisite. Moreover, a separate indicator on availability during the evening verifies that the supply is able to cope with the evening peak.

(iii) *Reliability.* Frequent unscheduled interruptions prevent an effective provision of electricity services and represent a barrier to socio-economic development. They may be caused by breakdowns or by curtailments to comply with technical constraints. Reliability is assessed measuring number of interruptions and their duration.

(iv) *Quality.* Voltage levels are evaluated because very low voltages prevent some appliances to be used and may damage equipment. Poor quality of service can be caused by an overload of the system or by long-distance cables.

(v) *Affordability.* If the price is too high, the new service would intensify inequalities among villagers, enabling the richest with a new set of opportunities to increase their income, while the poorest would suffer increased marginalization. Hence, the expenditure should not overcome a certain portion of the household income.

(vi) *Legality.* Illegal connections may lead to a system overload, worsening the reliability and quality of supply, and put at risk the economic viability of the service. Moreover, they usually do not comply with safety standards. The number of illegal connections may be estimated by information related to bill payments.

(vii) *Health and Safety.* Installations should follow national standards and households should be aware of basic electrocution risks. This attribute is evaluated by verifying the presence of accidents related to electrical risks.

In general, to pave the way for successful access to electricity programs, practitioners could design composite projects to stimulate the demand by supporting the technological aspect with actions to facilitate access to credit, to train on the productive uses of energy and raising awareness on the positive repercussions, to increase the availability and affordability of energy-efficient appliances [4]. Moreover, complex and comprehensive planning, accurate demand estimation and good governance are needed to foster the achievement of SDG7 [8]. The more the goal of universal access to electricity gets close, the more the people left behind become difficult to reach, because living in extremely isolated lands or in areas of conflict. This is the so-called "last-mile" electrification process, which calls for public intervention to make the investment viable [4].

1.4 Electrification strategies

As highlighted in Figure 1.5, access to electricity can be characterized by very different features, mainly determined by the technologies adopted to provide the service. Electrification planning tools usually evaluate three main strategies: grid extension, microgrids,

			TIER 0	TIER 1	TIER 2	TIER 3	TIER 4	TIER 5
1. Peak Capacity	Power capacity ratings (in W or daily Wh)			Min 3 W	Min 50 W	Min 200 W	Min 800 W	Min 2 kW
				Min 12 Wh	Min 200 Wh	Min 1.0 kWh	Min 3.4 kWh	Min 8.2 kWh
	OR Services			Lighting of 1,000 lmhr/day	Electrical lighting, air circulation, television, and phone charging are possible			
2. Availability (Duration)	Hours per day			Min 4 hrs	Min 4 hrs	Min 8 hrs	Min 16 hrs	Min 23 hrs
	Hours per evening			Min 1 hr	Min 2 hrs	Min 3 hrs	Min 4 hrs	Min 4 hrs
3. Reliability							Max 14 disruptions per week	Max 3 disruptions per week of total duration <2 hrs
4. Quality							Voltage problems do not affect the use of desired appliances	
5. Affordability						Cost of a standard consumption package of 365 kWh/year <5% of household income		
6. Legality							Bill is paid to the utility, prepaid card seller, or authorized representative	
7. Health & Safety							Absence of past accidents and perception of high risk in the future	

ATTRIBUTES

Figure 1.5: The ESMAP Multi-tier Framework for Electricity Access [11].

stand-alone systems [12–14]. The most suitable option for a specific area may be selected according to a wide range of criteria.

The first significant discriminating factors are the distance from the bulk power system and the density of population. Expanding the main network is usually feasible in case the unserved area is adjacent to already existing infrastructure; this comes with a significant upfront investment that utilities are often wary of facing, due to the risk of not recovering costs in a reasonable time horizon. With the increasing efforts in rural electrification, the areas where the least-cost option is the connection to the bulk power system are slowly being exhausted. If the economic and geographic conditions do not justify the expansion of the main grid, but density of population and demand level are still adequate for a centralized source of power, loads are aggregated through microgrids, which are usually hybrid energy systems. In particular, microgrids based on Renewable Energy Sources (RESs) allow to reduce the carbon footprint of the power generation, in accordance with the national energy

plans setting objectives of decarbonization of the sector. These systems may be identified either as microgrids or as minigrids: the two words are used interchangeably because there is no clear indication about the size that determines the boundary between one category and the other. Finally, in case of scattered population and low demand, stand-alone systems are adopted, which power each user individually. The most common devices employed for this electrification approach are Solar Home Systems (SHSs), composed by a Photovoltaic (PV) panel and a Battery Energy Storage System (BESS), usually powering lighting and few additional basic needs, e.g., phone charging.

The latent demand and the target Tier of electrification influence the cost of each solution and may push towards one option or the other. In particular, in case the implementing entity aims at Tier 1 or Tier 2, stand-alone solutions would almost certainly be the least expensive, regardless the distance from the grid and the density of the community. As the desired quality of service and the latent demand to be fulfilled increase, shared infrastructure becomes more and more viable. The trade-off between the different options moves in favour of microgrids and grid extension at growing sizes and densities of the settlements to be electrified, with the tendency to lean toward the connection to the national grid in conditions of proximity to pre-existing lines. These trends are confirmed in Figure 1.6, showing the application of the OnSSET electrification planning tool on SSA evaluating different scenarios of target Tier of electricity access [12]. When aiming at supplying only basic appliances with limited availability along the day (Tier 1), the stand-alone option is predominant. Improving the target quality of service forces a much higher reliance on minigrids or grid extension. Nonetheless, similar demographic conditions may be associated to different electrification strategies due to different unit cost of grid transmitted power: a lower cost of grid electricity increases the competitiveness of grid connection, making it viable for more combinations of population density and distance from the grid [15].
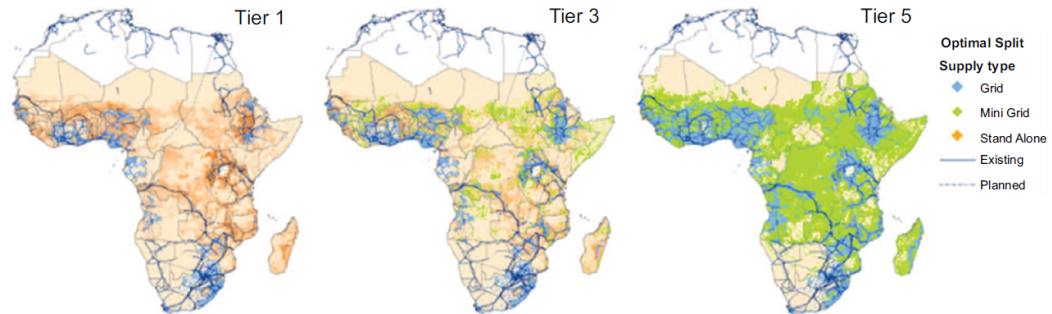
Figure 1.6: Least cost electrification mix for different target Tiers of electricity access [12].

Connection to good quality bulk power systems can enable access levels up to Tier 5 [16], as they easily accommodate demand growth and allow scalability. However, grid reliability is often an issue in SSA; in several countries, houses and small businesses register several hours of outage per day [17, 18]. The International Energy Agency analysed in [19] the impacts of reliability on the shares of grid connections and decentralized solutions in reaching universal access to electricity, using the Reference Electrification Model (REM) [13]. The results obtained for a region in Rwanda are shown in Figure 1.7. At lower

9

grid reliability levels, microgrids and stand-alone systems result more attractive. On the other hand, investments in additional centralized generation to cover load peaks result in reduced specific cost of fulfilling the demand from the bulk power system, increasing the competitiveness of grid extension. Nonetheless, decentralized solution would still cover about one third of the connections at 100% grid reliability, remaining relevant in the achievement of universal access.
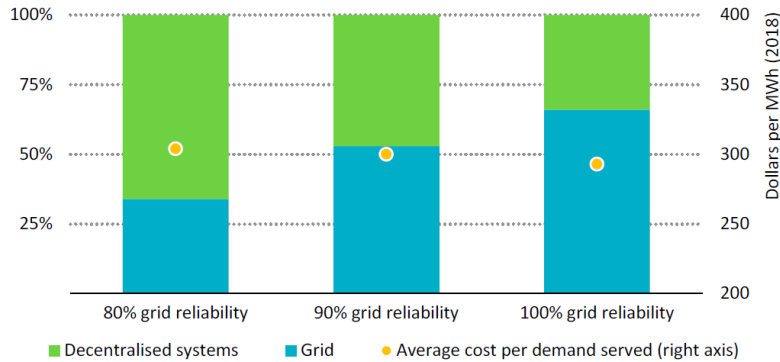
Figure 1.7: Connections by type to reach universal access to electricity with different grid reliability levels in a region of Rwanda [19].

Figure 1.8 compares the shares of the three electrification strategies to 2030 in the Business As Usual (BAU) scenario, i.e., projections based on historical trends, and in case stronger efforts are made to reach universal access to electricity, that would require the electrification of 110 million more homes. In this desired condition, SHSs play a more marginal role while microgrids are estimated to account for about half of the total household connections.
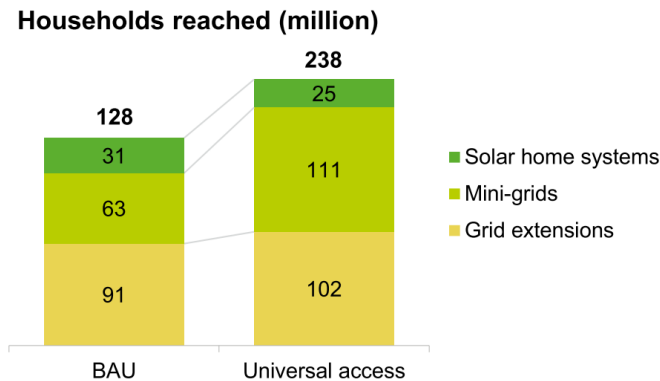
Figure 1.8: Technology use 2020-2030, assuming all minigrids are solar hybrid systems [16].

Given the numerous aspects influencing decision making for access to electricity, these shares are not evenly distributed in unelectrified areas and significant differences emerge

in the optimal electrification plans to be adopted in different countries. As an example, Figure 1.9 shows the energy access solutions to be adopted in Angola and Ethiopia to reach universal access by 2030 [19]. In Angola, the electricity grid supplies only the main settlements in the eastern part of the country; hence, grid extension would power only 38% of the population, while microgrids will likely cover 46% of the projected needs, supported by stand-alone systems in the most remote areas. On the contrary, Ethiopia is expected to advance from a current access rate of 45% up to 100% by relying largely (80%) on network densification and extension for new connections, as most of the population lives in proximity to the network. In conclusion, the potential of the different technologies varies widely across SSA, depending on the peculiarities of the area.
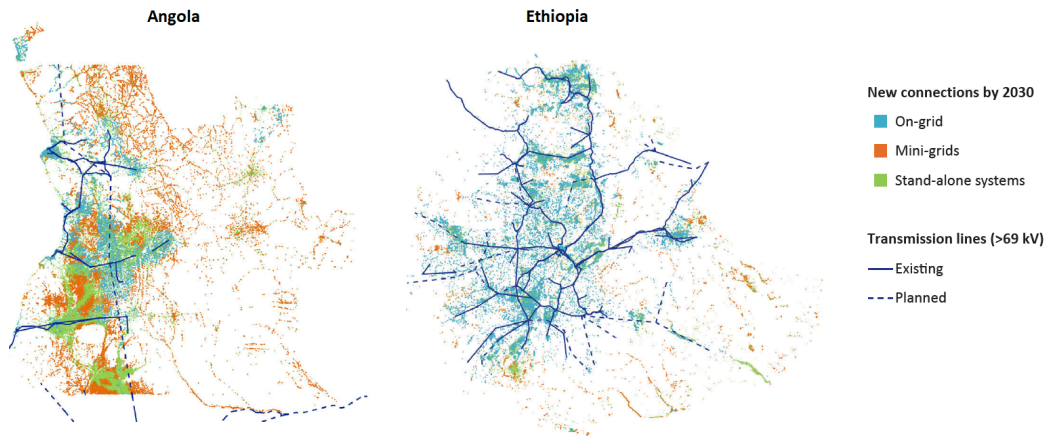
Figure 1.9: Electrification strategy for universal access by 2030 in Angola and Ethiopia [19].

1.5 The role of microgrids in reaching universal access

As highlighted in the previous section, a significant boost in microgrid installation is necessary to reach universal access by 2030. Figure 1.10 highlights the conditions in which microgrids would be the most suitable electrification option, according to a wide range of indicators, including but not limited to size and density of the settlement, socio-economic development of the community, distance from the national grid [20, 21]. Geographical and cultural peculiarities of the target area play a role in electrification plans, too, e.g., in case of decentralized solution, stand-alone systems are preferable in case the terrain is not flat [21, 22].

Hence, the potential for microgrid installations is particularly high in densely populated areas characterized by a significant distance from the bulk power system. The presence of energy-intensive productive activities, e.g., mining, helps reducing the specific cost of energy also for residential users, making the investment more robust [15]. In case the implementing entity intends to provide electricity access levels of Tier 3 or beyond, microgrids are very promising in the rural areas where decentralized solutions are preferred, as
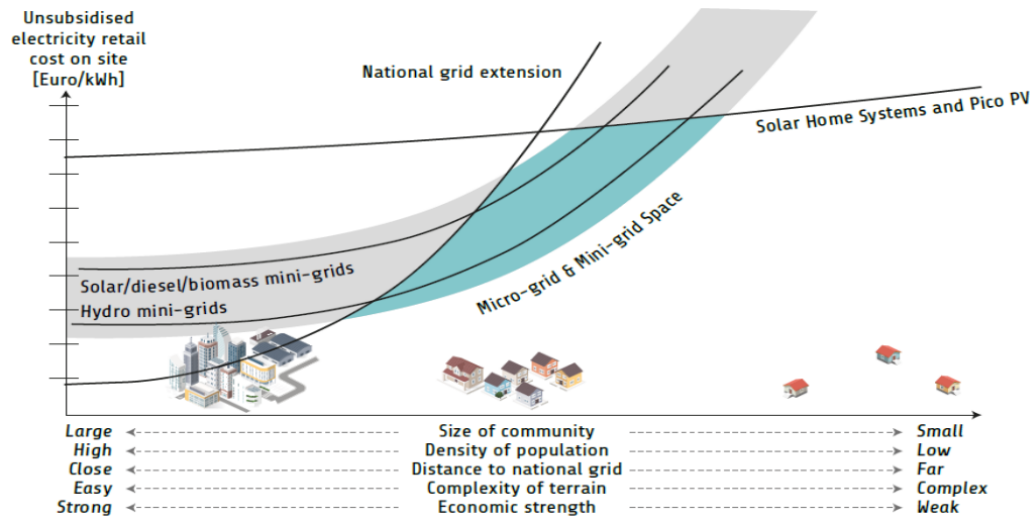
Figure 1.10: Competitiveness of microgrids/minigrids compared to alternatives [21].

stand-alone systems are usually able to cover only basic needs, limiting the opportunities of development and self-determination.

The practical implementation of the different strategies is also strictly linked to the local regulatory framework and electrification plans. In particular, robust and safe investments in microgrid installation require clear rules on tariff schemes, subsidies, interaction with the grid, etc. The absence of such clear regulations may hinder the path to universal access to electricity. On the contrary, advanced regulatory frameworks favour the flourishing of microgrid projects, as proven by the experience of several Sub-Saharan countries (Tanzania, Kenya, Rwanda, Nigeria) [19].

As the current average electrification pace is not sufficient to reach SDG7 by 2030, microgrids can represent a significant support for speeding up the process, providing reliable energy also to communities that would be reached by the grid in a few years. This is plausible only if the system is designed to interact effectively with the grid at the time of connection and if the tariff scheme allows to make the investment sustainable in the long term. Hence, regional planning tools may support multi-step electrification plans. Such approach is proposed in [14], which recommends a stepwise electrification strategy that rapidly reaches the whole population with a mix of decentralized and centralized solutions, to be partially and gradually integrated in the long run. This approach is particularly suitable for countries characterized by low grid reliability, as it also allows to improve the service provided to the new connections. Moreover, microgrids can support governments in meeting environmental objectives through the decarbonization of the energy sector.

Therefore, microgrids are a precious tool in the race towards the achievement of SDG7 and, according to local conditions, may have a variable but always relevant weight in pursuing the objective.

There are currently 47 million people connected to 19,000 microgrids, mostly hydro and diesel-powered and predominantly in Asia [17]. With the significant decrease in costs of

storage and RES generators (excluding hydro, which is a well-established technology with steady price trends) and with the advancements in control systems [16], hybrid energy systems are the most common configuration for newly installed microgrids. A typical layout is shown in Figure 1.11, where a diesel generator is combined with PV panels and storage to supply households and income-generating activities.
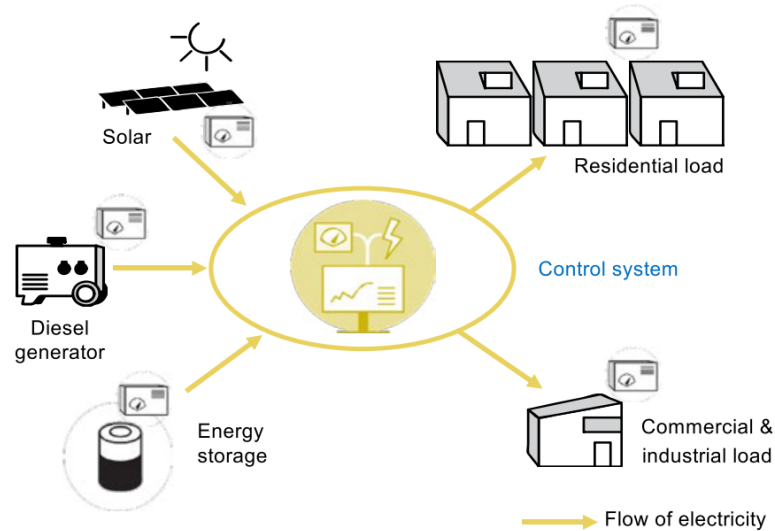
Figure 1.11: Architecture of isolated microgrid systems [16].

The costs of modern microgrid components are expected to keep on decreasing and ESMAP estimates that, in case actions to reduce the upfront investment and the operation costs, e.g., smart meters and remote-controlled management system, are implemented, the Levelized Cost of Electricity (LCOE) would fall down to 0.20$/kWh in 2030 [17], which would make these systems economically comparable with national grids [15]. In particular, PV-battery-based systems are undergoing the most dramatic cost reductions and have the additional advantage of being less constrained to the characteristics of the area with respect to other renewable sources like wind and hydro. This could trigger a vast implementation of microgrid projects, reaching extremely isolated communities at affordable cost.

Recent projections foresee that universal access to electricity could be achieved by 2030 reaching 490 million people with 210,000 microgrids, mostly solar-hybrid in SSA [17].

Hence, microgrids will play a crucial role in guaranteeing equal opportunities to electricity access in the next years, and it is of pivotal importance to plan such systems in a comprehensive and accurate way, to favour the effectiveness and durability of projects. Advanced computer tools are very powerful means to support decision makers in successfully planning rural electrification projects [23] and have been widely employed to guide policies and practical implementations. The next chapter summarizes the state of the art on microgrid planning algorithms, identifying the main literature gaps in effectively modelling these systems and their direct impact on the local community.

Chapter 2

State of the art and contributions

2.1 Introduction

Isolated microgrids are taking on great importance in pursuing universal access to electricity [17]; hence, an effective and accurate modelling to size and operate these systems is essential to enable their dissemination in rural areas and to efficiently allocate investments and funds from private and public donors. This chapter discusses the state of the art to identify the main literature gaps and define the objectives of the research. First, a detailed review on rural microgrid planning tools is provided in Section 2.2; this allows to thoroughly acknowledge in Section 2.3 the features missing in the current literature but necessary for designing an effective and comprehensive tool and thus to derive the main goals of the work, whose main contributions are resumed in Section 2.4. The structure of the thesis is presented in Section 2.5 and publications are listed in Section 2.6.

2.2 Overview on rural microgrid planning

The typical framework of a microgrid planning algorithm is shown in Figure 2.1: data on load profile, RES availability and techno-economic characteristics of components are the main inputs, while the microgrid architecture, its expected operation and the values of the objective functions are the most significant outputs.

The mathematical formulation fully representing the technical aspects and the decision-making process typically involves a large number of binary, integer and continuous variables and requires the use of complex and computationally-intensive algorithms. Hence, a compromise between accuracy and complexity should be sought for; this often leads to significant simplifications of the problem under analysis and to overlooking characteristics that play a pivotal role in determining the most suitable option.

15
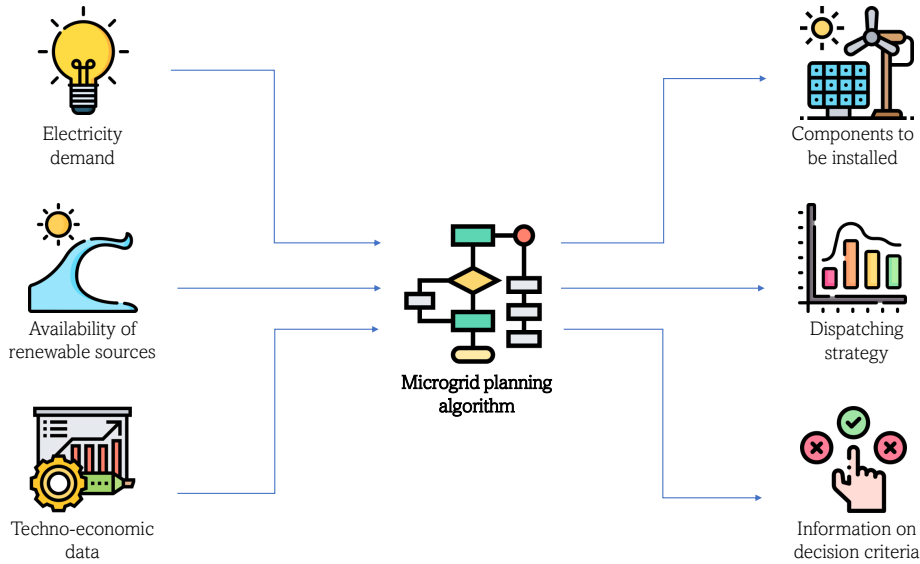
Figure 2.1: Block diagram of microgrid planning algorithms.

2.2.1 Traditional microgrid sizing approaches

Many approaches have been developed for microgrid planning, and there are increasing efforts on this topic, given its urgency. In particular, the approach in [24] involves a Genetic Algorithm (GA) to identify a population of possible generation portfolios, on which different rule-based operating strategies are tested over one typical year, with the objective of minimizing costs, fuel use and pollutant emissions. Heuristic methods are popular when aiming to quickly find an approximate sizing, but the search space needs to be limited, often to two technologies only, to avoid incurring combinatorial explosion [25–27]. Priority rules are identified for the employment of the available units, whose operation is analysed on the whole project lifetime in [25] and on one year in [26, 27]. A non-dominated sorting GA (NSGA-II) is used in [28] for sizing purposes, minimizing the total cost and the load curtailment probability. Similarly, [29] implements a multi-objective NSGA-II for the design, entrusting the optimal dispatching to a 24-hour Mixed Integer Linear Programming (MILP) problem. The work presented in [30] couples a GA-based sizing with a MILP optimized operation performed on 8 typical days that represent weekdays and weekends of the four seasons. A further evolutionary approach recently presented to solve the sub-problem of selecting valid-size scenarios is Particle Swarm Optimization, also in this case followed by a MILP procedure employed to solve the downstream sub-problem of optimizing the scheduling of system components; this approach can be performed either on a 1-week interval to be averaged on the whole month, as in [31], or run on a complete year with a Rolling Horizon (RH) technique, as in [32]. A GA is used in [33] to identify suitable sizing scenarios, while a MILP procedure optimizes the unit commitment from weekly averaged data; then, an RH technique with a 1-hour resolution verifies the validity of the results and

adjusts the sizing values if needed. Finally, the approach proposed in [34–36] adopts a one-shot MILP, i.e., optimizing sizing and operation all at once: the time-frame under analysis is the first year of the project, represented by one typical day per month in [34] and by three typical days (week, weekend and peak) per month in [35]. In addition, [36] uses the same typical days as in [35] but employs a multi-year approach in which the number of years to be optimized is flexible and adjusted to the user's knowledge of the input data and their forecast. An approach similar to one-shot MILP is proposed in [37], where the optimal size and operation of a rural microgrid are identified by means of a Linear Programming (LP) problem, which drastically reduces the computational complexity of the problem at the expense of limited precision in describing the behaviour of fuel-fired generators and storage assets.

One of the main issues faced in these works is the trade-off between accuracy and tractability: the size of the problem is so large that, in order to guarantee the convergence of the routine, several simplifying assumptions usually need to be implemented. According to the literature review, the following three approaches are the most popular:

  (i) heuristic sizing of generating and storage units coupled with rule-based dispatching of resources [24–28];

 (ii) heuristic sizing coupled with MILP-based dispatching criteria [29–33];

(iii) one-shot MILP performing both sizing and operation phases [34–36].

The first two methodologies split the formulation into two sub-problems; this usually guarantees fast computations, with the main drawback being that the optimality of the solution cannot be assured. In contrast, optimality is not an issue in the case of the one-shot MILP. Nonetheless, the computational burden increases dramatically with the number of integer variables and time steps. For this reason, the time-frame of the simulation is usually reduced to a few representative days and strong simplifying assumptions are made to avoid non-linearities, reducing the number of non-continuous variables, and to legitimize the compression of the time interval.

2.2.2 Multi-year characteristics

A significant research gap in traditional microgrid planning is the simulation and assessment of projects expected to last a considerable number of years by means of a few representative days, or at most one year, with the exception of [25, 31, 36] and of the commercial softwares HOMER [38] and iHoga [39] that use heuristic methods to size microgrids and have recently incorporated a multi-year feature. Figure 2.2 compares the architecture of single-year (top) and multi-year (bottom) approaches, highlighting that the traditional single-year method forces the modellers to assume that the simulated time interval is perfectly replicable along the project lifetime and to overlook any evolution over the years, thus most likely resulting in inaccurate designs. Contrarily, multi-year approaches allow to explicitly represent lost-lasting phenomena and improve the accuracy of the outputs, as long-term variations are proven to have a greater impact on the cost and configuration of the system with respect to short-term variations, e.g., daily fluctuations [40].

In particular, when access to energy is provided for the first time to a rural community, it is sensible to include load growth in the model. A common approach consists in assuming a plausible constant growth factor [36, 41–43]. Furthermore, asset degradation significantly affects the microgrid operational strategy during its lifetime, thus influencing the optimal design of the system and vice versa. In particular, the degradation of RES generators can be easily modelled by means of a linear decrease in productivity over time [44, 45], but this aspect is seldom included when planning isolated hybrid energy systems [43, 46, 47]. For what concerns BESS, the pace at which they degrade strictly depends on how they are used, and usually the replacement of the component is implemented when the capacity falls below 80% of its initial value [48, 49]. An accurate description of this phenomenon, together with other battery dynamic characteristics, e.g., variable efficiency, is pivotal for a consistent design of the microgrid.
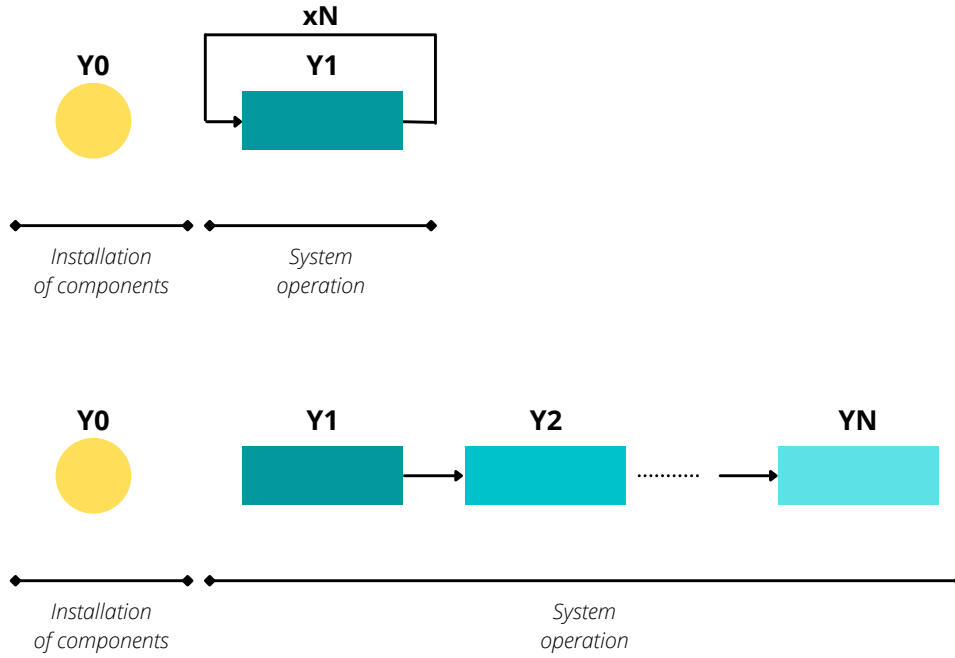
Figure 2.2: Algorithm structure of single-year (top) and multi-year (bottom) approaches.

Few works have managed to accurately model BESS behaviour within the scope of a MILP optimization, given the numerous non-linearities. The works [50, 51] adopt the concept of Coulomb efficiency explained in [52] to model the capacity degradation: this efficiency varies with the way the bank is operated in [50], while [51] identifies an approximation valid for any possible operating condition, which is used to compute the weekly storage degradation and update the available capacity accordingly. The battery life loss is a non-linear function of the State Of Charge (SOC); this curve is split into linear seg-

ments in [53] to include it into a MILP scheduling. The approach presented in [54] sets the working conditions of the storage system (C-rate, temperature) and the maximum number of cycles allowed is consequently defined, while [55] limits the number of changes of state of the batteries to reduce degradation. Finally, a common approach is to model the capacity reduction as a function of the total throughput, regardless of how the batteries are operated [31, 36, 46]. The available storage capacity is an input parameter in most of these works, while in the case of microgrid sizing, it constitutes a variable to be optimized; this poses further linearization problems. Furthermore, none of the papers mentioned in Section 2.2.1 dealing with microgrid design and, consequently, with storage sizing, adopts a capacity reduction model that considers the way the battery is managed. In conclusion, currently, there are no papers that address a MILP planning problem accounting for a detailed battery model and its effects on the system operation on the entire lifespan of the project.

2.2.3 Analysing the three dimensions of sustainability

Standard microgrid sizing tools usually reduce the complexity of the problem by means of a twofold approach: limiting the time frame under analysis adopting single-year approaches, as per Section 2.2.1, and focusing on economics-only optimizations. Therefore, cost is usually considered as the only determining factor in the effectiveness of the rural electrification process [26, 32, 33]. This assumption hardly matches the complex circumstances of off-grid microgrids in the Global South, given the multiplicity of impacts on the community involved, the intrinsic long-lasting nature of the system, the significant load growth and the assets degradation over the years.

A growing interest in environmental protection issues has led various scholars to also include an assessment of carbon emissions in their analyses, as a limit not to be exceeded [34, 38], or as monetary cost to be minimized [30, 36], or as additional objective function [24, 35, 39, 56–59]; however, Life Cycle Assessment (LCA), which quantifies the emissions along the whole life cycle of an asset, is rarely adopted [34, 39, 56], and generally only direct emissions are taken into account [24,30,35,36,38,57–59], resulting in incomplete and sometimes misleading evaluations.

In addition to this, the importance of considering the social impact of rural electrification projects is increasingly recognized and demanded as an indispensable element of system planning tools [60]. Nonetheless, very few multi-objective algorithms have been developed including social assessments, mostly through the evaluation of employment generation [39,58,59]. The maximization of the Human Development Index (HDI) in relation to energy consumption is rarely adopted [39], and although the relationship between HDI and energy use is widely recognized nowadays, as discussed in Section 1.3, it can hardly describe the local impact on the electrified community, while job creation is an understandable and measurable criterion; this is why the latter is used more extensively in multi-objective optimization.

A popular and consolidated approach for holistic analysis of rural electrification projects is to use Multi-Criteria Decision Analysis (MCDA) [61–64], which is more prone to including social and qualitative decision criteria. However, the purpose of MCDA is limited to prioritizing the preferred technologies according to scores assigned to the different options, weighted on the decision marker's preferences, so it cannot size generation mix and pro-

vide the scheduling strategy and is not able to efficiently manage different configurations of hybrid systems. Hence, these aspects must be analysed separately and MCDA is used for ex-ante [63] or ex-post [64] assessments, but planning tools are still needed.

Therefore, the literature lacks a holistic multi-objective optimization that addresses all the aforementioned shortcomings.

2.2.4 Long-term uncertainty in rural electrification projects

The outcome of rural electrification projects is extremely uncertain, because the design of the power system is based on specific assumptions in terms of electricity demand projections over time that may turn out to be very far from their actual realization. The evolution of the load depends on two main aspects, i.e., the increase in the number of users and the adoption of more energy-intensive appliances, and they are both subject to high uncertainty because related to complex socio-economic and environmental dynamics (closeness to other electrified areas, demand stimulation programs, access to financial capital, resilience to climate change, etc.) [65].

The formulation of realistic demand forecasts is key to robust microgrid planning. Some methodologies have been developed, but there is no standard yet: the most common approaches to estimate the demand are econometric (top-down) and end-use (bottom-up). The former is based on macroeconomic data which are easily accessible but cannot effectively represent the peculiarities of a community, while the latter provides more realistic appliances-based projections but data are hardly available [66]. In this regard, efforts have recently been made to gather and classify load profiles of existing remote microgrid projects, to derive replicable patterns and guide developers [67].

For what concerns forecasts of load evolution in the long term, they are often based on arbitrary trends; some works adopt a deterministic scenario based on a constant growth factor [36,41,42,44], while the uncertainty of such pivotal input has prompted many scholars to use scenarios to evaluate different possible realizations of the load. In particular, different projections have been derived from historical data on similar projects [47] or according to different assumptions either in terms of appliances penetration [68,69], or of macroeconomic trends (GDP, population,etc.) [70], or from a combination of these elements [40].

Given the significant impact of long-term uncertainties on the optimal configuration of an isolated hybrid power system, a few studies approaching the problem through multi-step sizing have recently been published; in these works, the installation of assets is not limited to the beginning of the project, but may be integrated in the following years, allowing to plan deferred investments linked to the increase in demand over time and components degradation.

The problem may be decomposed into subsequent deterministic single-year optimizations [36], or through a two-stage process that first determines the asset capacities of each year separately and then evaluates the total life cycle cost [42]. Similarly, [71] describes a capacity expansion planning problem of a remote power system, broken down into stochastic yearly optimizations. A capacity expansion problem is also presented in [72], in which a system dynamics model and the DER-CAM software [35] are iteratively solved until convergence, to accurately estimate the socio-economic phenomena stimulating the load growth and plan the investments accordingly.

As the difficulty of making accurate predictions is a pivotal issue in evaluating the hardly predictable evolution of rural electrification projects, stochastic methods are well suited for the optimization of such long-lasting systems subject to a high degree of uncertainty. Figure 2.3 shows an illustrative example of the framework adopted: the demand scenarios correspond to the different branches, all departing from the common starting point of the initial load curve, and the nodes correspond to the moments when the installation of components is allowed. The developer may set multiple capacity expansion windows, which are common to all scenarios; then, the optimizer will define for each scenario and for each capacity expansion window whether to upgrade the system and how.
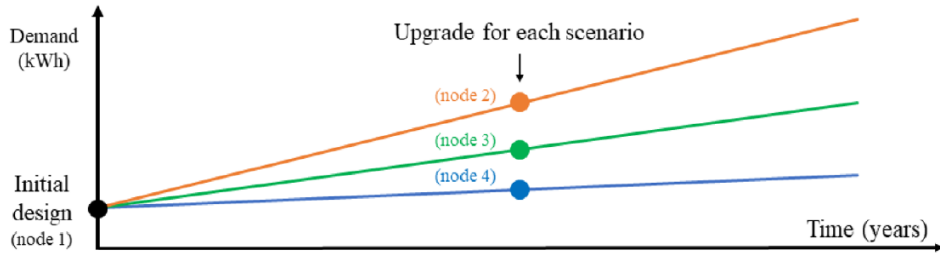
Figure 2.3: Example of tree structure to consider stochastic load growth and components upgrades [47].

Such methods have recently gained attention in the scope of multi-step sizing of rural microgrids [47,69]; in particular, [47] uses Particle Swarm Optimization to assess the least-cost option according to three demand growth scenarios and two installation windows; a Linear Programming (LP) problem is formulated in [69] to evaluate the best investment plan, given four capacity expansion steps and four load scenarios. However, these few stochastic multi-step sizing tools available in the literature use optimization methods that favour the speed of execution over the accuracy of the results. In particular, [47] adopts a heuristic method that may provide a local optimum as output configuration; the LP approach [69] efficiently reaches the global optimum but the strict linearity hinders the accurate technical description of the components, as, for example, it is not possible to set a minimum power threshold for fuel-fired generators. There are still no examples of multi-step sizings using MILP techniques, that do not pose optimality issues and can thoroughly describe the behaviour of the components but are usually associated to a heavy computational burden.

2.3 Literature gaps and research objectives

The previous sections presented the state of the art in microgrid planning algorithms, highlighting the gaps that reduce the effectiveness of such tools. Table 2.1 summarizes the characteristics of the most significant works on the topic, grouping the modelling aspects under analysis into four main categories:

(i) *Optimization method.* Defines whether the article adopts a one-shot MILP approach, i.e., component sizing and resource scheduling optimized jointly within one algorithm.

(ii) *Multi-year characteristics.* Identifies the presence of a long-term perspective, in contrast with single-year approaches. In particular, the presence of load growth, of degradation of RES generators and of BESS capacity reduction depending on its operation are detected.

(iii) *Multi-objective optimization.* Highlights the presence of multiple decision criteria, grouped into economic, environmental and social objective functions.

(iv) *Long-term uncertainty.* Points out the evaluation of long-term uncertainty in terms of multiple demand scenarios and of presence of capacity expansion opportunities along the project lifetime.

The table highlights that the only common feature among all the papers under analysis is the presence of an economic objective function, typically considered as the most significant - if not the only - information driving the selection of the generation and storage assets and their operation.

The prominence of traditional single-year least-cost approaches is gradually decreasing to make room for a twofold advancement: multi-year methods, enabling a long-term perspective on the evolution of the system, and multi-objective optimization, widening the decision-making process to a comprehensive and considerate approach. However, these two features are rarely combined because of the considerable impact on the computational burden. The only example available in literature is the commercial software iHoga [39], whose algorithm is not publicly available. This tool adopts a genetic algorithm and allows to expand with a multi-year module the basic single-year version minimizing the total Net Present Cost (NPC) or maximizing the Net Present Value (NPV), but without being able to evaluate different scenarios of demand growth and possible system upgrades. Moreover, the user may choose among several decision criteria to integrate the objective function: carbon emission, unmet load, HDI and job creation.

One-shot MILP algorithms have the advantage of optimizing sizing and operation phase in a simultaneous and effective way, guaranteeing the identification of the global optimum, but they usually employ a significant simulation time, compared to heuristic methods; for this reason the works adopting this technique are provided with only few of the important aforementioned features (see Table 2.1). Therefore, advancements in the formulation of MILP problems are required in order to extend their application to more complex models.

This research aims at filling the gaps identified in the literature, which concern both the way the microgrid planning problem is described and the mathematical programming tools adopted to identify the optimal solution. Hence, two main research objectives are pursued by this work:

Objective 1. To formulate a holistic MILP microgrid planning model, describing the full project lifetime and enabling an informed and comprehensive decision-making process, accounting for long-term uncertainty.

Objective 2. To develop novel algorithms enabling the use of MILP methods for complex and computationally-intensive applications.

Table 2.1: Main features of the most significant works on microgrid planning.

| | Method | Multi-year characteristics | | | Multi-objective optimization | | | Long-term uncertainty | |
	One-shot MILP	Load growth	RES degradation	BESS variable degradation	Economic	Environmental	Social	Demand scenarios	Multi-step sizing
[24]					✓	✓			
[25]		✓			✓			✓	
[26]					✓				
[27]					✓				
[28]					✓				
[29]					✓				
[30]					✓				
[31]					✓				
[32]					✓				
[33]					✓				
[34]	✓				✓				
[35]	✓				✓	✓			
[36]	✓	✓			✓				✓
[37]					✓				
[38]		✓	✓	✓	✓				
[39]		✓	✓	✓	✓	✓	✓		
[41]	✓	✓			✓			✓	
[42]		✓			✓				✓
[46]	✓		✓		✓				
[47]		✓	✓		✓			✓	✓
[54]	✓				✓				
[56]					✓	✓			
[57]					✓	✓			
[58]					✓	✓	✓		
[59]					✓	✓	✓		
[72]	✓	✓			✓				✓
[69]		✓			✓			✓	✓

2.4 Main contributions

The main contributions of the thesis can be summarized as follows:

- Comprehensive description of a rural microgrid planning problem, including long-term uncertain phenomena and the evaluation of the economic, environmental and social impacts of the project. The methodology is tested on a real case study of a community in Soroti, Uganda.

- Formulation of a novel iterative algorithm to account for complex non-linear phenomena, e.g. power-dependent BESS degradation, in one-shot MILP problems with an efficient and reliable approach.

- Development of A-AUGMECON2, which represents an advancement of the well-established AUGMECON2 method, for solving multi-objective MILP optimizations. It introduces an online Pareto filter that skips redundant iterations and dramatically reduces the computational burden, while improving the readibility of the results.

2.5 Thesis outline

The rest of the thesis gradually addresses the features and gaps discussed in Sections 2.2 and 2.3, while concurrently pursuing the two research objectives. Part II fully explores the modelling approach proposed to effectively tackle the rural microgrid planning problem, by dealing with one aspect at a time and building on the findings of the previous chapters to finally present the complete approach. Each chapter introduces the features under study, thoroughly describes the methodology and its application on a real case study, analyses the results. Part III concludes the thesis with a summary and a discussion on the contributions of the work, with reference to possible future developments. In detail, the thesis is organized as follows:

Chapter 3. An iterative procedure to reduce the computational burden of multi-year MILP planning problems is presented, including load growth, RES degradation and BESS power-dependent capacity reduction. The accuracy over single-year methodologies is highlighted.

Chapter 4. The model presented in Chapter 3 is adopted as the core problem to be optimized within the framework of a novel multi-objective method with online Pareto pruning. The significant advancement with respect to the traditional approach is discussed. Net Present Cost (NPC), life cycle carbon emissions, land use, job creation and public lighting coverage are evaluated to build the set of non-dominated solutions.

Chapter 5. The findings of the two previous chapters are capitalized to further expand the features of the model, including a stochastic approach for a sound evaluation of the possible long-term load growth scenarios and the possibility to upgrade accordingly the generation and storage assets along the project lifetime.

Chapter 6. The main results are summarized and discussed, highlighting the main advantages of the approach and its versatility.

Chapter 7. This chapter concludes the thesis with final remarks and possible future developments of the work.

2.6   List of publications

The following is a list of publications derived from the research presented in the thesis and from related activities:

- M. Petrelli, A. Berizzi, C. Bovo and E. Amaldi, "Robust optimization for the scheduling of isolated RES-based microgrids in developing countries," *Mediterranean Conference on Power Generation, Transmission, Distribution and Energy Conversion (MEDPOWER 2018)*, Dubrovnik, Croatia, 2018, pp. 1-8.

- A. Vaccaro, M. Petrelli and A. Berizzi, "Robust Optimization and Affine Arithmetic for Microgrid Scheduling under Uncertainty," *2019 IEEE International Conference on Environment and Electrical Engineering and 2019 IEEE Industrial and Commercial Power Systems Europe (EEEIC / I&CPS Europe)*, Genova, Italy, 2019, pp. 1-6.

- M. Petrelli, P. V. A. Melià, "A literature review of the integration of optimization algorithms and LCA for microgrid design: a replicable model for off-grid systems in developing countries", *XIII Convegno della Rete Italiana LCA*, Roma, June 13-14, 2019.

- M. Petrelli, D. Fioriti, A. Berizzi and D. Poli, "Multi-Year Planning of a Rural Microgrid Considering Storage Degradation," *IEEE Transactions on Power Systems*, vol. 36, no. 2, pp. 1459-1469, March 2021.

- M. Petrelli, D. Fioriti, A. Berizzi, C. Bovo, D. Poli, "A novel multi-objective method with online Pareto pruning for multi-year optimization of rural microgrids", *Applied Energy*, Volume 299, 2021, 117283.

- N. Stevanato, S. Corigliano, M. Petrelli, F. Tonini, M. Merlo, E. Colombo, "Rural Areas Electrification Strategies Through Shadow Costs Analysis - Bolivian Highlands Case Study", *Energy for Sustainable Development*, Volume 65, Pages 162-174, 2021.

Part II

Modelling framework for microgrid planning

Chapter 3

Deterministic multi-year planning

3.1 Introduction

This chapter paves the way to overcoming the literature gaps identified in Chapter 2. In particular, it describes a methodology able to find out the optimal sizing of the plant, taking into account optimal scheduling during operation, pursuing the least-cost objective, while capturing the complexity of such a system in terms of multi-year features, namely load growth, linear degradation of the RES generators and variable BESS capacity decrease. The Iterative Multi-Year (IMY) methodology here proposed is based on an iterative approach updating specific constants of the MILP planning core and accounting for a detailed description of the battery efficiency and power-dependent degradation, while preserving convergence quality. By doing so, the burden of each MILP problem is significantly reduced, thus making the overall approach able to simultaneously take into account both the operational planning and the degradation of the asset performances over time, which in turn depend on the hourly scheduling. The approach makes it possible to solve this very complex problem in a both accurate and computationally efficient way, overcoming traditional single-year methodologies [26, 32]. The MILP optimization is not directly used in a single shot, as in the literature (see Section 2.2.1), but it is embedded in an iterative scheme for the purpose of accuracy, while preserving tractability.

The chapter is structured as follows: the main contributions of the novel methodology are summarized in Section 3.2 and described in detail in Section 3.3, that presents the objective function and constraints of the optimization algorithm and the iterative procedure adopted to accurately account for the non-linear BESS degradation; Section 3.4 introduces the case study that will be used throughout the whole thesis and lists the tests performed to validate the methodology; Section 3.5 discusses the results, highlighting the reliability and computational efficiency of the procedure in comparison with standard approaches and it shows the significant influence of a detailed battery model on the optimal design; finally, Section 3.2 concludes the chapter with a summary of the most relevant considerations.

3.2 Contributions

The main contributions of this chapter include (1) a novel iterative algorithm for multi-year planning of isolated microgrids in developing countries that (2) accurately models the variable charging-discharging efficiency of the battery and its capacity degradation as a function of the hourly power-to-energy ratio, (3) considering detailed multi-year simulations spanning the entire lifetime of the project at an hourly time resolution. The effectiveness of contribution (1) is validated by proving the infeasibility of taking into account degradation and variable efficiency of batteries in a traditional one-shot MILP. The impact of contributions (2) and (3) on the total cost of an isolated microgrid in Uganda is shown, highlighting the importance of the results for real applications.

3.3 Methodology

In the IMY approach, a typical planning problem is integrated with the battery power-dependent efficiency and degradation, and the long-term simulations are decomposed in the iterative algorithm depicted in Figure 3.1. The main steps of the procedure are as follows:

1. Initialize the parameters describing the degradation of the battery and its power-dependent efficiency.

2. The MILP planning problem is run over the project lifetime, including the optimization of the hourly scheduling of the storage battery bank, using the most updated parameters modelling the battery. These parameters are constants for the MILP problem.

3. The parameters associated with capacity degradation and efficiency variation related to the optimized scheduling are updated.

4. If the convergence criterion on the variation of the parameters is met, the procedure stops; otherwise, the parameters are updated and a new MILP is run (go to 2).

   In contrast to the standard MILP formulation that would require a large number of continuous and binary variables to be optimized inside the MILP framework, the non-linearities of the battery are modelled in the IMY method through constants updated in each iteration. This reduces the computational burden of each MILP without significantly compromising the optimality of the solution. The iterative procedure runs until the variation of the parameters in two consecutive iterations falls below a threshold. The following subsections present the details of the IMY approach.

3.3.1 MILP sizing algorithm

The IMY approach is very general and can be applied to any system architecture. However, for the sake of simplicity and with no loss of generality, the mathematical formulation of the method is described referring to the typical microgrid shown in Figure 3.2, composed by Diesel Generators (DGs), Photovoltaic plants (PVs), Wind Turbines (WTs), and Battery
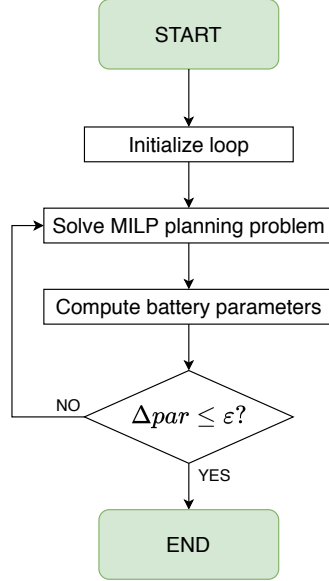
Figure 3.1: The optimization algorithm.

Energy Storage Systems (BESSs). Every technology is connected to an alternate current (AC) busbar; hence, the sizing of Converters (CONs) is embedded into the design of the direct current (DC) units, namely, PV and BESS. An hourly time interval is considered and time-variant quantities are assumed to be constant during each interval.

The IMY model of the system aims at capturing the most significant phenomena that should be considered in the optimal design of the microgrid. Moreover, given the MILP formulation aimed at minimizing the Net Present Cost (NPC) of the system, the model automatically tends to reduce the operating costs, hence maximizing the use of renewable energy sources, when available, or providing time-shifting to reduce reliance on fuel-fired generators when economically profitable.

The following subsections describe the model in detail and the full nomenclature is resumed in Appendix A.

Objective function

The function to be minimized is the NPC, formulated as in (3.1), where IC_i is the initial investment, $O\&M_i$ represents the operation and maintenance expenses, RC_i denotes the replacement cost and finally, RV_i is the residual value.

$$NPC = \sum_i (IC_i + O\&M_i + RC_i - RV_i) \tag{3.1}$$

where $i \in \{g, p, w, b\}$ is the set of indexes of the available technologies, namely, DG, PV, WT and BESS, respectively; each element represents the set of available types of components

31
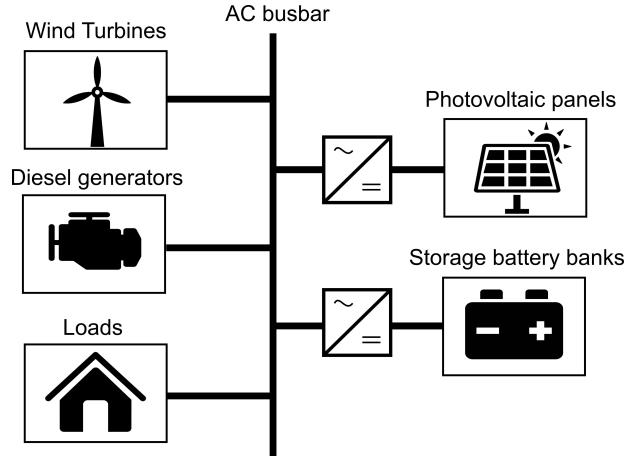
Figure 3.2: Microgrid architecture.

for each technology.

The initial investment cost of each technology type is defined as in (3.2), where c_i is the capital cost of a single unit and N_i is the number of installed units.

$$IC_i = N_i \cdot c_i \tag{3.2}$$

The O&M costs are defined in (3.3a) for PV, WT and BESS as a fixed amount per year y, supposed to be encountered at the last hour of the year. On the other hand, the O&M costs of DG, detailed in (3.3b), depend upon their operation hours and on fuel expenses. m_i is the yearly O&M cost of one unit of i, $\overline{Y}$ is the project lifetime in years, H is the number of hours in one year, $\overline{H}$ is the project lifetime in hours, d_h is the discount factor in hour h, $U_{h,g}$ is the integer variable stating the number of active DG of type g in hour h, f is the cost of fuel and $FC_{h,g}$ is the hourly fuel consumption of g.

$$O\&M_{i\setminus\{g\}} = N_i \cdot m_i \cdot \sum_{y=1}^{\overline{Y}} d_{H \cdot y} \tag{3.3a}$$

$$O\&M_g = \sum_{h=1}^{\overline{H}} d_h \cdot (m_g \cdot U_{h,g} + f \cdot FC_{h,g}) \tag{3.3b}$$

Given the usual time horizon of microgrid projects, the only components with a lifetime possibly shorter than the project duration are DG and BESS, and their replacement costs must be taken into account, unlike the other technologies. The life of DG is expressed in (3.4a) assuming H_g^{life} total working hours before replacement. The related cost is distributed along the corresponding lifetime, instead of being concentrated at the time of the actual replacement. This is a conservative approach that tends to overestimate the cost of DG, pushing towards a configuration based on renewables.

On the other hand, the presence of a replacement counter $k_{h,b}$ for BESS, increasing every time the relative residual capacity falls below the minimum threshold $\underline{\alpha_b}$, enables allocating the whole replacement cost when needed, as detailed in (3.4b).

$$RC_g = \frac{c_g}{H_g^{life}} \cdot \sum_{h=1}^{\overline{H}} d_h \cdot U_{h,g} \tag{3.4a}$$

$$RC_b = N_b \cdot c_b \cdot \sum_{h=1}^{\overline{H}} d_h \cdot (k_{h,b} - k_{h-1,b}) \tag{3.4b}$$

Finally, the residual value of the components whose lifetime Y_i^{life} is assumed longer than the project lifetime $\overline{Y}$, namely, PV and WT, is computed in (3.5a). Since the DG replacement cost is addressed as a distributed cost, there is no need to consider its residual value, which is instead evaluated for BESS in (3.5b) based on the residual capacity available. $\alpha_{h,b}$ is the per-unit BESS residual capacity, bounded in between a maximum ($\overline{\alpha_b}$) and a minimum ($\underline{\alpha_b}$) threshold. Factor $\rho_{h,i}$ is the degradation rate of component i.

$$RV_{i\setminus\{g,b\}} = d_{\overline{H}} \cdot \rho_{h,i} \cdot N_i \cdot c_i \frac{Y_i^{life} - \overline{Y}}{Y_i^{life}} \tag{3.5a}$$

$$RV_b = d_{\overline{H}} \cdot N_b \cdot c_b \cdot \frac{\alpha_{\overline{H},b} - \underline{\alpha_b}}{\overline{\alpha_b} - \underline{\alpha_b}} \tag{3.5b}$$

Constraints

The power balance constraint at the AC busbar is reported in (3.6), where $P_{h,b}^{dch}$ is the discharging power from BESS of type b, $\overline{\eta_b}$ is the maximum BESS efficiency of b, $\beta_{h,b}$ is the per-unit BESS efficiency of hour h, $P_{h,b}^{ch}$ is the BESS charging power of BESS of type b, P_h^{ren} is the renewable power injected into the system, $P_{h,g}^{dg}$ is the power produced by the DG units of type g, D_h^u is the unmet demand and D_h is the demand.

$$\sum_b \left(P_{h,b}^{dch} \cdot \overline{\eta_b} \cdot \beta_{h,b} - \frac{P_{h,b}^{ch}}{\overline{\eta_b} \cdot \beta_{h,b}} \right) + P_h^{ren} + \sum_g P_{h,g}^{dg} + D_h^u = D_h \tag{3.6}$$

To avoid the oversizing of the system, load shedding is typically admitted in these contexts. In particular, in the IMY formulation, the constraint is enforced to be below a given threshold of the yearly demand (see (3.7)), so that significant mismatches of unmet demand along the project lifetime are avoided. In the literature, sometimes the same problem is modelled by using economic penalties in the objective function for every unit of Energy Not Served (ENS) [73], while other studies have proposed the formulation by hard constraints [25, 74], as developed in this work. Both models involve considerations on continuity of supply and provide similar results, but the former is more computationally demanding, as highlighted in [73]. Moreover, given the scope of application of the model, it may be difficult to identify a suitable numerical value to be used as penalty in such contexts. Lastly, public calls for tender may often have requirements in terms of a cap on

ENS rather than estimating its equivalent economic cost. Therefore, the second approach is selected: load curtailment is admitted and capped in (3.7) through the $\overline{ENS}$ factor.

$$\sum_{h=1}^{\overline{H}} D^u_{(y-1)\cdot\overline{H}+h} \leq \sum_{h=1}^{\overline{H}} D_{(y-1)\cdot\overline{H}+h} \cdot \overline{ENS} \tag{3.7}$$

The renewable production injected into the system computed in (3.8) is at most equal to its availability, where $P^{pv}_{h,p}$ is the generation available from the PV generator of type p, and $P^{wt}_{h,w}$ is the generation available from the WT generator of type w, $\rho^{pv}_{h,p}$ and $\rho^{wt}_{h,w}$ are the linear degradation rates of PV and WT technologies respectively.

$$P^{ren}_h \leq \sum_p \rho^{pv}_{h,p} \cdot N_p \cdot P^{pv}_{h,p} + \sum_w \rho^{wt}_{h,w} \cdot N_w \cdot P^{wt}_{h,w} \tag{3.8}$$

The next block of constraints is devoted to defining the behaviour of DG. In particular, (3.9a) describes a linear fuel consumption curve according to coefficients A and B, suitable for small size DG; (3.9b) and (3.9c) limit the working area of the units within $\overline{P_g}$ and $\underline{P_g}$ and consider the reserve $R^{dg}_{h,g}$ to be provided; (3.9d) limits the total number of active generators.

$$FC_{h,g} = A \cdot U_{h,g} + B \cdot P^{dg}_{h,g} \tag{3.9a}$$

$$P^{dg}_{h,g} + R^{dg}_{h,g} \leq \overline{P_g} \cdot U_{h,g} \tag{3.9b}$$

$$P^{dg}_{h,g} \geq \underline{P_g} \cdot U_{h,g} \tag{3.9c}$$

$$U_{h,g} \leq N_g \tag{3.9d}$$

The behaviour of BESS is ruled by (3.10a)-(3.10g), where (3.10a) defines the energy level $Q_{h,b}$, limited by (3.10b) and (3.10c); the discharging and charging power are capped in (3.10d) and (3.10e) by the maximum power-to-energy ratio $\overline{PQ}_b$; and (3.10f) and (3.10g) aim at avoiding that the batteries discharge and charge during the same time interval. Δh is the selected time interval, $\overline{C_b}$ is the maximum capacity of one unit of b, DOD_b is the depth of discharge, $R^{sb}_{h,b}$ is the reserve to be provided by BESS of type b, $w^{dch}_{h,b}$ is a binary variable equal to 1 in the discharging mode and 0 in the charging mode, and M is a large constant.

$$Q_{h,b} = Q_{h-1,b} + (P^{ch}_{h,b} - P^{dch}_{h,b}) \cdot \Delta h \tag{3.10a}$$

$$Q_{h,b} \geq N_b \cdot \overline{C_b} \cdot (1 - DOD_b) + R^{sb}_{h,b} \cdot \Delta h \tag{3.10b}$$

$$Q_{h,b} \leq \alpha_{h,b} \cdot N_b \cdot \overline{C_b} \tag{3.10c}$$

$$P^{dch}_{h,b} \leq N_b \cdot \overline{C_b} \cdot \overline{PQ}_b \tag{3.10d}$$

$$P^{ch}_{h,b} \leq N_b \cdot \overline{C_b} \cdot \overline{PQ}_b \tag{3.10e}$$

$$P^{dch}_{h,b} \leq w^{dch}_{h,b} \cdot M \tag{3.10f}$$

$$P^{ch}_{h,b} \leq (1 - w^{dch}_{h,b}) \cdot M \tag{3.10g}$$

To account for the unpredictability related to real-time dispatching of the system, a reserve requirement R_h to be provided by DG and BESS is established in (3.11), proportional

to the unpredictability of load (γ_d) and of renewable sources (γ_{pv} and γ_{wt}). The literature is rich with multiple methods to deal with short-term variations and they differ in terms of data and computational requirements; however, the use of reserves is generally computationally efficient [26,30], and the approach was regarded as a good compromise between tractability and representation of the problem, especially with respect to stochastic [25,73] or robust [75] optimization. In stochastic optimization, uncertainties are modelled by means of scenarios, which proportionally increase the size of the problem with often more than a linear increase of computational requirements. Moreover, the formulation of scenarios and of their probability distribution requires an amount of data that is hardly available for developing countries. On the other hand, robust optimization provides a configuration able to completely fulfil the demand for any realization of the inputs [75]. The method is computationally efficient, but it tends to oversize the generating units, leading to a higher overall cost [76,77]. Hence, it is likewise unsuitable for the purpose of this work, because affordability is often a priority over reliability of service in cases of first access provided to rural communities. For these reasons, the approach involving reserve requirements is preferred.

$$R_h = \gamma_d \cdot D_h + \gamma_{pv} \cdot \sum_p \rho_{h,p}^{pv} \cdot N_p \cdot P_{h,p}^{pv} + \gamma_{wt} \cdot \sum_w \rho_{h,w}^{wt} \cdot N_w \cdot P_{h,w}^{wt} \tag{3.11a}$$

$$R_h \leq \sum_g R_{h,g}^{dg} + \sum_b R_{h,b}^{sb} \cdot \overline{\eta_b} \cdot \beta_{h,b} \tag{3.11b}$$

3.3.2 The iterative procedure

Updating parameters

As shown in the previous subsection, the dynamic behaviour of BESS in terms of capacity degradation and variable efficiency is accounted for in the MILP optimization by means of the parameters $\alpha_{h,b}$ and $\beta_{h,b}$, respectively. The former quantifies the relative residual capacity at hour h, depending on the total throughput $Q_{h,b}^{thr}$ and on the working power-to-energy ratio $PQ_{h,b}$. The latter indicates the relative charging or discharging efficiency, and it varies according to the working $PQ_{h,b}$, which is computed as in (3.12) after each MILP problem is solved:

$$PQ_{h,b} = \frac{P_{h,b}^{ch} + P_{h,b}^{dch}}{N_b \cdot \overline{C_b}} \tag{3.12}$$

The value of $PQ_{h,b}$ has to comply with the maximum power rate of the component ($PQ_{h,b} \in [0; \overline{PQ_b}]$), and it is discretized in subintervals, each characterized by a constant maximum number of cycles $n(PQ_{h,b})$ (i.e., the BESS cycle lifetime if always operated at that $PQ_{h,b}$) and charging and discharging efficiencies $\eta(PQ_{h,b})$. At each hour h, $n(PQ_{h,b})$ and $\eta(PQ_{h,b})$ are assigned according to the relevant interval of $PQ_{h,b}$. The computation of the parameter $\beta_{h,b}$ in (3.13) is now straightforward.

$$\beta_{h,b} = \frac{\eta(PQ_{h,b})}{\overline{\eta_b}} \tag{3.13}$$

To calculate $\alpha_{h,b}$, first, the total throughput is computed according to (3.14).

35

$$Q_{h,b}^{thr} = Q_{h-1,b}^{thr} + (P_{h,b}^{ch} + P_{h,b}^{dch}) \cdot \Delta h \tag{3.14}$$

The BESS residual capacity $C_{h,b}^{res}$ is modelled as a sawtooth function: in (3.15a), it degrades linearly as $Q_{h,b}^{thr}$ increases, with a growing slope for increasing $PQ_{h,b}$, i.e., decreasing $n(PQ_{h,b})$, and no replacement is needed; conversely, in (3.15b), it returns to its initial value when $\alpha_{h,b}$ falls below $\underline{\alpha}_b$, i.e., a replacement is put in place.

$$\text{if } \alpha_{h-1,b} \geq \underline{\alpha}_b \begin{cases} C_{h,b}^{res} = C_{h-1,b}^{res} - \dfrac{1 - \underline{\alpha}_b}{2 \cdot n(PQ_{h,b}) \cdot DOD_b} \cdot (Q_{h,b}^{thr} - Q_{h-1,b}^{thr}) \\ k_{h,b} = k_{h-1,b} \end{cases} \tag{3.15a}$$

$$\text{if } \alpha_{h-1,b} < \underline{\alpha}_b \begin{cases} C_{h,b}^{res} = N_b \cdot \overline{C_b} \\ k_{h,b} = k_{h-1,b} + 1 \end{cases} \tag{3.15b}$$

Finally, the parameter $\alpha_{h,b}$ is computed as detailed in (3.16).

$$\alpha_{h,b} = \frac{C_{h,b}^{res}}{N_b \cdot \overline{C}_b} \tag{3.16}$$

Convergence criteria

Convergence of the algorithm is achieved when the following criteria are met. First, the NPC is compared with the value obtained in the previous iteration NPC^*, and the relative change ΔNPC, calculated as in (3.17), shall fall below a given threshold.

$$\Delta NPC = \frac{|NPC - NPC^*|}{NPC} \tag{3.17}$$

Furthermore, in order to stress the convergence of the algorithm and improve the NPC, convergence criteria on the power-dependent behaviour of BESS, modelled by the parameters $\alpha_{h,b}$ and $\beta_{h,b}$ were introduced. In two consecutive MILP optimizations, only the degradation parameters ($\alpha_{h,b}$ and $\beta_{h,b}$) are modified; therefore, when limited changes occur on these parameters, limited differences in the optimal design of the master MILP problem are expected; hence, this strengthened convergence criterion is supposed to provide more reliable solutions.

The relative change in the parameters $\alpha_{h,b}$ and $\beta_{h,b}$ is detailed in (3.18a)-(3.18c), describing the additional convergence criteria.

$$\Delta\alpha = \frac{\sum_{h,b} \left| \alpha_{h,b} - \alpha_{h,b}^* \right|}{\sum_{h,b} \alpha_{h,b}} \tag{3.18a}$$

$$\Delta\beta = \frac{\sum_{h,b} \left| \beta_{h,b} - \beta_{h,b}^* \right|}{\sum_{h,b} \beta_{h,b}} \tag{3.18b}$$

$$\Delta\alpha_{\overline{H}} = \frac{\left| \alpha_{\overline{H},b} - \alpha_{\overline{H},b}^* \right|}{\alpha_{\overline{H},b}} \tag{3.18c}$$

$\Delta\alpha$ and $\Delta\beta$ focus on the average absolute variation of the parameters, while $\Delta\alpha_{\overline{H}}$ evaluates the relative change in the battery energy degradation occurring at the end of the project. The rationale behind using the average criterion of $\Delta\alpha$ and $\Delta\beta$ instead of the maximum deviation is justified by the fact that stability issues may arise when a relative mipgap (tolerance on best integer objective) [78] higher than zero is adopted, which is extremely common when dealing with complex and computationally expensive problems. Indeed, it may happen that, in two consecutive iterations, the algorithm may replace the battery in the same day, but not exactly in the same hour, which may lead $\Delta\alpha$ up to $(\overline{\alpha_b} - \underline{\alpha_b})$ in the replacement hour, preventing the convergence of the procedure but with no significant effect in terms of optimality of the solution. By using the average absolute criterion, the above numerical instability is mitigated. Nevertheless, (3.18c) guarantees congruity in terms of residual capacity at the end of the project and, consequently, of time of replacement. In fact, even if the time of replacement slightly changes at convergence, the variation in the residual capacity would be negligible; therefore, equation (3.18c) increases the stability of the approach with respect to convergence criteria on the maximum difference at any hour.

3.4 Case study

3.4.1 Location and input data

The IMY methodology described in the previous section has been tested on a rural community based in Soroti, in central-east of Uganda (1.72N 33.6E), where a load assessment data collection campaign was performed and documented in [79] and detailed in Appendix B. Data on local availability of solar and wind power production have been acquired by means of the Renewable.ninja web platform [80,81].

To represent the multi-year behaviour of the proposed community and its hourly uncertainties, the load profile, shown in Figure 3.3, has been estimated by accounting for the dynamics of the social behaviour of the community over the considered time horizon (10 years), based on the results of the study on social dynamics following access to electricity in similar contexts developed in [72]. The LoadProGen tool [82], adopted in [79] to estimate the profile resulting from the data collected on field, has been run with different input data for each year, in order to reproduce the relative load growth estimated in [72], due to the growth in the users and the higher penetration of appliances; the latter was estimated by using the income percentiles for the community [83]. Users were grouped in 17 different classes (6 residential, 11 business activities and local services), whose size and number of appliances per customer grow over time; in particular, given the wide variety of appliances used by the community, the demand estimated in [79] is assumed to be referred to the last year of the project, then the profiles of the previous years are estimated by reproducing "backwards" the growth trends analysed in [72]. By using LoadProGen [82], 20 load profiles were calculated for every year of the simulation to assess the hourly uncertainties of the typical profile, which was calculated by averaging the 20 profiles. A Monte Carlo technique was used to draw the daily profiles of the entire year: a Gaussian noise was added to the daily average load, whose standard deviation equals the one calculated for the 20 different profiles of the corresponding year. The granularity of both renewable

generation and demand profiles is 1 hour.

The capital and maintenance costs of the different units are shown in Table 3.1 together with their maximum lifetime. A DG fuel cost of 0.75 €/l is considered. Table 3.2 shows the features of the selected Li-ion battery model. The parameters in Tables 3.1 and 3.2 were derived from a literature review and the author's experience. Realistic ranges of the power-to-energy ratio dependent characteristics were derived from the literature [84–86] and are provided in Table 3.3. Renewable asset degradation was included in the analysis by considering a 1% annual decay of PV panel [44], a 0.53% annual deterioration of wind turbines [45].
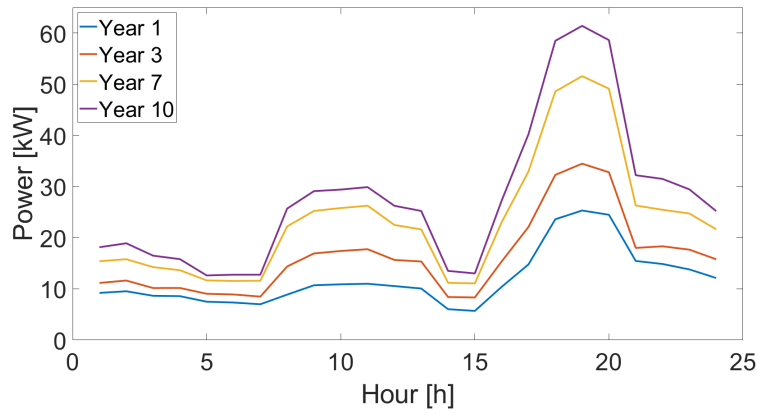
(a)
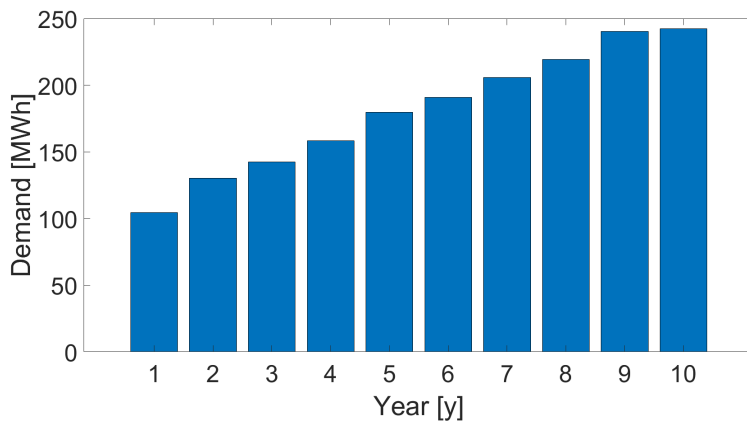
(b)

Figure 3.3: Estimated load profiles (a) and total yearly demand (b)

Table 3.1: Components costs and lifetimes [26, 28, 31, 32]

	Unit size	c_i	m_i	Lifetime
Photovoltaic panel	1 kW	1.1 k€	10 €/y	20 y
Wind turbine	10 kW	27 k€	810 €/y	20 y
Diesel generator	16 kW	11 k€	0.208 €/h	15,000 h
Battery	1 kWh	0.4 k€	10 €/y	15 y
Converter	1 kW	0.3 k€	0 €	20 y

Table 3.2: BESS specifications [25, 26, 86]

Nominal capacity of one BESS unit $\overline{C}_b$	1	kWh
Maximum power-to-energy ratio $\overline{PQ}_b$	1	kW/kWh
Depth of Discharge DOD_b	90	%
Initial State-of-Charge SOC_b^{init}	100	%
Minimum residual capacity before replacement $\underline{\alpha_b}$	80	%

Table 3.3: BESS characteristics depending on $PQ_{h,b}$ [84–86]

	$PQ_{h,b} \leq 0.2$	$0.2 < PQ_{h,b} \leq 0.6$	$PQ_{h,b} > 0.6$
$\eta(PQ_{h,b})$	99%	98%	95%
$n(PQ_{h,b})$	3500	3200	3000

3.4.2 Simulation parameters

When dealing with electrification projects in the Global South, it is advisable to consider a limited project duration with respect to the expected lifetime of the components to limit risks, given that many changes can arise in a newly electrified community. For this reason, a project lifetime of 10 years is considered. Moreover, as in these contexts a limited loss of continuity of service comes with almost null social cost, a yearly loss of load of 5% is admitted [25]. The discount factor d_h is computed based on an 8% nominal interest rate and a 2% expected inflation rate.

3.4.3 Test procedure

To prove the effectiveness of the method, the following models have been developed, tested and compared:

1. Iterative Multi-Year (IMY): the IMY iterative procedure, depicted in Figure 3.1, accounting for battery degradation and variable efficiency in a multi-year environment at an hourly time resolution.

2. One-Shot Multi-Year (OSMY): a standard literature-based methodology equivalent

to IMY but developed in a full MILP environment with no iterative algorithm.

3. IMY without battery details (IMYwoB): the IMY iterative method (IMY) without accounting for the battery degradation and variable efficiency. This simulation aims at highlighting the importance of considering the battery degradation since the planning phase.

4. IMY and OSMY with representative days (IMYrd/OSMYrd): in order to facilitate OSMYrd to converge and to be able to validate the results of IMY and OSMY, both IMY and OSMY are developed using 20 representative days (1 per season, with each year characterized by a rainy and a dry season in the area of interest).

5. Sensitivity on battery lifetime (IMY$\pm$25%): in order to evaluate the effects of the battery lifetime on the optimal design, a sensitivity analysis is performed by increasing and decreasing the lifetime of the battery ($n_{h,b}^{cyc}$) by $\pm$25%.

The convergence of the MILP optimization has been ruled by a maximum gap [78] of 3%, the tolerances of the external loop related to BESS behaviour (see (3.18)) have been all set to 1%, and the convergence criterion on the stability of the objective function (see (3.17)) has been fixed at 3%, coherently with the mipgap. A limit of 5 days has been set for the duration of the simulations. These values have been tailored according to the literature and experience of the author. It is worth noticing that information regarding the optimality gap is rarely disclosed, even if it plays a pivotal role in the tractability/accuracy trade-off. The optimal microgrid sizing is found in [73] and [87] by setting a 5% mipgap for a similar formulation; both the algorithms are run on one year with hourly time steps but no long-term phenomenon is taken into account. Nevertheless, the time employed by the two algorithms to converge is in the range of a few hours, comparable with the computational burden of the work presented here, which is characterized by a much larger size (1.66 million constraints and 1.31 million variables) and a lower mipgap.

The algorithm has been modelled in GAMS 24.0.2 and solved with CPLEX. The simulations have been run on a 6-core 3.20 GHz Intel Core i7 computer with 16 GB RAM.

3.5 Results

The main results of all the IMY tests are discussed in the following subsections. The main outcomes in terms of computational burden, objective function, cost components, sizing, BESS replacement year Y_b^{repl} and residual capacity at the end of the project $\alpha_{\overline{H},b}$ have been summarized in Tables 3.4 and 3.5.

3.5.1 The advantages of the iterative approach

The first noticeable result is that OSMY has not converged within the time limit of 5 days: CPLEX was still branching to find a first integer-feasible solution for the IMY problem; hence, no mipgap [78] was available. This underlines the complexity for standard MILP formulations to handle full multi-year planning problems, while the IMY approach discussed in this chapter successfully converged in 6.9 hours, reaching the target tolerances in 3 iterations. Therefore, the gain in terms of tractability of the algorithm is impressive,

Table 3.4: Optimization outputs (I)

	Time	NPC	IC	O&M	RC	RV
	[h]	[k€]	[k€]	[k€]	[k€]	[k€]
IMY	6.9	323	235	112	18	42
IMYwoB	4.4	278	271	86	14	93
OSMY*	>120	/	/	/	/	
IMYrd	$7.5 \ 10^{-4}$	306	225	104	16	39
OSMYrd	29.7	303	226	101	14	38
IMY-25%	16.2	341	146	181	51	37
IMY+25%	7.2	314	230	113	18	47

* No feasible solution found in the given time limit.

Table 3.5: Optimization outputs (II)

	PV	WT	DG	BESS	Y_b^{repl}	$\alpha_{\overline{H},b}$
	[kW]	[kW]	[kW]	[kWh]	[y]	[%]
IMY	91	/	16	215	/	83
IMYwoB	101	/	16	263	/	100
OSMY*	/	/	/	/	/	/
IMYrd	88	/	16	203	/	82
OSMYrd	86	/	16	214	/	82
IMY-25%	62	/	32	80	9	96
IMY+25%	89	/	16	209	/	86

* No feasible solution found in the given time limit.

and this confirms that the IMY iterative algorithm can easily contend with multi-year planning problems with power-dependent battery degradation and variable efficiency with low requirements in contrast to other standard techniques such as OSMY. Finally, the optimization IMYwoB, which neglects battery degradation and variable efficiency ($\alpha_{h,b} = 1$ and $\beta_{h,b} = 1$ in every time step), converged in 4.4 hours, which strengthens the robustness of IMY in reducing the requirements of one-shot methodologies.

Given that the results are characterized by a 3% mipgap, the comparison underlines the computational efficiency of the IMY method with respect to the literature [73,87].

3.5.2 Impact of BESS degradation on planning and operation

To evaluate the effects of the battery degradation and variable efficiency, the IMY methodology (IMY) is compared to IMYwoB, which neglects the above. The results show that NPC with IMY is approximately 16% higher than IMYwoB, which suggests that ne-

glecting such phenomena may lead to a suboptimal design of the system. As a matter of fact, in IMYwoB, the load is largely powered by renewable sources, especially during the first three years, due to a larger PV plant supported by higher storage capacity; as the load grows, the diesel production takes over, but its share never exceeds 34% of the total demand (see Figure 3.4a). With respect to IMY, this configuration comes with higher investment costs but limited O&M costs; moreover, as no battery degradation is accounted for, the components have high residual value at the end of the project and the replacement costs are only related to the DG working hours, as described by equation (4.5e). However, in real operation the battery degradation would reduce the capability of the system to defer the use of renewable production in compliance with the load needs; hence, increased reliance on the fuel generator or higher ENS are likely to occur.
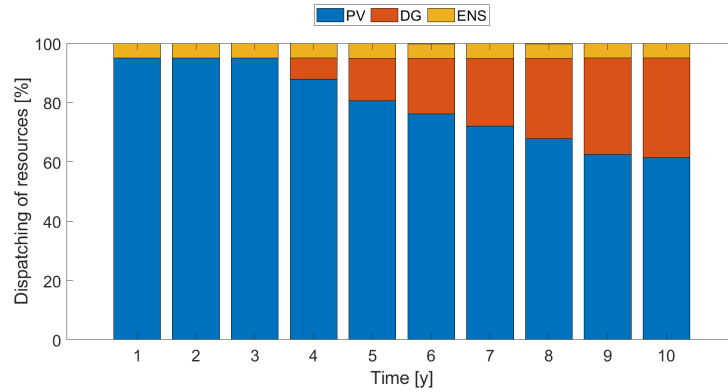
(a)
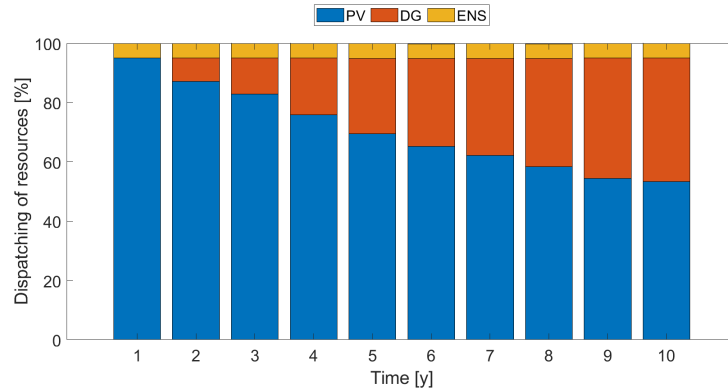
(b)

Figure 3.4: Dispatching of resources in IMYwoB (a) and IMY (b)

If the operation of the system resulting from IMYwoB is optimized considering BESS degradation and variable efficiency, the total investment rises from 278k€to 327k€. There-
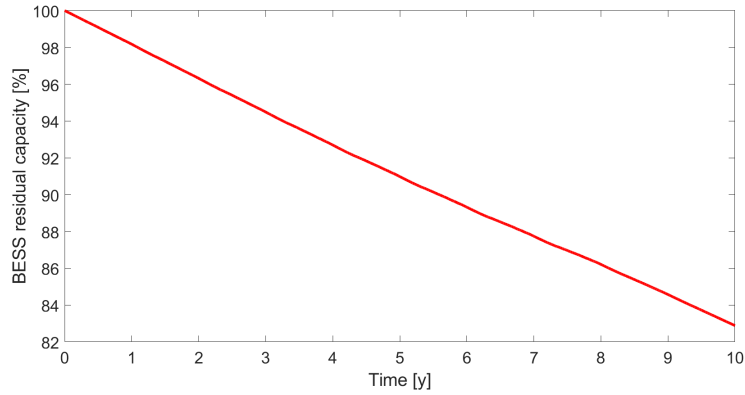
Figure 3.5: Storage capacity degradation in IMY

fore, if a developer neglects this aspects would end up with 18% more costs than expected, which may jeopardize the success of the project. By considering battery degradation and variable efficiency since the planning phase as in IMY, the result will be tailored to the actual system's behaviour; in fact, the optimizer tends to employ more DG and to leave a less prominent role to PV and BESS, whose size is reduced by 10% and 18%, respectively, and which are able to cover autonomously only the load of year 1 (see Figure 3.4b). In the last year of the project, PV panels are only providing energy to 53% of the demand, compared to the 61% of IMYwoB. Now, the NPC is 16% higher, characterized by a more consistent portion of O&M costs, approximately 30% higher than the O&M in IMYwoB and mainly related to fuel consumption, while the initial investment is reduced by 13%.

The results show that the model tends to avoid the replacement of the battery: the net capacity level at the end of the optimization period (83%) is very close to the replacement threshold (80%), as shown in Figure 3.5. Hence, the accurate modelling of the storage behaviour has a strong impact on the optimization results, as the system gradually ends up working with a way smaller BESS availability.

The trend of fuel consumption along the years in the two tests is compared in Figure 3.6: in both cases, the growing utilization of diesel generators follows the increase in the demand, but the degradation of BESS in IMY makes the use of DG necessary two years in advance. Furthermore, the use of discounted cash flows for NPC evaluation induces the optimizer to favour outflows in the late years, leaning towards a more frequent utilization of diesel units, rather than oversizing the renewable plant and the storage capacity, which explains the delay in the employment of DG in both cases. The local wind availability is not sufficient to induce the optimizer to consider the installation of wind turbines, neither in IMY nor IMYwoB.

3.5.3 Stability and computational efficiency of the results

To highlight the good convergence performances of the IMY algorithm, IMY has been run for 5 additional iterations after the convergence criteria were met, and the corresponding
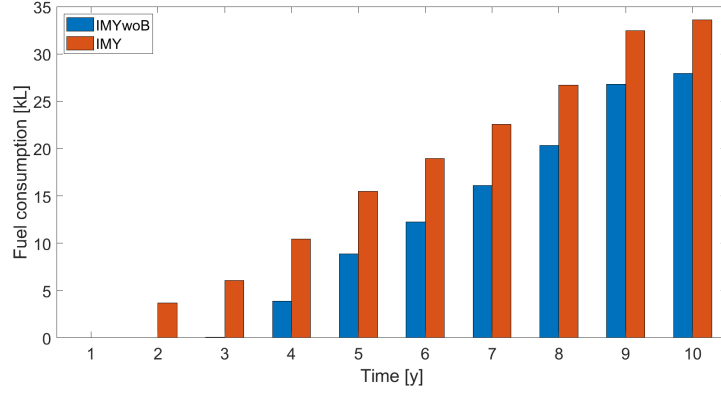
Figure 3.6: Fuel consumption in IMYwoB and IMY

behaviour of the convergence parameters and of the objective function are shown in Figure 3.7. It is worth noticing that the value of the objective function is stable after 3 iterations as well as parameters $\alpha_{h,b}$ and $\beta_{h,b}$. This is the reason why the corresponding relative changes, namely, ΔNPC, $\Delta\alpha$ and $\Delta\alpha_{\overline{H}}$, fall below the convergence threshold in few iterations and the procedure stops. The large NPC error of the first iteration occurs because the first MILP is initialized with no battery degradation; hence, the sizing corresponds to the output of IMYwoB. Starting from the second iteration, the effects of battery degradation and variable efficiency commence and PV and BESS are downsized, and the reliance on diesel increases. Along the iterative procedure, the available DG power remains constant and the number of PV and BESS units installed undergoes slight oscillations. The convergence is reached not only when the final sizing is attained, but also when the algorithm selects the optimal operation of the installed components. The IMY convergence criteria meet both: ΔNPC accounts for the total project costs, considering both the investment and operating costs, while $\Delta\alpha$ and $\Delta\beta$ focus on the operating effects. In the IMY simulations, battery degradation has a more significant impact than variable efficiency. $\Delta\alpha$ parameters experience a larger dynamic than $\Delta\beta$, as shown in Figure 3.7, which can be explained by the fact that the hourly power-to-energy ratio $PQ_{h,b}$ usually stays below the 0.2 threshold since it is profitable to install a large battery to be operated at low power levels to perform time-shifting of the energy produced by the PV source.

3.5.4 Validation of the procedure

As OSMY could not find a feasible solution, the quality of the results obtained with the IMY methodology are validated using typical days, to reduce the total computational burden and to be able to compare the outputs of the two procedures. The results reported in Tables 3.4 and 3.5 highlight that when representative days are used, the IMY methodology (IMYrd) and the one-shot one (OSMYrd) converge towards similar designs and values of the objective function; small differences are justified by the 3% mipgap. It is worth noticing that the error in terms of NPC is below 1% and the difference in terms of installed com-
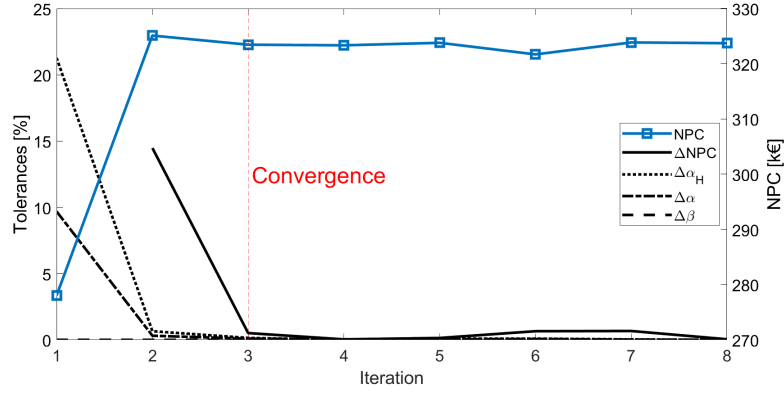
Figure 3.7: Evolution along the procedure's iterations of the convergence criteria and of the objective function

ponents is very limited. Despite the low number of representative days, the computational requirement of OSMYrd is still very high (more than 1 day), while IMYrd requires a few seconds to converge, which emphasizes the advantages and benefits of the IMY approach, as already discussed. Furthermore, the results obtained with IMYrd and OSMYrd are also similar to the values of IMY and OSMY, which strengthens the quality of the approach, but IMY is still preferable to OSMYrd, given its faster convergence and its higher capability of describing the real dynamics of the system; in fact, NPC with IMY is 6.7% higher than that with OSMYrd. However, methodologies with representative days, such as IMYrd, can be useful tools for preliminary designs and for initializing the full model, given their low computational requirements.

In order to generalize the validity of the approach, further simulations comparing IMYrd and OSMYrd on different test cases are presented in Appendix C, confirming the advantages of the proposed algorithm over traditional methods. In particular, the procedure is applied to St. Mary's Lacor hospital, Uganda, and Ngarenanyuki secondary school, Tanzania. The two load profiles derive from on-site measurement campaigns and have completely different shapes and peaks with respect to the master case study of Soroti, as they refer to peculiar services rather than a traditional mix of residential and income-generating activities. As the three case studies are located in different areas, the availability of renewable resources changes. Hence, this further validation increases the robustness of the analysis, as it confirms the reliability and the computational efficiency of the IMY approach, regardless of the input profiles.

3.5.5 Sensitivity analysis on BESS degradation parameters

Since battery lifetime is a critical element in planning phases, subject to significant uncertainties, a sensitivity analysis on the BESS lifetime parameters has been performed, and the results are shown in Tables 3.4 and 3.5. As expected, the higher the battery lifetime, the lower the total NPC, as in the test IMY+25% (lifetime 25% higher than IMY), the

NPC is 2.8% lower than IMY, while it increases by 5.6% in IMY-25%. The IMY-25% configuration is the only scenario in which the battery capacity drops below 80% and is replaced at year 9. Its more intense utilization is given by the fact that a much smaller storage bank is installed, together with a reduced PV capacity, compensated by the adoption of two diesel generators (only one is installed in all the other test cases). Therefore, the battery lifetime reduction has a significant impact on both the initial design and the dispatch of resources, leaning much more heavily on fuel use.

These results suggest how the cost of using batteries with a lower lifetime is higher than the benefit of increasing the lifetime by the same amount, and it underlines the great importance and urgency of developing a planning methodology able to cope with battery degradation in real applications. The above achievement is also enforced by the low computational requirements of the approaches, as shown in Table 3.4.

3.6 Conclusion

The novel IMY procedure proposed in this study, based on an iterative approach with an internal MILP core, successfully addresses the planning of a rural off-grid microgrid with a detailed multi-year horizon at an hourly time resolution. This approach enables analysing the dynamics of load growth, RES degradation and storage capacity reduction with its power-dependent efficiency throughout the entire project lifetime, with significant benefits for developers.

The IMY approach has been compared to traditional methods, validation tests have been performed by using representative days and alternative input profiles, and a sensitivity analysis over the battery lifetime has also been discussed. The results highlight significant improvements with respect to the equivalent literature-based one-shot MILP. The great advantage of the new method derives from outsourcing the calculations related to battery behaviour to an external loop, which reduces the computational requirements without affecting the quality of the results, as discussed in the IMY validation. Representative days can be used in preliminary analyses for rough evaluations, but the full methodology IMY in this chapter is recommended for the advanced design, given the higher accuracy of the results. Dedicated simulations highlight that neglecting the effects of battery degradation and power-dependent efficiency can lead to underestimating the cost of the system even by 16%, which may lead to sub-optimal allocation of resources and, most likely, energy shortages and financial issues. Similarly, the sensitivity over the battery lifetime has proven the battery to be a critical component, which can be accurately taken into account by the IMY approach.

This methodology is expected to significantly enhance the current state of the art in planning algorithms, including the non-linear constraints of the dynamics of the battery. In particular, it can be implemented in real case studies and sizing tools so that developers can benefit from more accurate simulations of the system behaviour, thus having a more appropriate understanding of the financial and technical requirements of their investments. The approach can be easily adapted to different system configurations and typologies.

Chapter 4

Holistic multi-objective optimization

4.1 Introduction

This chapter focuses on improving the decision making process, extending the algorithm presented in Chapter 3 into a multi-objective optimization evaluating economic, environmental and social decision criteria.

Multi-objective optimization has proven to enable assessing the trade-offs between different decision criteria in the energy sector, in particular for rural electrification projects [57,58], where different types of stakeholders with different priorities may be involved (companies, public institutions, NGOs) and a thorough analysis of the relationships between the economic, environmental and social impacts on the community is required [60]. The corresponding output, typically being a Pareto frontier, provides the decision maker with a more comprehensive view of the outcomes of their choices so that more informed decisions can be taken, also based on cultural and site-specific characteristics which could hardly be described within the algorithm. Moreover, when dealing with rural areas, scarcity of information is often an issue hindering the effective calibration of a single-objective optimization including several decision criteria, which entails the identification of weights or bounds, heavily influencing the final solution [88,89].

Only few microgrid planning tools extended the traditional techno-economic optimization including a wider decision-making process (see Table 2.1). Hence, it is timely and useful to develop a multi-objective planning methodology able to address economic, social, and environmental objectives, besides accounting for the multi-year characteristics of the project and including the degradation model of the assets. On the other side, in order to tackle the increased complexity in planning methodologies, it is also important to develop novel techniques to more efficiently address multi-objective optimization, especially within the scope of MILP algorithms, that guarantee very good quality of the results but may incur prohibitive computational burdens in case of particularly complex problems.

This chapter summarizes in Section 4.2 the state of the art concerning multi-objective MILP optimizations and describes in Section 4.3 the main advancements provided by

this work in terms of multi-objective methodologies and applications to energy systems. Section 4.4 recalls the main basic concepts on multi-objective optimization, ε-constraint method and AUGMECON2, while Section 4.5 presents the novel Advanced AUGMECON2 (A-AUGMECON2) developed in this work. The application of A-AUGMECON2 to a rural microgrid planning problem is introduced in Section 4.6, that describes the objective functions adopted as decision criteria and pertaining the scope of economic, environmental and social sustainability of the project. Section 4.8 discusses the data employed for the numerical simulations. The results of the procedure are presented in Section 4.9, where the resulting Pareto frontier is compared to the one deriving from the standard AUGMECON2, highlighting the significant savings of computational time and density of the frontier. The trade-offs between the different objectives and the decision making process are discussed. Final considerations are reported in Section 4.10.

4.2 Multi-objective approaches and AUGMECON2

In the scope of Mixed Integer Linear Programming (MILP) optimization, which is the formulation adopted in this study, the most common approaches to solve multi-objective problems are the weighted sum method [90,91] and the ε-constraint method [92–94]. The latter has the advantage of being able to represent the entire Pareto frontier independently of its shape; moreover, its results are not influenced by normalization issues and it generally has better computational performances [88,89]. In particular, the Improved Augmented ε-constraint Method (AUGMECON2) has been developed as an advancement of the traditional ε-constraint method [95,96] and, currently, it is a well consolidated approach, widely adopted to solve a diverse portfolio of problems in the energy sector [93,94,97,98].

However, AUGMECON2 presents two interrelated drawbacks: (1) when complex algorithms with more than two objective functions are optimized, the computational burden may become extremely large because of the presence of redundant iterations; (2) the higher the desired resolution of the Pareto frontier, the more the redundant points. The former issue needs an enhancement of the methodology, while the latter, which is related to the readability of the results and the choice of the final point, could be faced by one of the post-Pareto selection methods available. These can be grouped into three major categories: offline pruning algorithms to reduce the number of Pareto points [99,100]; clustering algorithms to identify and group similar solutions [101]; mathematical methods to select a single final point [102,103]. This additional step requires further computational resources, thus exacerbating the first issue.

Most of the recent literature still considers AUGMECON2 as the most up-to-date and efficient development of the ε-constraint method, as proven by its recent use in a wide variety of scientific literature also beyond the energy sector [104,105]. The very first efforts in advancing the methodology have been proposed in [106], partially addressing the issue of redundant optimizations. Nonetheless, the scope of [106] is limited to a theoretical approach applied on a test knapsack problem to highlight the efficiency of the algorithm, yet the performances of AUGMECON2 could be further improved.

Hence, the AUGMECON2 method is selected as the best option available in the literature to solve the MILP multi-objective multi-year optimization under study, and its two main shortcomings are faced by developing a novel methodology, aimed at providing better

computational performances and improved readability of the Pareto frontier by means of an online filter of redundant optimizations.

4.3 Contributions

The proposed modified version of AUGMECON2, here denoted as A-AUGMECON2, goes beyond the state of the art both in terms of advancements of the mathematical properties of the algorithm, fully addressing the issue of redundant simulations, and in terms of practical application of such novel approach, being it its first application to energy systems. Moreover, this is the first study providing such a comprehensive evaluation of rural microgrid projects, discussing both the multi-objective and multi-year features of the problem. In short, the main novelties presented in this chapter are listed below.

1. Development of a multi-objective multi-year planning methodology able to efficiently optimize and simulate the operation of the entire lifetime of a project, using economic (Net Present Cost), social (Job Creation and Public Lighting), and environmental (Life cycle emissions and Land use) objective functions.

2. Development of the A-AUGMECON2 methodology that reduces the computational requirements of the standard AUGMECON2, using a novel pruning algorithm that avoids the simulation of redundant iterations and enables the introduction of the first novelty while keeping a good tractability of the algorithm.

4.4 Multi-objective optimization

A generic multi-objective optimization can be expressed as follows:

$$
\begin{aligned}
\max \quad & f(\mathbf{x}) = [f_1(\mathbf{x}), f_2(\mathbf{x}), ..., f_p(\mathbf{x})]^T \\
s.t. \quad & y_i(\mathbf{x}) \leq 0 \qquad i \in 1...m \\
& h_l(\mathbf{x}) = 0 \qquad l \in 1...q \\
& \mathbf{x} = [x_1, x_2, ..., x_n]^T
\end{aligned}
\tag{4.1}
$$

where $f(\mathbf{x})$ is the p-dimensional vector of objective functions, defined by the n-dimensional vector of decision variables $\mathbf{x}$. The problem is subject to m inequality constraints and q equality constraints. For the sake of simplicity, a problem where all objective functions are maximized is described, but the same considerations stand also for minimization or mixed maximization/minimization problems.

The goal of multi-objective optimizations is to find the solutions of the Pareto frontier, which is composed by the set of so-called non-dominated points, i.e. solutions in which the performance of one objective function cannot be improved without worsening at least one other objective function [89, 107].

4.4.1 ε-constraint method

Classic formulation

One of the most common and efficient techniques for solving multi-objective problems is the ε-constraint method [89], where the multi-objective problem is transformed into several single-objective optimization problems, as shown in (4.2), by using an iterative approach. In particular, only the first objective function is optimized, while the others are constrained to be higher than a constant value e_k^{it}, which is modified in every iteration it. By varying e_k^{it} between the maximum $(\overline{e}_k)$ and minimum $(\underline{e}_k)$ values of each objective function, calculated beforehand, the procedure is able to calculate the Pareto frontier [89, 107]. It is worth noticing that the maximum and minimum values of e_k^{it} are calculated before solving (4.2), by performing p preliminary optimization problems corresponding to the maximization of each $f_k(\mathbf{x})$ one at a time, disregarding the other $f_{j \neq k}(\mathbf{x})$. The results are stored in the payoff table and upper and lower bounds for each objective function are identified.

$$
\begin{aligned}
\max \quad & f_1(\mathbf{x}) \\
s.t. \quad & f_2(\mathbf{x}) \geq e_2^{it} \\
& f_3(\mathbf{x}) \geq e_3^{it} \\
& ... \\
& f_p(\mathbf{x}) \geq e_p^{it} \\
& y_i(\mathbf{x}) \leq 0 \qquad i \in 1...m \\
& h_l(\mathbf{x}) = 0 \qquad l \in 1...q \\
& \mathbf{x} = [x_1, x_2, ..., x_n]^T
\end{aligned}
\tag{4.2}
$$

As typically done, the parameters e_k^{it} span between $\overline{e}_k$ and $\underline{e}_k$ with a uniform distribution divided into g_k intervals and $(g_k + 1)$ points, with a resolution of $step_k = \frac{r_k}{g_k}$, where $r_k = \overline{e}_k - \underline{e}_k$ represents the range of variation of the objective function k. With this formulation, each optimization (4.2) is carried out on a specific subspace of the search space, which can be described as a p-dimensional matrix of points. For every iteration it, the values of parameters e_k^{it} can be calculated as $e_k = \underline{e}_k + i_k^{it} \cdot step_k$, where $i_k^{it} \in \{1, ..., g_k+1\}$ is the integer value representing the current position in the grid.

The total number of points in the grid is $(g_2+1) \cdot (g_3+1) \cdot ... \cdot (g_p+1)$, which leads to an exponential behaviour. Therefore, the computational complexity can be very challenging as the number of objective functions increases.

When the optimization of a grid point leads to a better performance with respect to the thresholds forced by the vector $\mathbf{e}$, all the optimizations with intermediate positions of $\mathbf{e}$ will be characterized by very similar results (exactly the same Pareto point in case of null optimality gap [78]). Moreover, the information from initial optimizations used to identify the limits of the e_k^{it} parameters ($\overline{e}_k$ and $\underline{e}_k$) is not used in the main iterative algorithm (4.2). This means that the standard ε-constraint method can lead to a large number of redundant optimizations that significantly increases the computational requirements, without adding any insight.

AUGMECON2

The augmented ε-constraint method, a significant improvement of the ε-constraint method, was proposed by Mavrotas and named AUGMECON2 in its most recent development [95, 96]. Conversely to the classic approach in which the extreme values ($\overline{e}_k$ and $\underline{e}_k$) of the objective functions are calculated by simply optimizing one objective function at a time, AUGMECON2 makes use of lexicographic optimization for every objective function: problem (4.3), with J initially empty, is sequentially solved over the set of p objective functions by adding at the end of every iteration the constraint $(f_j(\mathbf{x}) \geq \hat{f}_j)$ updating J, with $\hat{f}_j$ objective function value resulting from the previous iteration. This guarantees that the forthcoming optimization does not deteriorate the optimality of the previous objective functions, as $\hat{f}_j$ represents the best value of objective function j. This limits the search space only to Pareto optimal solutions. The procedure is solved p times, covering the entire set of objective functions, for a total of p^2 optimization problems to solve.

$$
\begin{aligned}
\hat{f}_k = \max \ & f_k(\mathbf{x}) \\
s.t. \quad & f_j(\mathbf{x}) \geq \hat{f}_j \qquad j \in J \\
& y_i(\mathbf{x}) \leq 0 \qquad i \in 1...m \\
& h_l(\mathbf{x}) = 0 \qquad l \in 1...q \\
& \mathbf{x} = [x_1, x_2, ..., x_n]^T
\end{aligned}
\tag{4.3}
$$

Moreover, problem (4.2) is modified as follows, where $\mathbf{s} = [s_2, s_3, ...s_p]^T$ is the vector of slack variables introducing a penalty when objective functions do not correspond to their desired values e_k^{it}; *eps* is an adequately small number:

$$
\begin{aligned}
\max \quad & (f_1(\mathbf{x}) + eps \cdot (s_2/r_2 + 10^{-1} \cdot s_3/r_3+ \\
& + ... + 10^{-(p-2)} \cdot s_p/r_p)) \\
s.t. \quad & f_2(\mathbf{x}) - s_2 = e_2^{it} \\
& f_3(\mathbf{x}) - s_3 = e_3^{it} \\
& ... \\
& f_p(\mathbf{x}) - s_p = e_p^{it} \\
& y_i(\mathbf{x}) \leq 0 \quad i \in 1...m \\
& h_l(\mathbf{x}) = 0 \quad l \in 1...q \\
& \mathbf{x} = [x_1, x_2, ..., x_n]^T
\end{aligned}
\tag{4.4}
$$

This configuration of the objective function allows avoiding weakly efficient points. Moreover, to partially reduce the above stated problem of the presence of redundant points, the ratio $s_2/step_2$ is exploited to bypass the redundant iterations of the innermost loop only, i.e., the loop on e_2. This is a significant limitation that would lead to a considerable increase in computational requirements when more than two objective functions are used.

4.5 The novel methodology: A-AUGMECON2

Even if AUGMECON2 is one of the most efficient multi-objective methodologies, the computational burden is still a big issue, especially for computationally intensive algorithms like multi-year microgrid planning problems; hence inefficiencies, such as redundant simulations, shall be preemptively removed.

In AUGMECON2, the number of grid points to be analysed grows exponentially with the number of objective functions and with the desired density of solutions on the Pareto curve. Moreover, the curve tends to present conglomerates of almost identical points, not of interest for the decision maker. This is due to the fact that the very valuable information contained in the slack variables is only used by AUGMECON2 to bypass redundant points on the innermost loop.

A-AUGMECON2, whose source code is publicly available (see Appendix D), tackles the problem by limiting the calculation of points only to those whose embedded information is worth to be included in the curve, thus reducing the computational time.

Two main actions allow limiting the number of points computed:

1. Redundant simulations are preemptively recognized and not performed for all objective functions: slack variables **s** are used to identify the redundant grid points.

2. Redundant simulations corresponding to the points obtained to draw the extreme points ($\bar{e}_k$ and $\underline{e}_k$) of the search space are not repeated.

4.5.1 Payoff table

The priority order adopted in AUGMECON2 for the lexicographic optimization of the payoff table, does not reflect the optimization order used in the iterative algorithm for the creation of the Pareto frontier; hence, payoff table points cannot be used to remove simulations in the following step. Conversely, the priority among the objective functions is designed in A-AUGMECON2 to reflect the procedure of the iterative loop and avoid redundant optimizations.

To achieve this, the priority order of the objective functions in the lexicographic optimization needs to be modified in such a way that, instead of simply following the order in which the objective functions are listed in the set as in AUGMECON2, once the k-th objective function with the highest priority has been optimized, the second highest priority is attributed to $f_1(\mathbf{x})$; after these two rounds, the rest of the objective functions can be sequentially optimized following the order in which they are listed in the set. As in AUGMECON2, constraints are added at the end of every iteration to prevent the optimizer from worsening the optimality of the previous solutions. The mathematical description is detailed in Algorithm 1.

For the sake of clarity, Table 4.1 compares the order followed in the lexicographic optimization for the computation of the payoff table in AUGMECON2 and A-AUGMECON2, in the case of p=3 objective functions. While the former simply follows the order in which the objective functions are listed in the pertaining set, the latter employs Algorithm 1 to always have f_1 as second highest priority (apart from the first optimization, in which it is optimized as first). The A-AUGMECON2 approach allows obtaining a payoff table that contains points belonging to the Pareto curve; those points can be automatically included

---

Algorithm 1 Defining the bounds with the new priority order for lexicographic optimization.

1: **for** $k \in \{1, 2, ..., p\}$ **do**
2:     **for** $kk \in \{1, 2, ..., p\}$ **do**
3:         **if** $kk = 1$ **then**
4:             Solve (4.3) with $f_{j=k}(\mathbf{x})$ obj. function; store solution $\hat{f}_{k,k}$
5:         **else if** $kk \leq k$ **then**
6:             Solve (4.3) with $f_{j=kk-1}(\mathbf{x})$ obj. function; store solution $\hat{f}_{k,kk-1}$
7:         **else**
8:             Solve (4.3) with $f_{j=kk}$ obj. function; store solution $\hat{f}_{k,kk}$
9:         Add constraint $f_j(\mathbf{x}) \geq \hat{f}_j$
10:     Save final solution into payoff table
11: Calculate bounds: $\underline{e}_k = \min_{\hat{k} \in \{1..p\}} \hat{f}_{\hat{k},k}$ and $\overline{e}_k = \max_{\hat{k} \in \{1..p\}} \hat{f}_{\hat{k},k}$

Table 4.1: Priority order in lexicographic optimization for $p=3$, in AUGMECON2 and A-AUGMECON2.

	AUGMECON2			A-AUGMECON2		
$it=1$	$f_1 \to$	$f_2 \to$	f_3	$f_1 \to$	$f_2 \to$	f_3
$it=2$	$f_2 \to$	$f_3 \to$	f_1	$f_2 \to$	$f_1 \to$	f_3
$it=3$	$f_3 \to$	$f_1 \to$	f_2	$f_3 \to$	$f_1 \to$	f_2

in the final results, thus avoiding their re-optimization in the iterative procedure to build the Pareto frontier.

Moreover, the hard constraints on the objective functions introduced by the sequential optimizations (see line 9 of Algorithm 1) are turned into soft constraints, i.e., penalties are associated to the differences from the desired values $\hat{f}_j$, in order to avoid infeasibilities that may occur in case of non-null optimality gap [78].

4.5.2 Building the Pareto frontier

The procedure to find the efficient solutions is shown in Figure 4.1 and described in this section.

First, the payoff table is completed and the ranges of variation r_k of objective functions $f_2(\mathbf{x}), ..., f_p(\mathbf{x})$ are divided into g_k intervals to identify the grid of $(g_2+1) \cdot (g_3+1) \cdot ... \cdot (g_p+1)$ points, corresponding to the maximum number of iterations to be performed, as detailed in the previous section. Then, after the initialization of given indices, the main iterative loop starts.

In order to improve the computational performances and the readability of the results, an online filter skipping the redundant points is implemented in every iteration. Each point is associated with a parameter $v_{\mathbf{i}}$, where $\mathbf{i} = [i_2, ..., i_p]^T$ is the position vector of the point
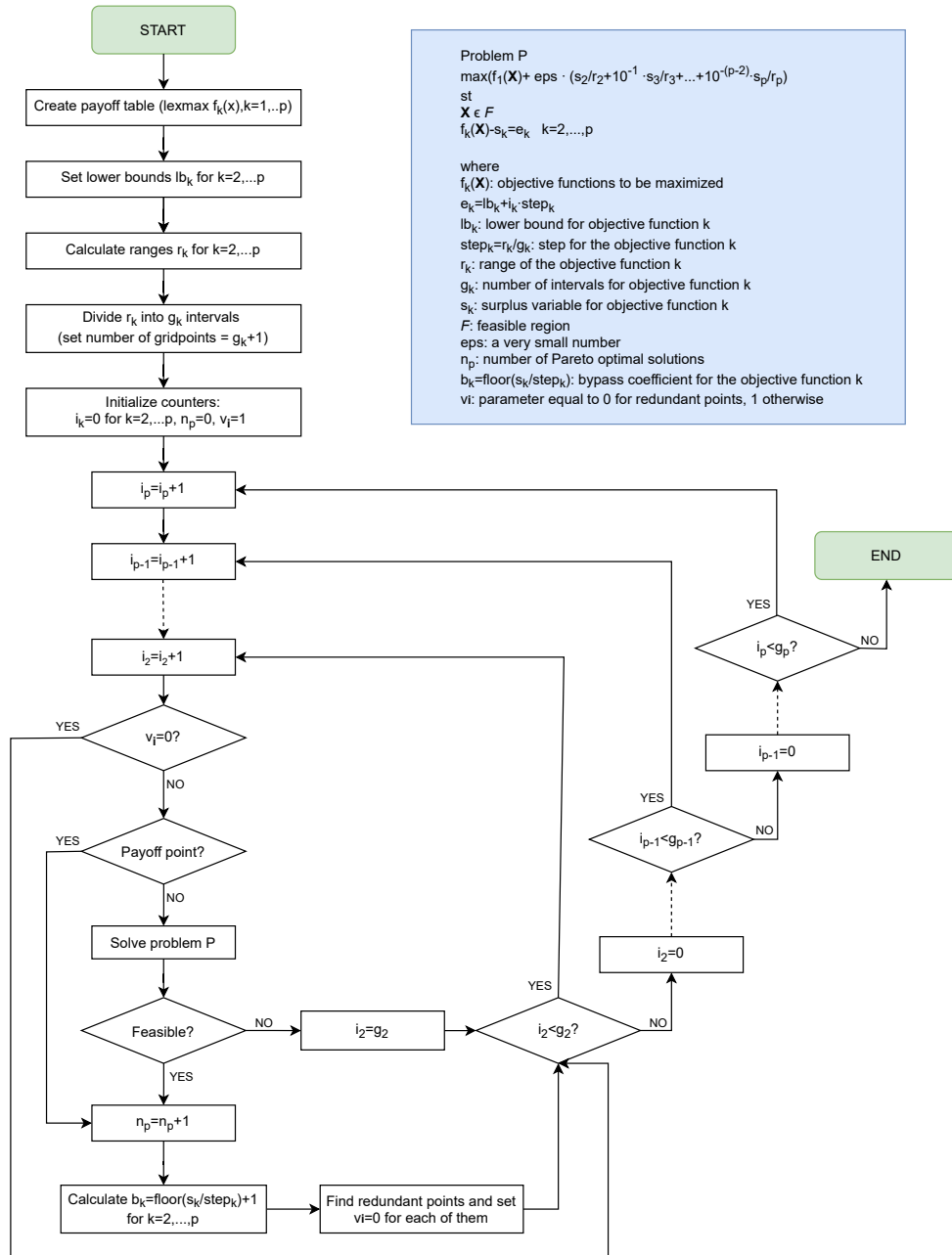
Figure 4.1: Flowchart of the proposed methodology.

in the grid. The parameter has value 1 if the point shall be analysed, 0 if it shall be skipped. At the beginning of the procedure, the vector $\mathbf{v}$ of all $v_{\mathbf{i}}$ is initialized to analyse all points (vector of ones).

The optimization of a given iteration is performed only if the corresponding $v_{\mathbf{i}}$ equals 1 and if the position of the point in the grid does not correspond to a point already calculated in the payoff table. If this last condition occurs, the results obtained from the lexicographic optimization to form the payoff table, as per Section 4.5.1, are directly included in the Pareto frontier, thus avoiding the repetition of its calculation.

When the current iteration corresponds to a non-redundant solution, then the optimization is performed and the outcome is collected; when a non-feasible solution is returned, points characterized by more stringent thresholds are skipped, as they are expected to provide non-feasible solutions, too.

When a feasible solution is obtained, it is stored in the repository of the Pareto curve and the result is analysed to evaluate whether some redundant simulations shall be removed by setting the corresponding $v_{\mathbf{i}} = 0$. To do so, the bypass coefficient $b_k = floor(s_k/step_k) + 1$ is computed for $k = 2, ..., p$, where $floor(\cdot)$ returns the integer part of the number. Then, Algorithm 2 is adopted to determine all the N_{comb} combinations of $i_2, ..., i_p$ identifying the points of the grid that would produce a similar result, where $comb$ and Δi_k are parameters and $mod(\cdot)$ is a function that returns the remainder of the division. The parameter $v_{\mathbf{i}}$ of the N_{comb} redundant points is set to zero.

Algorithm 2 Defining the positions of redundant points.

1: $b_k = floor(s_k/step_k) + 1,\ k \in 1, 2, ..., p$
2: $N_{comb} = \prod_{k=2}^{p} b_k$
3: **for** $comb \in 0, ..., N_{comb} - 1$ **do**
4:      **for** $k \in 2, ..., p$ **do**
5:          $\Delta i_k = mod(comb/b_k)$
6:          $comb = floor(comb/b_k)$
7:          $i_k = i_k + \Delta i_k$
8:      $v_{\mathbf{i}} = 0$

Finally, the parameters $i_2, ..., i_p$ are updated to move forward in the grid. The procedure stops when the condition $i_k = g_k + 1$ holds for $k = 2, ..., p$.

For the sake of clarity, Figure 4.2 illustrates the procedure in presence of redundant optimizations for the case of $p=3$ objective functions, where $f_1(\mathbf{x})$ is optimized, while $f_2(\mathbf{x})$ and $f_3(\mathbf{x})$, both varying in the range 1÷4, are turned into constraints. Point U_{it}, identified by the green square, is the grid element to be analysed. It lies in position $\mathbf{i}_U = [2, 1]$, i.e., problem (4.4) is subject to the constraints $(f_2(\mathbf{x}) - s_2 = 2)$ and $(f_3(\mathbf{x}) - s_3 = 1)$. As $v_{\mathbf{i}_U} = 1$, the optimization is not redundant and must be carried out. The problem corresponding to the grid point U_{it} is solved; the results, shown in Figure 4.2, are characterized by $s_2 = 1$ and $s_3 = 2$. Applying Algorithm 2, $v_{\mathbf{i}}$ is set to zero for $N_{comb} = 6$ points, including the current grid point and 5 redundant iterations, represented as red dots in Figure 4.2. Then, the grid is crossed in the direction of the blue arrow, according to the order in which objective functions are listed in the related set, i.e. along f_2 first, then along f_3. Therefore, the next point to be analysed is U_{it+1}.
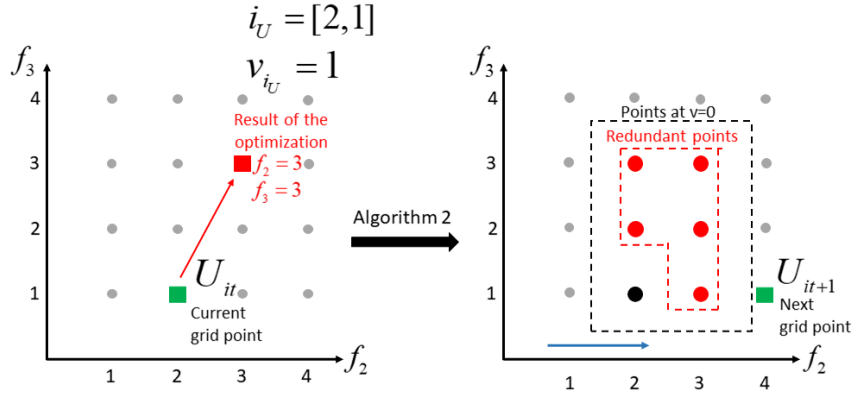
Figure 4.2: Procedure to skip redundant optimizations in case $p=3$.

4.6 Objective functions

The following set of objective functions is a valid representative of a holistic decision-making process, as it evaluates indicators pertaining to all the three dimensions of sustainability, namely economic, environmental and social, but it is not the only one possible. Depending on the type of stakeholders involved, there should be a preliminary discussion identifying the most pressing needs, in order to define the appropriate set of objective functions which reflect such necessities.

The algorithm has been tested on an unelectrified area in Soroti, Uganda, and the following objective functions have been considered relevant for a generic consortium involving public bodies: minimization of the net present cost, providing insights on the economic sustainability of the investment; minimization of CO_2 lifecycle emissions to account for global environmental impact and compliance with national targets on decarbonization of the power sector; minimization of land occupation to account for local environmental impact in an area with limited space availability; maximization of local job creation, providing insights on direct socio-economic development opportunities; maximization of street lighting to account for improvement in safety and social life.

4.6.1 Economic impact

Net Present Cost

As for microgrid investments, the Net Present Cost is typically considered as economic objective function to be minimized [25, 32]. It is adopted in Chapter 3 and its formulation is here reported in equations (4.5a)-(4.5h) for the sake of simplicity. It takes into account the investment costs IC_i, the operation and maintenance charges $O\&M_i$, the replacement costs RC_i of batteries and diesel generators (the other components are assumed to have service life longer than project duration), and the residual values RV_i of the assets at the end of the project lifetime. Given the cumulative modelling of DG replacement charges as

in (4.5e), there is no need to consider DG residual value.

$$\min NPC = \sum_i (IC_i + O\&M_i + RC_i - RV_i) \tag{4.5a}$$

$$IC_i = N_i \cdot c_i \tag{4.5b}$$

$$O\&M_{i\backslash\{g\}} = N_i \cdot m_i \cdot \sum_{y=1}^{\overline{Y}} d_{H \cdot y} \tag{4.5c}$$

$$O\&M_g = \sum_{h=1}^{\overline{H}} d_h \cdot (m_g \cdot U_{h,g} + f \cdot FC_{h,g}) \tag{4.5d}$$

$$RC_g = \frac{c_g}{H_g^{life}} \cdot \sum_{h=1}^{\overline{H}} d_h \cdot U_{h,g} \tag{4.5e}$$

$$RC_b = N_b \cdot c_b \cdot \sum_{h=1}^{\overline{H}} d_h \cdot (k_{h,b} - k_{h-1,b}) \tag{4.5f}$$

$$RV_{i\backslash\{g,b\}} = d_{\overline{H}} \cdot \rho_{h,i} \cdot N_i \cdot c_i \frac{Y_i^{life} - \overline{Y}}{Y_i^{life}} \tag{4.5g}$$

$$RV_b = d_{\overline{H}} \cdot N_b \cdot c_b \cdot \frac{\alpha_{\overline{H},b} - \underline{\alpha_b}}{\overline{\alpha_b} - \underline{\alpha_b}} \tag{4.5h}$$

4.6.2 Environmental impact

Emissions

Environmental objectives have been increasingly included in energy projects planning, due to climate change concerns. To perform an accurate evaluation of the microgrid global impact, emissions have been considered in the proposed methodology in terms of Life Cycle Assessment (LCA), i.e., accounting for construction, installation, operation and disposal of the assets. The minimization of total emission allows to evaluate solutions in line with the increasing pressure of governments for high shares of renewables. The mathematical formulation of CO_2 emissions is reported in (4.6a), where $CCO2_i$ represents the emissions for the installation and replacement of the asset i and $OCO2_i$ corresponds to the carbon emissions due to the operation phase, which is non-null only for fuel-fired generators, as detailed in (4.6e); e_i is the specific emission for each installed component and e_g^{op} represents the specific emission per unit of fuel consumption. $CCO2_i$ of renewable assets is detailed in (4.6b), while its formulation for the battery and the generator, (4.6c) and (4.6d) respectively, also accounts for their replacement.

$$\min CO2 = \sum_i CCO2_i + OCO2_i \tag{4.6a}$$

$$CCO2_{i\backslash\{g,b\}} = N_i \cdot e_i \tag{4.6b}$$

$$CCO2_b = \left[1 + \sum_h (k_{h,b} - k_{h-1,b})\right] N_b \cdot e_b \tag{4.6c}$$

$$CCO2_g = N_g \cdot e_g + \sum_h \frac{U_{h,g}}{H_g^{life}} \cdot e_g \tag{4.6d}$$

$$OCO2_g = FC_{h,g} \cdot e_g^{op} \tag{4.6e}$$

Land use

The local environmental impact of the microgrid is taken into account by including in the analysis the minimization of the space required for the installation of the different assets [58]. The importance of this variable for decision makers is strictly related to the specific conditions of the area where the system needs to be installed; for example, land occupation may become a sensitive issue when the community is based in a protected area; on the contrary, it may not be relevant for PV-base systems in presence of large rooftops. The minimization of the land use variable (LU) is here considered and its model (4.7) is proportional to the number of installed units and their land occupation lo_i.

$$\min LU = \sum_i N_i \cdot lo_i \tag{4.7}$$

4.6.3   Social impact

Jobs creation

Energy planning can promote local jobs, as a consequence of the assets installation and operation, which are incorporated in the proposed multi-objective method by means of a maximization problem [58, 59, 108]. The mathematical formulation of the job creation variable (JC), detailed in (4.8a), is a function of the jobs generated throughout the value chain of each asset (CJC_i). Moreover, the contribution related to fuel consumption for fuel-fired generators is accounted by means of a separate variable (OJC_g). The parameter j_i represents the specific job creation per installation and operation of each asset, while j_g^f is the per-unit job creation related to fuel consumption.

$$\max JC = \sum_i CJC_i + OJC_g \tag{4.8a}$$

$$CJC_{i\setminus\{g\}} = N_i \cdot j_i \tag{4.8b}$$

$$CJC_g = N_g \cdot j_g + \sum_h U_h^{dg} \cdot \frac{j_g}{H_g^{life}} \tag{4.8c}$$

$$OJC_g = \sum_h P_{h,g}^{dg} \cdot j_g^f \tag{4.8d}$$

Public lighting coverage

Finally, public lighting is considered and included in the optimization by means of the PL variable, as it is an important enabler of better living conditions, including but not limited to improved security, recreational and educational activities. For this reason, street lights are considered as priority loads and they are not subject to curtailments: once a street light is installed, it must be supplied during the dark hours. The total need of street lights

to cover the whole area and the related power profile L_h^{tot} are assessed. Equation (4.9) maximizes the coverage of the service, expressed as the share (%) of the total requirement which is actually fulfilled.

$$\max PL = \frac{L_h}{L_h^{tot}} \cdot 100 \tag{4.9}$$

4.7 MILP sizing algorithm

Besides the extension of the decision criteria, the MILP planning problem is the same as that presented in the previous chapter. Hence, the IMY methodology is used: a multi-year formulation is adopted and an iterative procedure allows to accurately describe the degradation of BESS.

The only constraint of the problem subject to a slight modification with respect to the formulation described in Section 3.3.1 is the power balance constraints (3.6), which now separately accounts for the public lighting portion of the load L_h:

$$\sum_b \left(P_{h,b}^{dch} \cdot \overline{\eta_b} \cdot \beta_{h,b} - \frac{P_{h,b}^{ch}}{\overline{\eta_b} \cdot \beta_{h,b}} \right) + P_h^{ren} + \sum_g P_{h,g}^{dg} + D_h^u = D_h + L_h \tag{4.10}$$

The rest of the formulation remains unaltered and includes constraints (3.7)-(3.11). The full nomenclature is listed in Appendix A.

4.8 Case study

4.8.1 Description

The proposed methodology has been tested on the case study of the rural community of Soroti, Uganda, presented in Chapter 3 and characterized by the load shown in Figure 3.3. The hybrid energy system in Figure 3.2 is considered, evaluating photovoltaic and wind energy, diesel generators and electrical storage. The specific solar and wind power production per unit of asset has been estimated using the Renewable.ninja platform [80,81].

4.8.2 Input parameters

According to the proposed multi-objective approach in line with the SDGs, the three sustainability dimensions, economic, environmental and social, are taken into account. The main economic parameters of the optimization are summarized in Table 3.1 and in Section 3.4.1; the data related to the environmental impact (global CO_2 emissions and land use) are reported in Table 4.2; the information related to job creation is shown in Table 4.3, and the need for public lighting has been estimated based on the on-field data collection [79] (details are provided in Appendix B).

It is worth noticing that, in order to investigate the global environmental impact of the proposed systems, the emissions have been evaluated by an LCA approach that allows a more in-depth and accurate impact analysis with respect to an evaluation limited to direct

emissions alone. The assessment of the local environmental impact of the electrification project has been accounted for in terms of land use of the different components. As for batteries, their space requirements are considered negligible, as racks can present a very compact layout.

Table 4.2: Components LCA emissions and land use [62, 109, 110].

	Emissions	Land use
Photovoltaic panel	2472.07 $kgCO_2/kW$	7.1 m^2/kW
Wind turbine	935.57 $kgCO_2/kW$	267.7 m^2/kW
Diesel generator	192.17 $kgCO_2/kW$	2.35 $m^2/unit$
Fuel	3.15 $kgCO_2/L$	-
Battery	56.45 $kgCO_2/kWh$	-

Many studies have analysed the impact of different energy technologies on the job market in industrialized countries [111, 112], but little has been done to investigate this topic for rural communities in the Global South. A methodology has been developed in order to estimate multiplicative factors that allow the data of industrialized countries to be applied to different contexts [113]. Given the interest of this work in evaluating the local impacts in terms of job creation, only construction and installation (C&I) and operation and maintenance (O&M) are included and shown in Table 4.3, as the manufacturing of components for rural electrification projects is very likely to be performed abroad, not contributing to local development.

4.8.3 Test procedure

The multi-objective problem has been modelled in GAMS 24.0.2 and solved with CPLEX, using A-AUGMECON2 method described in Section 4.5. The comparison with the standard AUGMECON2 algorithm is also proposed.

The simulations have been run on a 6-core 3.20GHz Intel Core i7 computer with 16GB RAM. A tolerance of 0.5% has been set on thresholds **e** and $g_k = 6$ for $k \in \{2, ..., p\}$; hence, a grid of $\prod_{k=2}^{p}(g_k + 1) = 2401$ points is analysed. Each optimization is bound by a time limit of 3 hours and the time frame under study is 10 years, described by means of one representative day per month.

The use of a comprehensive multi-objective optimization is suitable for a first evaluation of the planning options, as it provides a full picture of the problem and allows to evaluate the trade-offs between different decision criteria. Hence, the adoption of representative days is advisable because it reduces dramatically the computational burden without compromising significantly the results (see Tables 3.4 and 3.5 and Section 3.5.4). Furthermore, for the purposes of evaluating the mutual differences between the different points of the Pareto frontier, the results are perfectly valid since the same simplification is applied in the study of all points. If needed, an hourly simulation can be performed as subsequent step, only for the points of interest.

Table 4.3: Components job creation per phase [114].

	C&I [jobs/MW]	O&M [jobs/MW]	Fuel [jobs/GWh]
Photovoltaic panel	13.46	7.34	-
Wind turbine	3.06	4.90	-
Diesel generator	2.08	1.96	2.94

4.9 Results

4.9.1 Validation of the online Pareto pruning

Table 4.4 confirms that the novel methodology described in Section 4.5 allows a considerable reduction of the computational burden by skipping many redundant computations, while keeping the same quality of information about the Pareto curve. In particular, the total number of points in the curve is reduced by 75% with respect to the AUGMECON2 method, and the total time employed by A-AUGMECON2 is 63% lower. Hence, the tractability of the problem is highly improved.

Table 4.4: Computational performances with and without online Pareto pruning.

	Points	Computation time
AUGMECON2	362	262 h
A-AUGMECON2	89	96 h

In terms of Pareto frontier, Figure 4.3 highlights the quality of the results as the two curves show negligible differences (caused by a non-null mipgap), even though A-AUGMECON2 presents 75% fewer points. This means that the adoption of the proposed approach leads to better computational performances, tractability of the results and effectiveness of visualization, thus favouring a more efficient decision making process.

4.9.2 Discussion on numerical results

The algorithm deals with conflicting objectives and the search space is delimited by the points identified in the payoff table, in which the best performance of each objective function is evaluated as per Section 4.5.1. Figure 4.4 shows the value of the different objective functions in the payoff table points, highlighting the main trade-offs between these quantities, while Table 4.5 presents the units installed for each of these points.

The most relevant takeaway is the significant similarity of the points at minimum NPC (purple) and minimum emissions (green). The least-cost solution is characterized by 25% more emissions at a 22% lower overall cost. This suggests that the economic objective does not collide with the purpose of emissions reduction, but it automatically approaches decent environmental targets, given the technology and cost improvements of the recent years. In both cases, the public lighting service is not provided at all, as a reduced load

61
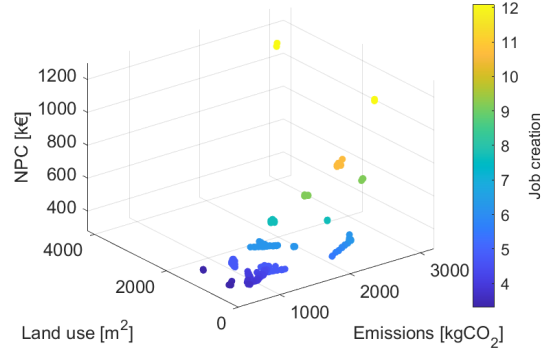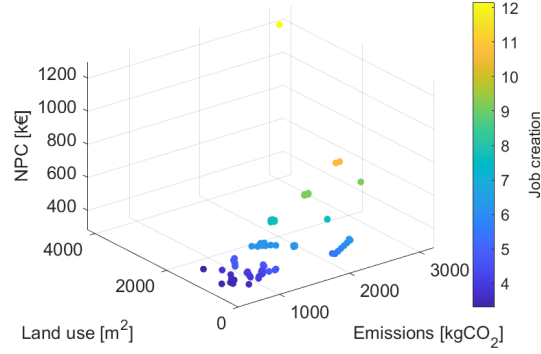
(a) AUGMECON2

(b) A-AUGMECON2

Figure 4.3: Comparison of the Pareto curves.

allows to decrease the size of the system and consequently costs and emissions. The curve at maximum public lighting coverage (yellow), besides satisfying completely the security target, presents limited impact on the overall cost (NPC about 20% higher than in the least-cost solution), which means that it may be considered as an affordable service, depending on priorities and budget constraints, and thus it may be recommended for new microgrid installations. However, these three solutions have a significant impact in terms of land use (in the range $835 \div 1055 m^2$) and a reduced employment generation (3.3÷3.8).

On the other hand, the minimization of land use (blue) manages to reduce the space requirement down to $7 m^2$ by heavily relying on diesel production, thus significantly increasing both NPC and emissions, although more local jobs (5.5) are created due to local maintenance and fuel procurement of the generators. Finally, the curve related to job creation (red) refers to the maximum employment of local human capital, associated to a surge in economic and environmental costs, because of a large oversizing and a complete reliance on DG during operation.

These results highlight the similarities and differences between the extremes of the
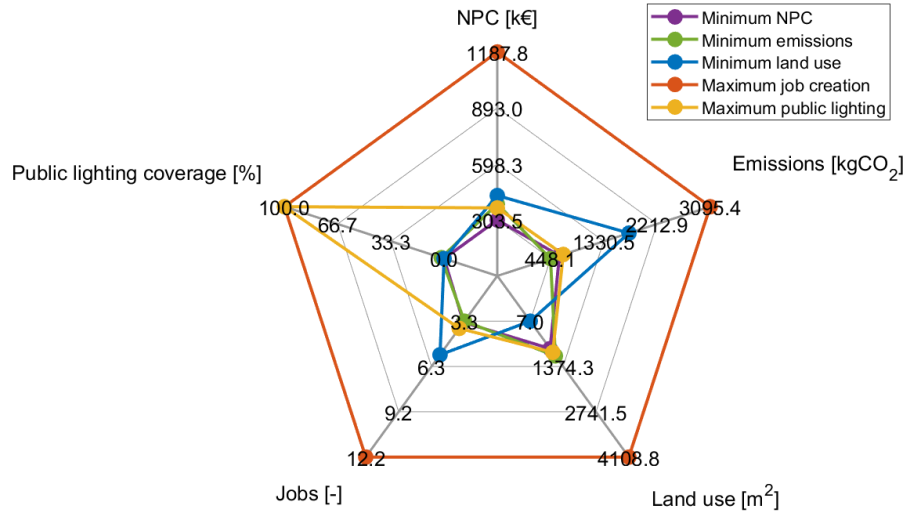
Figure 4.4: Payoff table points.

solutions to be investigated by local developers and governments, underlining the need for properly developing multi-objective methodologies that assist policy and business decision making.

Table 4.5 details the optimal design corresponding to the solutions of the payoff table, whose objectives are shown in Figure 4.4. It is worth noticing that the solutions focusing on the minimization of NPC and CO_2 emissions and the maximization of public lighting are comparable also in terms of optimal generation portfolio: a diesel generator is foreseen in all the three cases and the use of PV systems in the minNPC and maxPL cases is about 20% and 10% lower than in the CO_2 case respectively. In these three points, an increasing PV capacity is associated to a more significant presence of storage to effectively support the utilization of renewable energy and relegate DG to a more sporadic use. Moreover, the only solution where no PV devices are installed corresponds to the minimization of land use, and this result justifies the sharp increase in CO_2 emissions with respect to the least-cost option shown in Figure 4.4. Finally, the maximization of job creation pushes the solution towards the installation of all the available units, including wind turbines (which result to be unsuitable for any other solution analysed), while the operation relies entirely on diesel units. This generates the isolated point visible in Figure 4.3b at the extremes of the Pareto frontier (yellow point): the WT installation determines a much greater land occupation with respect to the other solutions and the oversizing leads to high costs, emissions and employment generation.

The information in Table 4.5 shall further guide policy makers and developers in fostering renewable sources and support public lighting, in areas where a relatively large land use is acceptable; yet, the Pareto frontier will be needed to identify the specific trade-off.

The renewable penetration of the solutions of the payoff table spans between 0% (minLU and maxJC cases) till about 97% in the least CO_2 emission case, reaching 84% in the least-

Table 4.5: Sizing of payoff table points.

	DG* [kW]	PV [kW]	WT [kW]	BESS [kWh]
min NPC	16 (1)	117	0	248
min CO_2	16 (1)	148	0	472
min LU	48 (3)	0	0	79
max JC	80 (5)	200	1	446
max PL	16 (1)	133	0	327

*: in brackets the number of installed units

cost option. Interestingly, the LCA approach for emissions accounting leads to a generating portfolio of the point at minimum emissions that is not entirely based on renewable sources: the diesel generator is occasionally employed at the end of the project, when the load is higher and the performances of PV panels are poorer. This is because the installation of an additional quantity of panels sufficient to cover the increasing load for the entire duration of the project, net of the degradation phenomena, would cause a greater quantity of life-cycle emissions than those associated with the installation and occasional use of a diesel generator, providing about 3% of the total energy. This result highlights the importance of an LCA impact assessment (from cradle to grave), because limiting the analysis to direct emissions could lead to distorted and incorrect considerations, driving sub-optimal business and policy outcomes.

Furthermore, Figure 4.5 compares the different use of resources in the configurations of the payoff table, in order to highlight the energy shares and the impact of multi-year characteristics, namely demand growth and asset degradation. The point at maximum jobs is not included in the analysis, as it corresponds to the installation of all the available units and the employment of the technologies that contribute the most to jobs creation in O&M phase, namely fuel-fired generators; hence, the full demand (including public lighting) is easily fulfilled by DG units. On the other side, the yearly cap on the Energy Not Served (ENS) is always hit in all the other points (see Figure 4.5), as it enables a reduction of costs, emissions and land use.

In the least-cost solution in Figure 4.5a, the demand of households and productive activities is entirely met by PV panels up to year 4. Then, as the load increases and the equipment degrades, the need to dispatch DG units gradually increases, up to about 32% of the total demand in year 10. The trends related to the solution maximizing the public lighting coverage (Figure 4.5d) show very similar behaviour to the least-cost solution(Figure 4.5a), confirming that public lighting needs can be met without significantly increasing the generation costs. In the minimimum CO_2 emissions case (Figure 4.5b), DG units start to be used in year 7, with a maximum contribution in the last year accounting for about 13%. On the contrary, when land use is minimized (Figure 4.5c), the demand is fully met by the fuel-fired generators or curtailed; no renewable sources are employed.

(a) Minimum cost

(b) Minimum emissions

(c) Minimum land use

(d) Maximum public lighting coverage
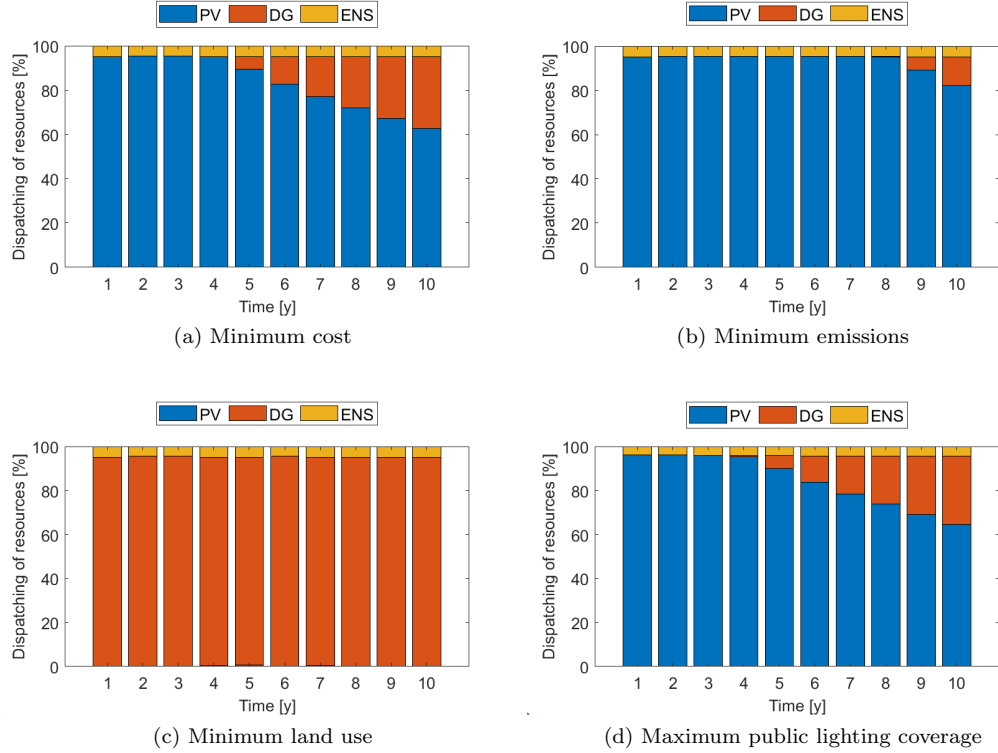
Figure 4.5: Yearly dispatching of resources.

4.9.3 Narrowing down possible solutions

Despite the filter, which removes redundancies and improves the readability of the results, some considerations can be made to further reduce the portfolio of available options and ease the decision making process, starting from the analysis of Figures 4.3b and 4.4 and from the considerations in Section 4.9.2. In particular, the points of the grid with high thresholds on jobs creation (> 7) can be excluded from the analysis, as they correspond to oversized microgrids. Moreover, given the limited influence of public lighting on the total cost of the system, it is sensible to guarantee a high share of the service, in light of the extremely positive impact it has on the well-being of the community. Therefore, only points with $PL > 90\%$ are taken into consideration. This allows narrowing the options down to the 9 points shown in Figure 4.6. Such reduced selection of points supports the decision maker in a more straightforward visualization of the trade-off between the objective functions, while preserving a rich portfolio of solutions.

Figure 4.6a highlights that higher emissions are associated with higher costs and more people employed. The top-right area of the graph corresponds to the points with the lowest renewable fraction: the higher the reliance on diesel generators, the greater the emissions

(a) Jobs variation

(b) Land use variation
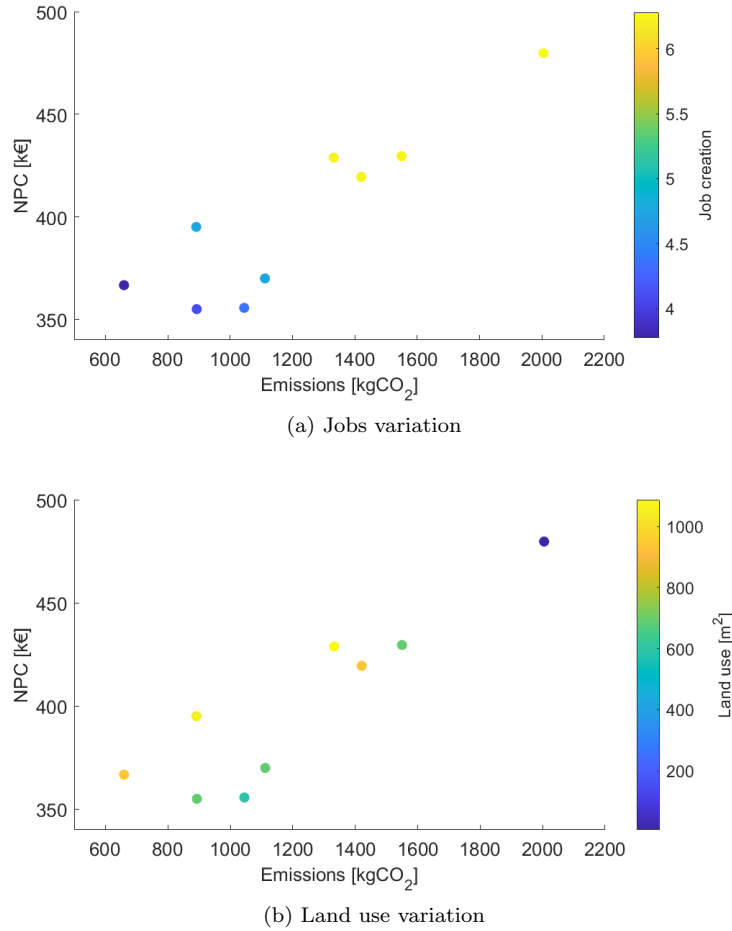
Figure 4.6: Reduced Pareto curve.

and the workforce needed to manage maintenance and fuel procurement. Moreover, these points are also characterized by very limited land use, as shown in Figure 4.6b, as diesel generators cover very limited space, unlike PV panels. It is worth noticing that comparable levels of land use, which, as a matter of fact, means similar PV capacity, correspond to wide ranges of emissions and costs (see Figure 4.6b), as the effectiveness in exploiting solar energy is strongly related to the capacity of the storage system. This, in turn, determines the need for diesel generators, whose operation significantly affects NPC and emissions.

A closer look at the selected points is provided in Figure 4.7, where the technical design and costs breakdown of the points in Figure 4.6 are shown in relation to LCA emissions. In particular, Figure 4.7a further underlines the impact of storage on the effective exploitation of renewable resources: BESS capacity is needed along with the renewable assets (PV panels) to further decrease CO_2 emissions. If a limited storage capacity is available, RES

(a) System design

(b) Costs breakdown
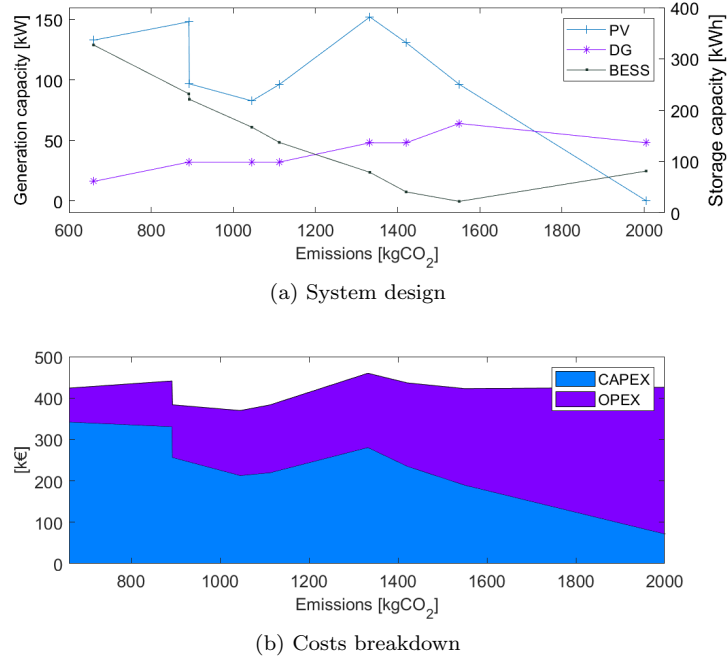
Figure 4.7: Technical and economical performances of the selected Pareto points.

generators need to be oversized and/or be supported by higher DG power. On the other hand, the higher the reliance on fuel-fired generators, the lower the CAPEX, thus the implementing entity can defer costs, reducing the initial investment at the cost of higher expenses along the project lifetime and larger CO_2 emissions (see Figure 4.7b). This element could have a decisive weight during the decision process, depending on the availability of funds, local regulation and company goals.

4.9.4 Decision making process

The peculiarity of the Pareto curve obtained from multi-objective optimization is that it preserves the complexity of the problem under analysis and allows the decision maker to have a full picture of the possible solutions and of their outcomes in different scopes.

Several works adopt procedures that lead to the selection of one single point of the curve by means of mathematical methods [102, 103]. In the author's opinion, the selection of the optimal microgrid for the purpose of rural electrification has so many impacts on the community, that it is preferable for the decision maker to be able to evaluate among a reasonable number of options and to select the most appropriate according to site-specific characteristics.

Among the various qualitative criteria that can facilitate the final evaluation based on the specificities of the community are: the willingness to pay for energy; the social acceptability of the different technologies; the compatibility with future expansion of the

plant; the resilience of the system, related to the local availability of components and spare parts and to the ease of maintenance and training of specialized personnel [61, 62, 64].

4.10 Conclusion

This chapter proposes a multi-objective planning method for off-grid microgrids able to optimize socio-economic, security and environmental concerns in a long-term perspective, accounting for detailed multi-year simulations of the system operation and assets degradation. In order to efficiently solve the corresponding non-linear multi-objective problem, the novel A-AUGMECON2 algorithm has been developed and its results proved to improve the convergence characteristics of the standard AUGMECON2, thanks to the novel Pareto pruning method that avoids repeating redundant optimizations. Each A-AUGMECON2 optimization is integrated with an iterative approach (presented in Chapter 3) that allows to efficiently deal with the non-linear problem by solving a number of MILP subproblems, where parameters are updated till convergence.

The results, obtained on a case study of a typical microgrid in Uganda, highlight that the reduction of life cycle emissions is compatible with cost-effective designs; hence, economic and environmental targets can be jointly met. Moreover, meeting the security goal, expressed by the public lighting penetration, increases costs by less than 20%, with considerable social benefits, thus recommending to institutional decision makers to include this service when planning rural electrification projects. On the other hand, maximizing local jobs and minimizing land use bring about a surge in costs, implying that when these needs are relevant, policy and business decision makers shall carefully select the optimal design and find the best compromise on the Pareto frontier, according to the specific needs of the community. These results, efficiently obtained by the proposed methodology, highlight the need for multi-objective multi-year optimization tools for optimizing rural microgrids in the Global South.

Moreover, the proposed methodology based on the novel A-AUGMECON2 has confirmed to reach the same optimal Pareto frontier than standard approaches (AUGMECON2) but with less than half of the computational requirements of the latter. This proves the approach discussed in this chapter to be an adequate tool to foster the practical use of multi-objective multi-year methodologies by developers and policy makers, given their constant need for fast optimization tools with far-reaching long-term perspective.

Furthermore, the proposed methodology can be applied to a large variety of energy systems, thus benefiting both policy/business decision makers and the research community, who may infer more accurate results and better tailor their projects, thus enabling cost savings, environmental benefits and improved social well-being.

Chapter 5

Dealing with long-term uncertainty

5.1 Introduction

Rural electrification projects are characterized by a significant long-term uncertainty, as their outcome is influenced by socio-economic and environmental factors which are hardly predictable during the initial design process. This chapter introduces the analysis of this further element in the microgrid planning problem described in Chapters 3 and 4. In order to comply with this requirement, a stochastic approach is adopted to account for different demand growth scenarios and the possibility of deferring installation costs according to the demand realization is introduced. These new features of the model contribute to a further increase of the complexity of the algorithm and simplifications are needed to preserve its tractability.

The chapter is structured as follows: Section 5.2 describes the novelties introduced in the following sections; Section 5.3 recalls the two main approaches to deal with uncertainty in optimization problems, namely robust and stochastic methods, and highlights their characteristics, identifying stochastic techniques as the most suitable for the problem under study; Section 5.4 describes how the new features for evaluating a long-term uncertain horizon are included in the model presented in the previous chapters; Section 5.5 discusses the manifold considerations that may be done to reduce the complexity of the model, ranging from the simplification of the decision process to the identification of the most efficient mathematical representation of the long-term stochasticity of the microgrid planning problem; Section 5.6 presents the input data adopted in the simulations; Section 5.7 shows the obtained results, highlighting the advantages of a multi-step investment approach over traditional single-step investments and discussing the Pareto frontier; finally, Section 5.8 draws some conclusions.

5.2 Contributions

A relevant contributions of this chapter stands in the analysis of the most appropriate method and practical implementation for the evaluation of long-term uncertainty for microgrid planning. Moreover, it includes for the first time a stochastic multi-step investment feature in a multi-objective problem, while keeping a good tractability of the algorithm. Hence, this chapter is the final step in building a comprehensive, integrated and accurate model of the planning problem of isolated microgrids.

5.3 Selecting an uncertainty modelling technique

5.3.1 Common frameworks

Two well-established approaches are available in literature to cope with the unpredictability of the inputs: robust and stochastic optimization, both adopted also within the framework of multi-objective optimization of energy systems [97, 115]. The former adopts a reformulation of the original problem to identify the optimal solution, given the worst possible realization of the inputs, of which only the width of the uncertainty interval needs to be known; the conservativeness of the solutions may be regulated by means of a user-defined parameter [76, 97]. The latter includes the formulation of multiple scenarios, each associated with a probability of occurrence; the method returns the optimal value of the expected objective function, given the input scenarios and their estimated occurrence probability [115, 116]. Depending on the characteristics of the problem, on the type of uncertainty to be analysed and on the computational requirements, the developer may tend to one or the other approach.

In particular, robust optimization is suited to conditions of data scarcity, interest of the user in a cautious and conservative approach, need of limited computational burden. However, this method tends to oversize components for the sake of prudence against any possible realization of the inputs, negatively impacting on the objective function to a degree which is not always acceptable [76]; this is particularly true when dealing with investments in the Global South. Moreover, this issue is exacerbated in case of long-term uncertainty, usually characterized by uncertainty interval limits expanding over time (see Figure 2.3), in contrast to bands usually describing short-term fluctuations: the wider the uncertainty on the final realization of the time-series, the greater the impact on the objective function derived from tailoring the solution to the worst case.

Differently from robust methods, stochastic optimization requires a minimum knowledge of the probability distribution within the uncertainty interval and increases the complexity of the problem because of the explicit analysis of the different scenarios. Nonetheless, the formulation allows to take into account the various possible realizations of the inputs and attribute them a weight when selecting the optimal solution and computing the objective function; this usually leads to more efficient options and limits the risk of oversizing [76].

5.3.2 Suitability for rural microgrid planning

As mentioned in Section 2.2, the optimal planning of rural electrification projects is mainly affected by long-term trends, subject to high degree of uncertainty, rather than short-term fluctuations, i.e., hourly demand and RES variability [40], which can be efficiently handled by means of reserve constraints (see equation (3.11)). It is instead extremely difficult to forecast the evolution of the demand over the years and to cope with it within a deterministic optimization; hence, an uncertainty modelling technique shall be used.

Given that the trade-off between conservativeness and economic efficiency for the problem under analysis is usually in favour of an affordable service, robust optimization is not suitable to cope with long-term time series affected by growing uncertainty, as demand projections may foresee consistent growth rates but it is not realistic to plan the system according to the most extreme scenario. Hence, stochastic approaches are preferable in order to consider different possible long-term scenarios, assessing their probability and identifying the optimal solution accordingly. As mentioned above, this method comes with additional computational complexity, but this is not particularly relevant when analysing rural microgrids. Given the reduced data availability, it is not reasonable to formulate a very high number of scenarios and attribute them a probability of occurrence; it is usually sufficient to identify the most probable trends according to socio-economic and/or historic data. Different assumptions on appliances penetration and development of community services are used in [68] and [69] to describe three and four scenarios respectively. A combination of bottom-up and macro-economic indicators is adopted in [40] to derive nine demand scenarios. Three linear growth rates and the related probabilities are calibrated in [47] according to a database on 23 Kenyan microgrids. Long-term projections are formulated in [25] using six different arbitrary trends, while [41] considers all the combinations of six yearly growth factors, reduced to 15 final scenarios. In conclusion, the characteristics of the problem allow to adopt stochastic optimization defining a limited number of long-term demand projections, avoiding a prohibitive impact on the tractability of the model. Moreover, this method easily accommodates the presence of capacity expansion windows, referred to the pertaining scenario.

5.4 Methodology

The adoption of a stochastic framework for a multi-step investment planning problem implies little modifications on the algorithms presented in the previous chapters. Two additional sets are needed, namely the set of demand scenarios s and the set of capacity expansion windows c, expressed as the hours of the time series when additional investments are allowed.

As illustrative example, equation (5.1) shows the modifications undergone by the economic objective function to accommodate the features added to the algorithm. The only element of the total NPC which is not affected by the stochasticity of the problem is the initial investment IC_i, taking place before the system starts operating and common to every scenario. All the other cost components are now scenario-dependent and their contribution to the NPC is weighted on the occurrence probability of the scenario pr_s. Moreover, the cost of installing additional assets $N_{s,c,i}^{ce}$ during the capacity expansion win-

71

dow c is modelled by $CE_{s,i}$. The costs of operation and maintenance $O\&M_{s,i}$, the costs of replacement $RC_{s,i}$ and the residual values $RV_{s,i}$ are updated to account for the deferred investments, with $U^{ce}_{s,c,h,g}$ integer variable on active DG units installed as capacity expansions, $k^{ce}_{s,c,h,b}$ counter on replacement of capacity expansion BESS, Y^{ce}_c year of capacity expansion c, $\alpha^{ce}_{s,c,h,b}$ relative residual capacity of capacity expansion BESS. The rest of the nomenclature is listed in Appendix A and it refers to the models presented in Chapters 3 and 4; hence, the reference to the different scenarios by means of the index s is missing.

$$\min NPC = \sum_i IC_i + \sum_{s,i} pr_s \cdot (CE_{s,i} + O\&M_{s,i} + RC_{s,i} - RV_{s,i}) \tag{5.1a}$$

$$IC_i = N_i \cdot c_i \tag{5.1b}$$

$$CE_{s,i} = c_i \cdot \sum_c d_c \cdot N^{ce}_{s,c,i} \tag{5.1c}$$

$$O\&M_{s,i\setminus\{g\}} = m_i \cdot \sum_{y=1}^{\overline{Y}} d_{H\cdot y} \cdot (N_i + \sum_{c \geq H\cdot y} N^{ce}_{s,c,i}) \tag{5.1d}$$

$$O\&M_{s,g} = \sum_{h=1}^{\overline{H}} d_h \cdot \left[m_g \cdot (U_{s,h,g} + \sum_{c \geq h} U^{ce}_{s,c,h,g}) + f \cdot FC_{s,h,g} \right] \tag{5.1e}$$

$$RC_{s,g} = \frac{c_g}{H^{life}_g} \cdot \sum_{h=1}^{\overline{H}} d_h \cdot (U_{s,h,g} + \sum_{c \geq h} U^{ce}_{s,c,h,g}) \tag{5.1f}$$

$$RC_{s,b} = c_b \cdot \sum_{h=1}^{\overline{H}} d_h \cdot \left[N_b \cdot (k_{s,h,b} - k_{s,h-1,b}) + \sum_{c \geq h} N^{ce}_{s,c,b} \cdot (k^{ce}_{s,c,h,b} - k^{ce}_{s,c,h-1,b}) \right] \tag{5.1g}$$

$$RV_{s,i\setminus\{g,b\}} = d_{\overline{H}} \cdot \rho_{h,i} \cdot c_i \cdot \left(N_i \cdot \frac{Y^{life}_i - \overline{Y}}{Y^{life}_i} + \sum_c N^{ce}_{s,c,i} \cdot \frac{Y^{life}_i + Y^{ce}_c - \overline{Y}}{Y^{life}_i} \right) \tag{5.1h}$$

$$RV_{s,b} = d_{\overline{H}} \cdot c_b \cdot \left(N_b \cdot \frac{\alpha_{s,\overline{H},b} - \underline{\alpha_b}}{\overline{\alpha_b} - \underline{\alpha_b}} + \sum_c N^{ce}_{s,c,i} \cdot \frac{\alpha^{ce}_{s,c,\overline{H},b} - \underline{\alpha_b}}{\overline{\alpha_b} - \underline{\alpha_b}} \right) \tag{5.1i}$$

Similarly, the rest of the objective functions (4.6)-(4.9) and the constraints (3.7)-(3.11),(4.10) are reformulated to account for the multi-step investment approach. The Iterative Multi-Year (IMY) procedure to evaluate BESS variable efficiency and capacity reduction remains unaltered.

5.5   Reducing the computational complexity

The multi-step stochastic version of the model presented in this chapter brings about additional complexity; in particular, the increase in number of variables and constraints is basically proportional to the number of scenarios and the computational burden usually increases more than linearly with the size of the problem. Moreover, the presence of capacity expansion windows contributes to a further increase of number of variables and

constraints. The inclusion of the complete model within a multi-objective framework would likely make the routine very difficult to solve or even intractable. Hence, simplifying the problem while keeping the overall thoroughness and the pivotal features is essential.

5.5.1 Practical considerations

Some suitable simplifications may be inferred by discussing the scope of application of the problem and building on the results of Chapters 3 and 4 of the numerical application of the algorithms on the Soroti case study.

As discussed in Section 4.8.3, a comprehensive multi-objective optimization aims at providing the decision maker with information about the relationships between the different indicators and the related impact on the generating portfolio and on the operating strategy. Given the purpose of the algorithm, the use of representative days is suitable for an adequate description of the problem and is very effective to reduce the size of the MILP core, as already done in Chapter 4.

The description of ε-constraint methods to solve multi-objective optimizations provided in Section 4.4.1 highlighted that the number of grid points to be analysed grows exponentially with the number of objective functions. The novel A-AUGMECON2 presented in Section 4.5 dramatically improves the tractability of complex multi-objective problems by skipping redundant simulations, but the reduction of the size of the grid is certainly a fundamental aspect in simplifying the analysis. Given the discussion on the numerical results of A-AUGMECON2 obtained on the test case (see Section 4.9), two objective functions may be removed to diminish the points to be examined:

(i) *Public lighting.* This is a pivotal service to foster the improvement of the well-being of a community and it has a moderate impact on the total economic and environmental costs. Hence, guaranteeing a good level of the service is an advisable and considerate choice. For this reason, the objective function may be turned into a constraint imposing a fixed minimum service coverage.

(ii) *Job creation.* The maximization of jobs creation forces the installation of all the available units. This allows to limit the search space identifying one of the extremes of the Pareto frontier. In practice, the final working point is very likely to be within the search space defined by the other objective functions (total cost, life-cycle emissions and land use), avoiding an oversizing of the system. Therefore, the objective function can be removed, computing the jobs associated to each Pareto point as parameter to be evaluated in the decision process, but not adding a dimension to the size of the grid.

Moreover, from the output generation portfolios discussed in Chapters 3 and 4 it emerges that the wind resource in the studied area is not sufficient to justify a profitable investment in WTs; PV panels result to be more efficient also from the environmental perspective. WTs are removed from the possible generation assets, simplifying the microgrid architecture and reducing the number of parameters and variables. Hence, an initial assessment of the available resources through preliminary analyses is desirable because it allows to reduce the possible configurations of the system and fasten the optimization process.

Finally, choosing an adequate number of scenarios and capacity expansion windows helps to keep simulation times reasonable. Section 5.3.2 debated the suitability of a limited number of long-term demand projections for the analysis of rural electrification projects, thus avoiding a prohibitive impact on the tractability of the model. For what concerns the number of investment steps, several works suppose yearly capacity expansions [36, 42, 71]. However, it is not reasonable to imagine yearly installations in rural microgrids, where the remoteness of the area is often the reason why such electrification strategy is chosen. A modelling strategy resembling a possible practical approach consists in periodically assessing the evolution of the system and the potential need of additional assets. This option is adopted in [47], identifying one possible capacity expansion window at the fifth year of a 10 year project. Similarly, [69] allows four investments steps (including the initial installation) in 20 years. Therefore, few investment steps are adequate for the scope of application of the algorithm and have limited influence on the computational burden.

5.5.2 Solving a stochastic problem

The traditional solution of a stochastic optimization is a large scale monolithic MILP evaluating all the N realizations at once and identifying the optimal solution. When this option is too burdensome, decomposition techniques may be adopted to speed up computations. In particular, Aggregated-Rule-based Stochastic Optimization (ARSO) is a popular method that reduces the formulation to N deterministic subproblems and selects the final configuration according to an aggregation rule [117–119]. Figure 5.1 illustrates the framework of the two approaches.

(a) Stochastic Optimization (SO)

(b) Aggregating-Rule-based Stochastic Optimization (ARSO)
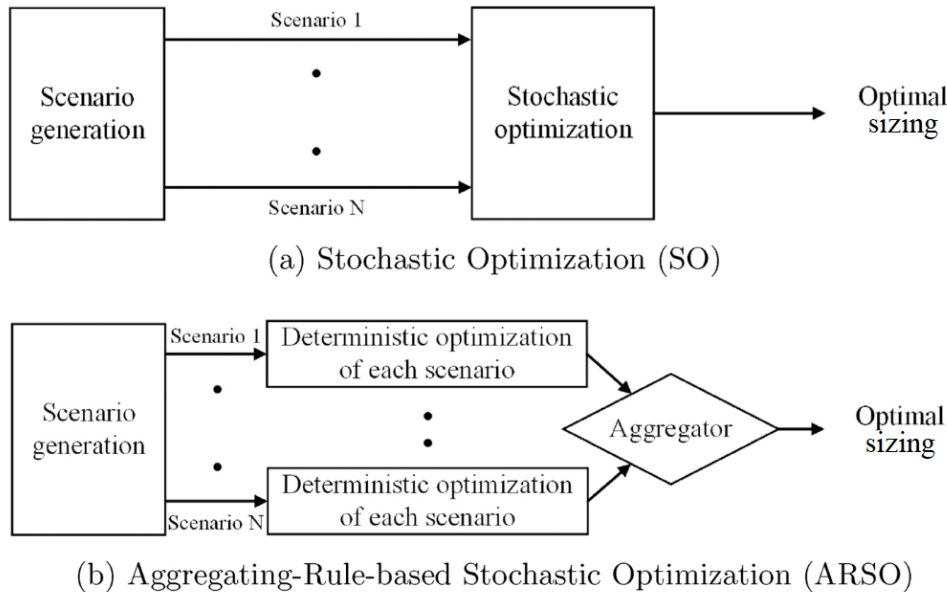
Figure 5.1: Approaches to stochastic sizing [119].

Both methods are tested on the stochastic reformulation of the algorithm presented in Chapter 3, specifically on the Iterative Multi-Year (IMY) model using representative days, to evaluate their performances and verify whether an ARSO appoach may contribute to reducing the complexity of the problem under analysis. The ARSO procedure using a cost-based aggregating rule is composed of the following steps:

(i) Deterministic optimization of the N scenarios.

(ii) For each solution of step (i), the sizing variables are fixed and the optimal dispatching for every possible realization of the input is computed (N^2 simulations in total).

(iii) The expected NPC is calculated according to the probability of occurrence of the scenarios.

(iv) Among the N solutions of step (i), the one associated to the lowest expected NPC is selected.

The two approaches are compared for an increasing number of scenarios, namely 3, 5 and 10, to assess the benefits and drawbacks of the methodologies in different configurations. The results are summarized in Table 5.1.

Table 5.1: Comparing Aggregated-Rule-based Stochastic Optimization (ARSO) and stochastic optimization (SO) performances.

			ARSO	SO	ARSO	SO	ARSO	SO
			3 scenarios		5 scenarios		10 scenarios	
Time		[s]	144	146	406	550	4477	2625
NPC		[k€]	341	339	341	339	364	360
	DG	[kW]	32	32	32	32	32	32
Sizing	PV	[kW]	86	86	86	86	86	94
	BESS	[kWh]	174	172	174	175	175	184

These simulations confirm the quality of results provided by ARSO: very limited differences with the corresponding stochastic version in terms of costs and assets installed are present. However, the main outcome is that the there is no evident gain of practical interest in adopting ARSO techniques on the selected test cases; on the contrary, stochastic optimization may consistently outperform ARSO, as in the 10 scenarios case. Moreover, traditional stochastic approaches provide better objective function values. For these reasons, the rigorous and consolidated stochastic method is adopted in the following sections. It is worth noticing that considerations on the computational time are case-dependent, as other works found significant benefit in adopting ARSO techniques over traditional stochastic optimization [119]; the gain may diminish as the number of scenarios decreases (limited impact on number of variables and constraints) and the complexity of the core MILP problem increases.

5.6 Case study

5.6.1 Description

The proposed methodology has been tested on the case study of the rural community of Soroti, Uganda, presented in Chapter 3. A hybrid energy system evaluating photovoltaic, diesel generators and electrical storage is considered. The specific solar power production per unit of asset has been estimated using the Renewable.ninja platform [80].

5.6.2 Input parameters

The main parameters of the optimization are summarized in Sections 3.4 and 4.8.

According to the considerations in Section 5.5, an accurate analysis of a rural electrification project can include a limited number of scenarios and few capacity expansion windows, for a comprehensive study that preserves also good tractability.

In particular, the use of 5 scenarios results to be a reasonable choice based on data availability and computational time (see Table 5.1). The long-term demand projections are formulated based on the literature review of growth trends in similar contexts [25,47,72]. The central scenario corresponds to the load profile adopted in Chapters 3 and 4 and shown in Figure 3.3, reproducing the social dynamics observed in [72].

Table 5.2: Load scenarios growth factor and probability of occurrence.

Scenario	1	2	3	4	5
Yearly growth factor	0%	10%	20%	30%	40%
Probability	5%	20%	50%	20%	5%

Table 5.2 presents the growth factors and the probability of occurrence of the scenarios and Figure 5.2 shows the trend of the profiles over time. The extreme scenarios (no growth and 40% yearly increase) capture the tails of the probability distribution and are associated to a low probability (5%). The central scenario responds to the social trends observed in [72] and is considered to be the most probable realization (50% probability) of the demand. Scenarios 2 and 4 are characterized by intermediate values.

In order to allow an update of the assets installed, two capacity expansion windows are identified on a 10-year project, namely at the end of year 3 and 6.

5.6.3 Test procedure

The problem has been modelled in GAMS 24.0.2 and solved with CPLEX, using the A-AUGMECON2 approach described in Section 4.5 as multi-objective method and the iterative procedure presented in Section 3.3 to efficiently describe the multi-year characteristics of the system.

The simulations have been run on a 6-core 3.20GHz Intel Core i7 computer with 16GB RAM. The problem has 3 objective functions and in its ε-constraint formulation the NPC is kept as objective function, while the life-cycle emissions and the total land use are reformulated as constraints and their range of variation is split into $g_k = 9$ intervals for
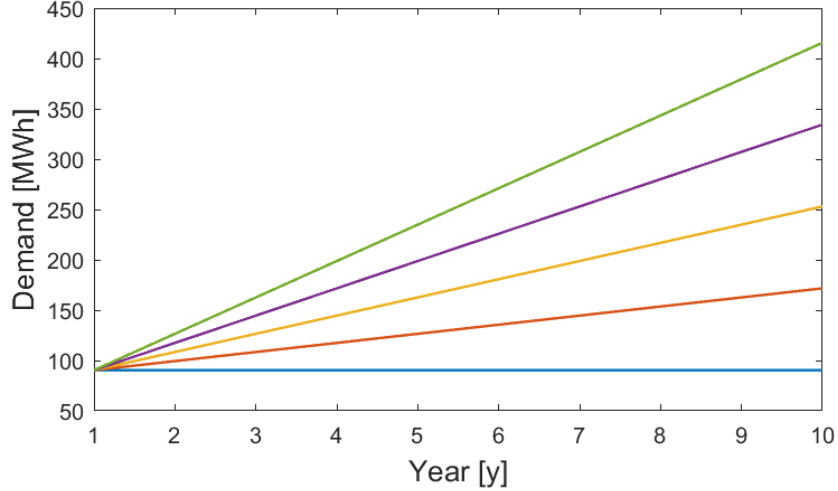
Figure 5.2: Long-term demand scenarios.

$k \in \{2, ..., p\}$, with p number of objective functions; hence, a grid of $\prod_{k=2}^{p}(g_k + 1) = 100$ points is analysed. The time frame under study is 10 years, described by means of one representative day per month. A minimum coverage of 90% of the public lighting needs is desired.

5.7 Results

5.7.1 Impact of capacity expansions

Accounting for different realizations of the inputs leads to more cautious solutions, that identify the best microgrid generation and storage portfolio allowing to operate the system in any evaluated condition. If the possibility of integrating such portfolio over the years is taken into consideration, the first installation is a starting point to satisfy the initial needs of the community and the following investments are tailored on the actual realization of the demand in time, reducing risks and improving the efficiency of the objective functions. On the contrary, in the single-step investment case, the installation at the outset of the project is the result of a long-term perspective accounting for all the scenarios in that initial evaluation.

Table 5.3 shows the payoff tables delimiting the search space of the routine run in single-step and the multi-step investment cases and highlights that the presence of capacity expansions improves the quality of the results, reducing the total cost by a significant amount, ranging from 10% in the least-cost solution up to 23% in case of minimum land use.

Given the reduced upfront cost associated to the installation of DG units and the presence of a discount factor that leads the optimizer to favour deferred expenses, the single-step version of the algorithm is characterized by higher reliance on the use of fuel.

Table 5.3: Payoff tables obtained in case of single-step and multi-step investment.

	single-step			multi-step		
	NPC	CO_2	LU	NPC	CO_2	LU
	[k€]	[$kgCO_2$]	[m²]	[k€]	[$kgCO_2$]	[m²]
min NPC	382	640	932	344	497	1112
min CO_2	444	554	1189	365	494	1143
min LU	617	2006	7	478	1987	5

Moreover, satisfying the total demand with the initial installation implies that more units are needed, as their degradation will reduce their capability of powering the load in the last years of operation, and that the residual value of the assets at the end of the project will be lower if compared to the multi-step case.

In light of these observations, the multi-step version of the model is adopted for the full evaluation of the system in a long-term perspective and its results are analysed in the following subsections.

5.7.2   Computational efficiency

The measures discussed in Section 5.5 allowed to significantly reduce the size of the multi-step stochastic problem. In particular, the most effective action was the removal of two decision criteria from the set of objective functions, namely jobs creation and public lighting coverage. Thus, while increasing the density of g_k points analysed for the single objective functions, the total size of the grid (100 points) is drastically reduced compared to Chapter 4 (2401 points). The payoff table and the full Pareto frontier, composed by 14 non-redundant points, are computed in about 52 hours. The number of available solutions enables a good readability of the results and the possibility to make an informed decision without further reducing the portfolio of available options.

5.7.3   Pareto frontier

The whole range of solutions is shown in Figure 5.3, where different views of the frontier are displayed. As in the Pareto points of Chapter 4, the main trend emerging from Figure 5.3 is the increase of emissions at reduced land occupations, associated to a prevalent reliance of DG units and a high total cost (see Figure 5.3a). On the contrary, the points associated with a consistent renewable fraction and low LCA emissions ($< 1000 kgCO_2$) are also cost-effective options ($NPC < 365k$€). This confirms the finding of Chapter 4, which supported a substantial alignment of cost and emission reduction objectives.

However, as shown in Figure 5.3b, low-emissions solutions entail a high initial investment, which is not always suitable for the implementing entity, depending on funds availability. This is because renewable and storage assets are characterized by a considerable upfront cost and almost null operation expenses. On the contrary, DG units entail a limited initial investment but O&M costs represent a substantial share of the total; hence,
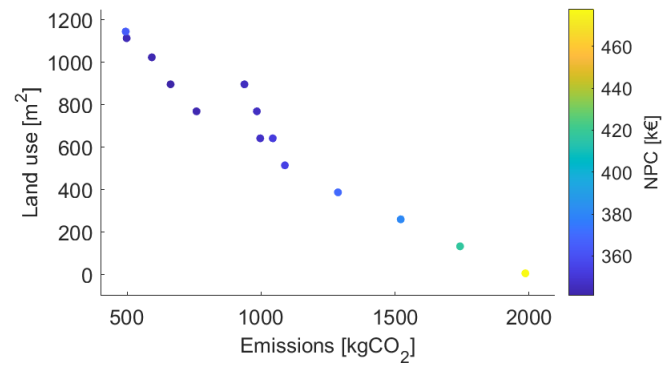
(a) NPC
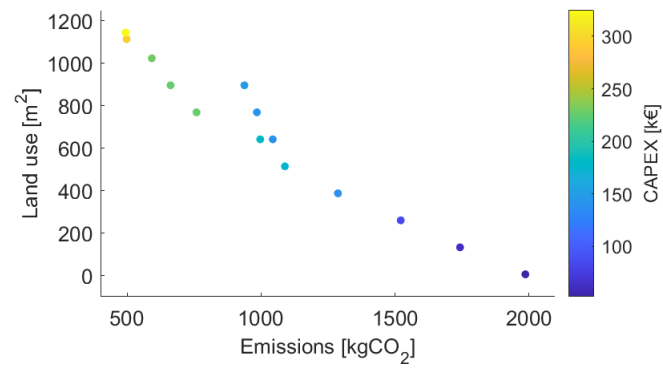
(b) CAPEX
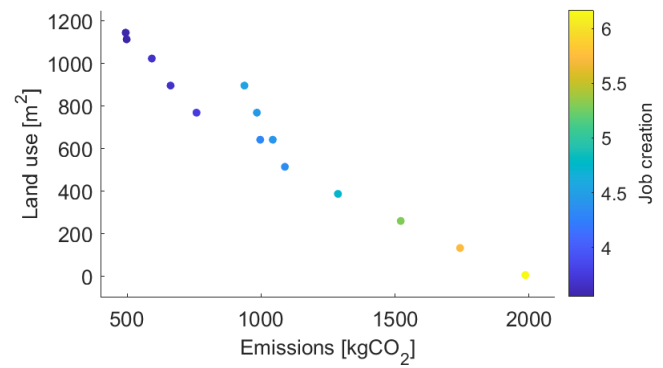
(c) Jobs

Figure 5.3: Views of the Pareto curve.

costs may be deferred and distributed along the project lifetime, which may be a significant advantage for the developer.

A further drawback of mostly RES-based options is that renewable assets have poor maintenance requirements, differently from fuel-fired generators that foster more employment opportunities because of more frequent maintenance and fuel procurement operations. Indeed, Figure 5.3c shows that the number of full-time jobs fostered by the microgrid project may vary from 3.5 in the least-cost solution up to 6.2 in the case of minimum land use, entirely based on the energy produced by DG units.

5.7.4 Sizing variables

Focusing on the three payoff table points for a more in depth analysis of the solutions delimiting the search space, Figure 5.4 shows the units installed before the coming in operation of the plant (Y0) and during the first (CE1) and second (CE2) capacity expansion window. The installation at Y0 is common to every scenario, while the different evolutions of the demand may lead to distinct sizing options in CE1 and CE2. The bars represent the ranges given by the different scenarios, the marker points out the solution of the central scenario, characterized by 50% probability of occurrence.

Only one DG unit is installed in Y0 in the minNPC and $minCO_2$ case, then the system entirely relies on renewable energy and batteries for further installations (see Figure 5.4a). In case land use is a priority, two fuel-fired generators are necessary in Y0 to power the total load, to be integrated by an additional DG unit in CE1 in the highest growth scenarios.

As in the numerical results of Chapter 4, the minLU case is characterized by a null renewable fraction and PV panels are never installed. On the contrary, Figure 5.4b highlights that about 100kW of PV are installed in Y0 in the least-cost and minimum emission options. Then, further panels are needed as the demand grows over time. Hence, no integration of the solar assets is foreseen in the first scenario, associated with a flat load behaviour.

The need for BESS in the payoff points is shown in Figure 5.4c. The minimization of emissions requires almost 400kWh of BESS in Y0, in order to optimally exploit the renewable energy provided by PV panels. As the degradation of the assets kicks in and the load increases, additional batteries may be needed in the following years. Only 40kWh are installed in Y0 in case of minLU, to support the operation of the DG units. In this solution, the load increase does not determine the installation of further generation assets, except in the case of the two most extreme growth factors, but there is a growing need for storage systems to improve the load shifting capability of the system and fully satisfy the demand with the generators installed in Y0.

5.8 Conclusion

Long-term uncertainty may play a pivotal role in determining the outcome of a project in the long run. For this reason, this chapter treats its evaluation at planning level. In particular, the model presented in the previous chapters has been enriched with two interrelated features: stochasticity to evaluate different demand growth scenarios and capacity expansion windows to defer investments according to the actual realization of the inputs
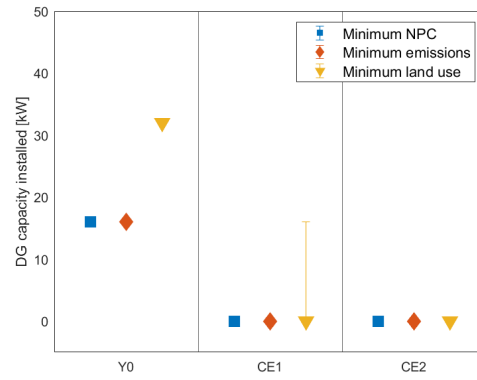
(a) Diesel generators
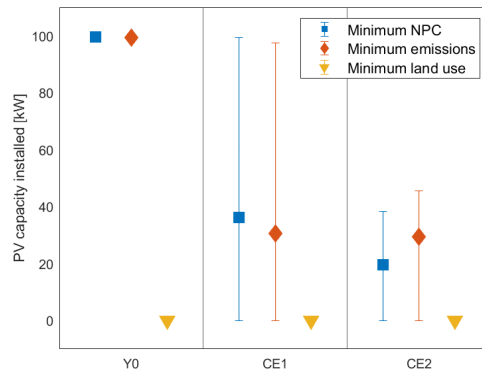
(b) PV panels
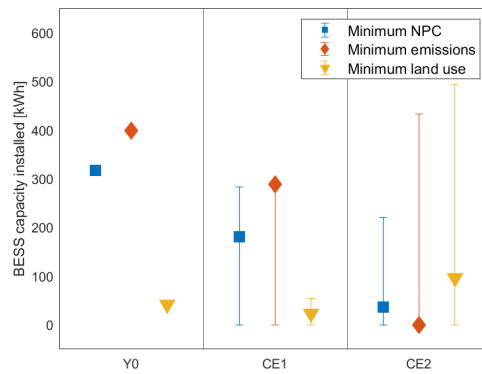
(c) Batteries

Figure 5.4: Assets installed in payoff points.

over time.

Five load scenarios and two additional investment steps allow to improve the representation of the system, abandoning the assumption of perfect knowledge which typically characterizes the deterministic approaches, and adopting a well-established uncertainty modelling technique, guaranteeing a feasible system operation in any realization of the inputs.

The inclusion of these features increases the size of the problem and preserving its tractability is essential to provide an efficient tool to developers and researchers. Hence, several measures are adopted to reduce the computational complexity of the model: the microgrid architecture, i.e., the available assets, is simplified; representative days are used; the points under analysis are reduced by a condensed decision making process.

The numerical results show that a stochastic approach leads to more prudent solutions, without leading to significant oversizings. This characteristic is mitigated by the presence of capacity expansion windows. Indeed, if two additional investment steps are considered, the NPC of the payoff points is reduced by $10 \div 23\%$. The multi-step investment approach allows to defer expenses and, consequently, to rely more intensely on renewable and storage components, characterized by a high upfront cost and thus less efficient with respect to fuel-fired generators in a single-step investment configuration.

Moreover, the results confirm the main trends identified in the previous chapter, i.e. the growth of the LCA emissions and total costs at decreasing land occupation and increasing jobs, the substantial alignment of economic and emission objectives.

This final configuration of the model represents a novel integrated approach to evaluate rural microgrid planning problems with a far-reaching perspective and a comprehensive analysis of sustainable options to foster the development of the target community.

Part III

Discussion

Chapter 6

Key takeaways and impact

6.1 Introduction

Two main objectives were declared for this work in Section 2.3, namely the formulation of a holistic MILP microgrid planning problem and the development of novel algorithms to preserve its tractability. Every chapter of Part II contributes to both objectives, improving the description of the problem and providing resolution approaches that drastically reduce the computational burden with respect to the state of the art.

The main features of the model are here discussed, pointing out the key findings. In particular, Section 6.2 compares the results of the procedure discussed in Chapter 3 with a traditional sizing method, highlighting the effectiveness of optimization tools over standard computations. Section 6.3 describes the measures adopted in the chapters of Part II to reduce the complexity of the problem under study and facilitate the analysis of the results. Section 6.4 summarises the main findings of Chapter 4, where a holistic multi-objective optimization is presented, and underlines the importance of a wide perspective in decision making processes for rural electrification. Section 6.5 compares the solutions of different configurations of the model to prove the impact of stochastic approaches and multi-step sizings on the objective functions. Section 6.6 describes the versatility of the proposed model, whose features can be easily adjusted to the specific application and to the needs and interests of the implementing entity. Finally, Section 6.7 resumes the key takeaways of this chapter.

6.2 Impact of using optimization tools

Advanced computer tools for microgrid planning have become a standard approach in research, but their use for practical applications is still limited: NGOs, firms and local institutions often adopt traditional sizing criteria which cannot account for the technical constraints of the different components and correctly plan the operational strategy. Moreover, traditional methods cannot efficiently size hybrid systems, accounting for the contribution of different resources and the impact on the needed BESS size.

In order to highlight the importance of adopting optimization tools for real projects,

a traditional sizing procedure [120] is applied in this section on the Soroti case study and compared with the results of Chapter 3, where a least-cost algorithm accounting for the multi-year characteristics of the system (load growth and assets degradation) is presented. As mentioned above, the traditional method does not allow to effectively plan hybrid microgrids; hence, as a high renewable fraction is a common requirement in recent projects, a solar-battery system is designed.

The size of the solar PV plant P_{pv} is given in (6.1) by the ratio between the monthly cumulative demand D_{month} and the minimum monthly solar energy produced per kW of PV. It is worth noticing that D_{month} refers to the last year of the project, to account for load growth and avoid energy shortages.

$$P_{pv} = \frac{D_{month}}{\min\{E^{pv}_{month}\}} = 172.42 \quad kW \tag{6.1}$$

The needed BESS capacity C_b is computed in (6.2) and depends on the days of autonomy Aut required in case of cloudy days. The Depth of Discharge of the battery needs to be taken into account to correctly size the storage bank. In (6.2) a two days autonomy is supposed. Analogously to (6.1), D_{day} is the maximum daily cumulative demand in Soroti, i.e., the load at the end of the project.

$$C_b = \frac{Aut \cdot D_{day}}{DOD} = 1471.22 \quad kWh \tag{6.2}$$

This configuration of the system is compared in Table 6.1 to the solution of the Iterative Multi-Year (IMY) procedure obtained in Chapter 3. The traditional sizing is characterized by a complete reliance of renewable energy, which comes with almost double PV power and a 7 times higher BESS capacity. The initial economic effort is quadrupled. Even without explicitly accounting for asset degradation, the traditional sizing method leads to a significant oversizing of the generation and storage portfolio. The installation of a back-up diesel generator would allow to reduce the autonomy required to BESS and to decrease the PV power installed, but no clear indications are usually provided to correctly coordinate the usage of different resources, without moving excessively towards a strongly fuel-based solution.

Table 6.1: Sizing initial investment (IC) using traditional approach and IMY procedure.

	PV [kW]	DG [kW]	BESS [kWh]	IC [k€]
Traditional sizing	172	/	1471	830
IMY	91	16	215	235

The numerical results in Table 6.1 confirm the importance of adopting optimization tools for an accurate planning of resources. The algorithm evaluates all the possible configurations that would satisfy the load and selects the one at the lowest overall cost, providing detailed information on the assets to be installed, on their operation over time and on pivotal economic indicators. This approach improves the reliability of the initial design and gives accurate information about the economics of the system, enabling more informed decisions and long-term plans and increasing the chances of a successful project.

6.3 Computational performances

As mentioned in Section 2.3 and recalled in Section 6.1, the first objective of the work, namely an effective and accurate modelling of microgrid planning for rural electrification, could not be separated from the second, which is a commitment to advance the state of the art in terms of optimization techniques. In particular, Chapters 3 and 4 present two novel approaches that contribute to a drastic reduction of the computational burden, while preserving excellent quality of the results.

The IMY procedure proposed in Chapter 3 adopts an iterative procedure to describe complex non-linear phenomena within a MILP optimization by means of constant parameters to be updated at each iteration. This method converges in few hours, while the corresponding traditional One-Shot Multi-Year (OSMY) could not even find a feasible solution in 5 days. Adopting representative days to push OSMY towards the optimal point allows to validate the results of IMY, which are essentially the same of the full MILP, with an impressive gain in optimization time (see Section 3.5 and Appendix C).

This method represents the core model of the multi-objective optimization performed in Chapters 4 and 5, as shown in Figure 6.1. The extension of the decision process beyond techno-economic evaluations is of pivotal importance when dealing with energy access in the Global South. However, depending on the number of objective functions and on the desired density of the Pareto frontier, i.e., set of efficient solutions, the computational burden may become prohibitive and hinder the resolution of such a complex problem. For this reason, Chapter 4 has a strong focus on facing the limitations of current multi-objective methods; it proposes the novel Advanced AUGMECON2 (A-AUGMECON2) procedure, provided with an online Pareto filter that skips all the redundant optimizations and drastically reduces the computational burden, being almost 3 times faster than AUGMECON2. Results in Section 4.9 show that the density of the Pareto curve is the same as in the standard AUGMECON2; hence, there is no loss of information and the decision making process is facilitated by a reduced number of options and the removal of recurrent solutions.
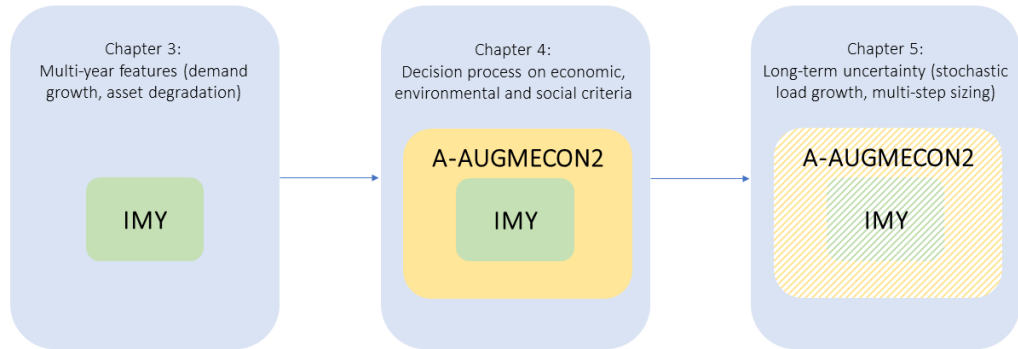
Figure 6.1: Methods proposed in Part II.

Dealing with long-term uncertainty accounting for the stochasticity of load scenarios and enabling capacity expansions along the project lifetime increases the complexity of

the problem. Hence, some practical considerations are made in Section 5.5 to improve the tractability of the full stochastic model presented in Chapter 5. A "lighter" version of A-AUGMECON2 and IMY is adopted, reducing the number of decision criteria, the available technologies, and selecting a reasonable number of demand growth scenarios and capacity expansion windows.

Both mathematical procedures and practical experience of the developer can contribute to improve the tractability of a model, identifying the features that is worth investigating in detail and those that can be neglected or simplified to ease the analysis.

It is worth noticing that the novel IMY and A-AUGMECON2 procedures are not limited to the specific application of rural microgrid planning. On the contrary, they have general validity and can be applied to any complex problem. In particular, the method proposed by IMY to represent non-linear phenomena within a MILP framework is easily replicable in any model. The algorithm of A-AUGMECON2 is an efficient resolution method for any multi-objective optimization; its advantages over traditional methods increase with the complexity of the problem under study. Its source code is publicly available (see Appendix D) and can be adopted by researchers and developers of any sector.

6.4 Holistic decision making

A comprehensive evaluation of a rural electrification project is necessary to its effectiveness and durability. A multi-disciplinary analysis allows to evaluate trade-offs between different needs and impacts and strengthen the role of the action of fostering development in the community while being economically efficient and environmentally sustainable.

It is possible to include social and environmental considerations in least-cost studies by bringing all the impacts into the form of cost: as an example, Appendix E proposes a methodology to evaluate the different development opportunities offered by different electrification technologies by means of a shadow cost analysis. A more explicit and detailed analysis of the manifold impacts related to energy access projects can be provided by multi-objective optimizations, whose output preserves the complexity of the problem and leaves room for site-specific evaluations of the decision maker.

The results of Chapter 4 highlight the value of multi-disciplinary approaches and discusses the relationships between the different indicators. In particular, it is worth noticing that the decrease in costs of RES generators and storage has led least-cost solutions to be characterized by high renewable fractions ($> 80\%$) and limited carbon emissions. Moreover, CO_2 accounting with a Life Cycle Assessment (LCA) approach, instead of limiting the analysis to direct emissions, has led to interesting conclusions, namely that the solution with minimum emissions for the analysed case study was not that entirely powered by renewable sources. On the contrary, the sporadic use of diesel in the last years of the project (higher load and worse component performances) has less impact than oversizing the PV panels at the beginning of the project.

A complete coverage of the public lighting needs brings about 20% increase in the total cost. Illuminated streets in the evening allow improving the safety conditions of the community and the quality of recreational activities, with a significant impact on general well-being. At least partial coverage of the service would therefore be recommended, based on budget availability.

If budget restrictions limit the initial investment of the implementing entity, a higher reliance on DG generators allows reducing installation costs and spreading expenses more evenly between CAPEX and OPEX. Fuel-based options are also characterized by limited land use and high employment opportunities, because of consistent O&M needs and fuel procurement operations.

The use of multi-objective optimizations introduces the added complexity of the availability of a portfolio of solutions instead of a single option. This is, however, necessary to enable the decision maker to have a holistic view of the possible configurations of the system and of their impacts on the different decision criteria. The choice of the final microgrid architecture and operation will derive from the experience of the decision maker, who may lean towards one solution or another based on specific characteristics of the site, which can be decisive in the success of a project and which are often difficult to model in an optimization.

6.5 Long-term perspective

One of the biggest challenges in planning rural microgrids is the formulation of realistic long-term scenarios. Wrong assumptions may hinder the durability of the project and leave the community without a reliable service.

First steps in the direction of careful multi-year planning were taken in Chapters 3 and 4, where the load trend was estimated according to the results of a system dynamic study in a similar context, accounting for increasing appliances penetration and number of customers in relation to socio-economic development of the community thanks to the presence of electricity [72].

Even though the long-term trend was derived from an accurate multi-disciplinary study, it is worth highlighting that a wide variety of environmental and socio-economic factors may intervene and determine an unforeseen load behaviour. Therefore, dealing with uncertainty in planning models is necessary to strengthen the reliability of the results.

Chapter 5 adopts a stochastic approach to evaluate different realizations of the demand over time. The trend in [72] represents the central scenario and is associated to a 50% probability of occurrence, while 4 additional scenarios are identified as less likely realizations. The resulting microgrid is able to cope with any realization of the input and represents the optimal compromise solution, given the probability of occurrence of the different scenarios.

The impact of adopting a long-term perspective and accounting for demand uncertainty is shown in Table 6.2, where the results of the deterministic multi-objective optimization using the growth trend from [72] is compared to the configuration that includes a stochastic analysis of the load in case of single-step and multi-step investment.

A stochastic approach provides more cautious solutions, whose feasibility is guaranteed in any scenario. Therefore, energy shortages are prevented and a reliable service to the community can be provided independently of the actual realization in time. This comes at the cost of higher expenses. Indeed, Table 6.2 shows that the stochastic least-cost option with a 90% coverage of the street lighting service has an NPC of 4% higher than the deterministic solution with full public lighting coverage. However, this effect is mitigated and even counterbalanced by the inclusion of capacity expansion windows: the possibility to defer investments allows to tailor subsequent installations on the actual realization of

Table 6.2: Least-cost solutions at high public lighting (PL) coverage in case of multi-objective (MO) optimization, multi-objective with stochastic long-term load scenarios (MOS) and multi-objective with stochastic long-term load scenarios and multi-step sizing (MOSMS).

	NPC	CO_2	LU
	[k€]	[$kgCO_2$]	[m^2]
MO - 100% PL	367	660	946
MOS - 90% PL	382	640	932
MOSMS - 90% PL	344	497	1112

the load and reduce risks and total costs. Moreover, multi-steps investment configurations favour higher RES penetration and, consequently, lower carbon emissions and higher land use. RES generators are characterized by relevant upfront costs and almost null O&M expenses and this leads the optimizer to penalise such assets in the first years; the investment reduction associated to discounted cash flows in later years reduces this economic downside of renewable assets with respect to fuel-fired generators.

6.6 Scope of application

A wide variety of stakeholders, including public institutions, NGOs, academia and companies, is involved in projects for access to electricity; therefore, the priorities and the objectives may vary depending on the funding sources and on the implementing entity. Moreover, microgrid planning studies may be part of wider analyses on regional and national plans or concern the electrification of specific communities.

These elements significantly impact on the type of tool to be used in planning phase, on the level of detail and on the criteria to be considered for the decision making process.

The work in Part II provides a number of features that can be easily included or excluded from the analysis, depending on the specific needs. In particular, Chapter 3 provided the least-cost solution derived from a detailed hourly simulation of the project lifetime including multi-year characteristics, namely load growth and asset degradation, with a focus on power-dependent capacity reduction of batteries. This type of study is particularly suitable for private companies focusing on a specific system to be installed and willing to estimate costs with very high accuracy in the implementation phase.

In pre-feasibility and feasibility studies, less details are needed to assess the viability of the project and condensed time series using representative days can be adopted to drastically reduce the computational burden and obtain rapidly good-quality results. Tables 3.4 and 3.5 in Section 3.5 highlight that the use of typical days has limited influence on the objective function and can provide good preliminary estimates of costs and optimal microgrid architecture. The further advantage of reducing the time frame analysed is that fast computational times enable the use of open-source solvers and extends the possibility of using advanced tools to stakeholders that traditionally do not have access to commercial solvers. Moreover, fast versions of the model could be integrated into more complex

frameworks, e.g. in rural electrification planning tools aimed at defining the most suitable electrification strategy for a region, defining whether to connect communities to the national network or to adopt isolated systems [121].

Representative days are also adopted in Chapters 4 and 5, where the multi-objective optimization significantly increases the computational burden. As discussed in Section 4.8.3, the use of a comprehensive multi-objective optimization is suitable for a first evaluation of the planning options, as it provides a full picture of the problem and allows to evaluate the trade-offs between different decision criteria. It could be followed by a more detailed simulation of the most suitable options. Holistic analyses are of particular interest for public and third sector actors, as they usually focus not only on the techno-economic feasibility of the system, but also on its effectiveness in stimulating development. Awareness is also increasing in the private sector on the importance of careful and comprehensive planning for the success of a project; complex and holistic decision-making processes are therefore essential regardless of the implementing entity and, if possible, given the available resources, they are always preferable to purely techno-economic studies.

6.7 Conclusion

The modelling framework proposed in this work aims at providing decision makers with an effective, accurate and comprehensive planning tool, whose available features could be easily adapted to the needs of the specific application. This objective is reached by also developing novel algorithms aimed at reducing the computational burden of complex problems.

The stakeholders active in the rural electrification sector can take advantage of the proposed approach, adapting it to their own budget and computational resource constraints and to the desired degree of detail in terms of component modelling and impact assessment.

The tool provides significant advantages with respect to traditional sizing methods, which tend to oversize assets and cannot effectively manage hybrid system design. On the contrary, the proposed approach can easily identify the least-cost solution, accounting for long-term phenomena, and evaluating the trade-offs between various decision criteria relating to the different scopes of sustainability, namely economic, environmental and social.

Chapter 7

Conclusions and future work

7.1 Conclusions

7.1.1 Wrapping up

This doctoral thesis analyses the energy access problem, focusing on isolated microgrids, which are playing a crucial role in fostering rural electrification. In particular, this work provides a holistic modelling framework to enable decision makers to make informed decisions, accounting for long term phenomena and for techno-economic, environmental and social aspects.

The general framework on access to electricity in the Global South is provided in Chapter 1, where the main global figures and the role of energy in unleashing development are discussed. Then, the main electrification strategies are presented and the attention of this work on microgrids is motivated by the current projections on the urgent need of isolated systems to accelerate the achievement of universal access to electricity.

Advanced optimization tools enable more accurate and efficient designs with respect to traditional methods. Hence, their adoption can support practitioners in effectively planning rural electrification projects. Chapter 2 reviews the available literature on microgrid planning, identifying the most common approaches, the gaps in the state of the art and the obstacles to formulate a comprehensive model. From these, the two main objectives of the doctoral work are derived, namely the development of a holistic MILP microgrid planning model and the improvement of current traditional algorithms to reduce the computational burden and enable accurate and detailed analyses.

The most common approach to optimize the design and operation of rural microgrids is to adopt single-year methods, assuming the perfect replication of the first year along the project lifetime. This methodology fails to consider the multi-year characteristics of the system, which may significantly impact the results. The model proposed in Chapter 3 describes a microgrid planning problem accounting for demand growth and asset degradation. In particular, it considers linear degradation of the RES generators and a BESS capacity reduction depending on its hourly operation. This last phenomenon is modelled by means of constant parameters to be updated in an iterative procedure. The results highlight that single-year methods lead to suboptimal solutions and may cause energy shortages and

underestimation of costs.

A crucial element in planning tools is the indicator chosen as objective function. Basically all the works in literature adopt an economic objective function, to ensure the efficiency of the investment. An increasing interest in environmental issues and the political pressure on the exploitation of renewable sources has encouraged some researchers to include also carbon emissions among the decision criteria defining the optimal configuration of the system. Social impacts are usually overlooked, despite being decisive in rural contexts in determining the success of the project and, consequently, its economic efficiency. The issue of a holistic decision-making process is tackled in Chapter 4, where a multi-objective optimization is solved minimizing costs, life-cycle emissions and land use, and maximizing job creation and public lighting coverage. Moreover, a novel methodology to skip redundant simulations is developed. It allows to drastically reduce the computational burden and it is a general algorithm which can be applied to any sector; hence, it represents a relevant advancement in the analysis of complex problems through multi-objective optimization.

Finally, the algorithm is extended in Chapter 5 with the analysis of long-term uncertainty by including stochastic load scenarios characterized by different linear growth factors. Moreover, capacity expansions windows are implemented to permit deferred investments and adapt the microgrid architecture to the actual realization of the demand over time. Multi-step investments allow significant savings and are robust solutions against highly uncertain inputs.

A wrap-up and critical discussion on the features of the model is provided in Chapter 6. A numerical example underlines the importance of adopting optimization tools rather than traditional sizing methods, that are based on strong simplifying assumptions and cannot efficiently handle hybrid systems. The main advancements introduced by the work are discussed, highlighting the flexibility of the model, whose functions can be easily adapted to the specific needs of the user in terms of computational resources, degree of detail, decision criteria.

7.1.2   Contribution to SDG7

Given the relevance of the topic investigated and of the results obtained, this work provides a significant contribution in facilitating rural electrification through microgrids and thus the achievement of SDG7, as it guides policy and business decision makers in effectively planning isolated systems.

In particular, the findings discussed in Part II confirm the economic efficiency of RES-based plants, to be supported by storage system, that also address the climate concerns by exploiting local resources and limiting the use of fuel. Moreover, when the stochastic feature and a comprehensive set of indicators are included, stakeholders are provided with robust options that reduce financial risks because of the thorough evaluation of uncertainty and of the trade-offs between different relevant decision criteria. Planning a stepwise installation of components, to be tailored on the long-term trends of the demand, in contrast with a full installation at the outset of the project, allows to defer costs, thus encouraging rapid and safe investments.

In conclusion, this doctoral thesis provides a sound methodology and valuable insights on the practical characteristics of isolated microgrid projects, fostering the realization of

universal access to electricity.

Computer tools provide a decisive support to the stakeholders in the sector for developing efficient and effective electrification plans. The synergy between different tools contributing to different aspects of the electricity access process is essential to foster the connection of unelectrified communities by 2030.

In particular, the algorithm presented in this thesis benefits from the interaction with bottom-up load estimation tools [82, 122] to accurately formulate the daily demand curves. Moreover, a simplified version of the deterministic least-cost formulation of the algorithm is adopted to size and estimate the cost of microgrids in GISEle [123], an open-source regional electrification planning tool aimed at defining the best electrification solution (grid extension or microgrid) to connect all people living in the target area.

7.2 Limitations and future developments

7.2.1 Accessibility of the tool

Although the procedure represents a significant advancement of the state of the art, the computational burden is still prone to improvements, as MILP optimizations are extremely sensitive to input data and number of variable and constraints. Currently, the size of the problem and the need of commercial solvers do not allow the extensive use of the tool by non-technical users, e.g. policy makers and NGOs. Hence, additional work is needed to enable the formulation of an efficient version to be made available to the stakeholders in the sector of energy access.

At the present status, the tool is currently usable by academic stakeholders, but it is hardly accessible to other entities. Hence, its use is plausible in the context of electrification projects developed in consortia that include researchers in the sector who have at their disposal the instruments necessary for the use of the routine.

However, this limitation does not constitute a barrier to the effective practical use of the tool, since very often national or regional plans and large electrification projects are implemented following the Quadruple Helix approach [124], where representatives of private players, civil society organisations, academia and public institutions are engaged and cooperate to identify the solutions that best meet the needs of communities.

7.2.2 Synergy with other electrification models

A comprehensive analysis of the electricity access problem would entail the synergy between different routines tackling different aspects, phases and/or scales of the electrification process. Even though the methodology here presented exploits tools and findings available in literature to make realistic assumptions on demand estimation and long-term trends [47, 72, 79], the heavy computational burden does not allow the interaction of the full routine with complex and large-scale models. At the moment, an extremely simplified version is included in the GISEle [123] regional electrification planning tool.

Further efforts in the development of efficient algorithms for computationally-intensive problems would enable the effective connection of the model here presented with others in

the literature, thus making available to stakeholders complete tools for planning electrification projects.

In particular, the formulation of long-term demand scenarios could be directly derived from system dynamic models [65,125], accounting for specific socio-economic characteristics and development opportunities unleashed by access to electricity. The system dynamic model could iteratively interact with the microgrid planning tool to correctly account for long-term evolutions, as proposed in [72].

Furthermore, the tool could exploit georeferenced data to design the system also in terms of optimal placement of the units, and plan the least-cost distribution system. This would also allow to increase the scale of the analysis and consider the aggregation, through a network of electrical connections, of several microgrids in the same area.

7.2.3 Numerical assumptions

When developing a model, assumptions are made in order to decide on what to emphasize, what to overlook and how to describe the phenomena involved. This concerns every aspect of the tool, including but not limited to input data, objective functions and constraints, and affects the numerical results, how they are presented and the derived insights.

As for the assumptions of the modelling of components, future versions of the algorithm may include considerations on fuel procurement, transport and storage for diesel generators. This would negatively impact on the economic convenience of such technological option. However, this is not supposed to significantly affect the results, as fuel-based options already play a marginal role in cost and emissions efficient solutions.

The choice on the reduced time frame to be represented and explicitly modelled using typical days has been defined following a thorough literature review and internal simulations. However, this process could be formalized: a sensitivity analysis could be performed to determine the most appropriate number of typical days and thus identify the optimal trade-off between computational burden and accuracy of the results.

The long-term evolution of the load is certainly the most challenging assumption a modeller must face when dealing with first access to electricity. This work tackles this issue by capitalizing on previous works available in the literature and real case studies [47,72] to estimate a reasonable number of growth scenarios, each characterized by a probability of occurrence. Such stochastic method allows to provide the user with robust and reliable options, that cover against any realization of the input load and avoid shortages of energy related to deterministic incorrect forecasts at planning stage. This approach could be extended to other uncertain parameters; for example, cost trends could be characterized by stochastic behaviour, strengthening the quality of the results against significant prices variations over time.

7.2.4 Relevance of decision criteria

Finally, multi-objective optimization requires a preliminary selection of the relevant indicators to be evaluated, because each additional objective function produces a significant increase of the computational burden. This drawback would play in favour of Multi-Criteria Decision Analysis (MCDA), that is extremely efficient and is not significantly affected by the inclusion of additional indicators. However, MCDA entails the assignment of weights

to the decision criteria, influencing the final solution. In contrast, multi-objective optimization allows a full evaluation of the trade-offs between the different objective functions. Therefore, the decision maker may tend towards multi-objective optimization when he/she wishes to fully analyse the reciprocal impacts of a limited number of aspects; MCDA is preferable when a wide variety of indicators needs to be included and when their priority is already known.

The objective functions selected in this work, namely net present cost, life-cycle emission, land use, local jobs creation and coverage of public lighting service, represent a valid selection of criteria which are usually relevant for the stakeholders. Nonetheless, there may be conditions in which such group of functions does not reflect the interests of the decision maker. For example, land use may not be a relevant issue if wide rooftop areas are available for PV installations. In that case, the objective function can be easily excluded from the analysis and, if desired, substituted by other indicators, for example the reliability of the different technologies or the social LCA of the available components.

If the model is effectively integrated in large-scale analysis, e.g. electrification planning at country level, as wished for future developments of the work, the current trade-offs between the objective functions may change and modify the resulting solutions. For example, the analysis of the potential for rural microgrids on a wide area and the evaluation of the related jobs generation at national level may even reveal compound effects on the total number of people employed in the sector, providing a more complete vision of the impacts of such systems. Hence, the scale up of the proposed model is desirable and would be beneficial to support decision makers in acquiring a thorough and comprehensive understanding of access to electricity.

Part IV

Appendices

Appendix A

Nomenclature

Table A.1: Definition of indexes, parameters and variables for the microgrid planning model presented in Chapter 3 and 4.

Indexes			
h	Hours	y	Years
g	Diesel generators (DG)	p	Photovoltaic panels (PV)
w	Wind turbines (WT)	b	Batteries (BESS)
i	Components, $i \in \{g, p, w, b\}$		
Parameters			
M	Big constant	H	Number of hours per year
$\overline{H}$	Project lifetime in hours	$\overline{Y}$	Project lifetime in years
Y_i^{life}	Component lifetime	c_i	Unit capital cost
m_i	Unit maintenance cost	e_i	Unit installation emissions
e_i^{op}	Unit operation emissions	lo_i	Unit land occupation
j_i	Unit jobs from value chain	j_g^f	Unit jobs form fuel use
δ	Demand growth rate	L_h^{tot}	Total lighting demand
d_h	Discount factor	$\overline{ENS}$	Max energy not served
γ_z	Forecast error of z	$P_{h,p}^{pv}$	Available PV power
$P_{h,w}^{wt}$	Available WT power	$\rho_{h,p}^{pv}$	Linear PV degradation rate
$\rho_{h,p}^{wt}$	Linear WT degradation rate	A, B	Fuel consumption coefficients
f	Cost of fuel	H_g^{life}	Total DG working hours
$\overline{P}_g$	Max DG power	$\underline{P}_g$	Min DG power
DOD_b	Depth of Discharge	$C_{h,b}^{res}$	Residual BESS capacity
$\eta(PQ_{h,b})$	Power-dependent efficiency	$\overline{\eta}_b$	Max BESS efficiency
$\beta_{h,b}$	Relative BESS efficiency	$\overline{C}_b$	Max BESS capacity
$\overline{\alpha}_b$	Max relative BESS capacity	$\underline{\alpha}_b$	Min relative BESS capacity
$\alpha_{h,b}$	Relative residual BESS capacity	$k_{h,b}$	BESS replacement counter
$\overline{PQ}_b$	Max power-to-energy ratio	$PQ_{h,b}$	Power-to-energy ratio
$Q_{h,b}^{thr}$	Cumulative throughput	$n(PQ_{h,b})$	Power-dependent max cycles

Table A.1: Definition of indexes, parameters and variables for the microgrid planning model presented in Chapter 3 and 4 (continued).

Variables			
NPC	Net present cost	IC_i	Initial investment cost
$O\&M_i$	O&M cost	RC_i	Replacement cost
RV_i	Residual value	$CO2$	Total LCA emissions
$CCO2_i$	Emissions from installation	$OCO2_i$	Emissions from O&M
LU	Total land use	JC	Total job creation
CJC_i	Jobs from whole value chain	OJC_g	Jobs from fuel use
PL	Public lighting coverage (%)	N_i	Number of units installed
D_h	Load demand	D_h^u	Unmet demand
L_h	Fulfilled lighting demand	P_h^{ren}	Renewable power injected
R_h	Total reserve requirement	$FC_{h,g}$	Fuel consumption
$P_{h,g}^{dg}$	Power produced by DG	$R_{h,g}^{dg}$	Reserve provided by DG
$U_{h,g}$	Active DG units (integer)	$w_{h,b}^{dch}$	Binary variable on BESS state
$P_{h,b}^{dch}$	Discharging power of BESS	$P_{h,b}^{ch}$	Charging power of BESS
$R_{h,b}^{sb}$	Reserve provided by BESS	$Q_{h,b}$	Energy level of BESS

Appendix B

Soroti load

The case study adopted to test the approaches proposed in Part II refers to the community of Soroti, where few households and business activities are reached by the electrical grid in the city centre, while the rest of the community uses small diesel generators or traditional energy sources to satisfy their needs. Mandelli performed surveys locally [79], investigating the typical conditions of the peripheral area and considering a hypothetical microgrid composed by 100 households and common businesses and services.

The information collected on field is elaborated in the LoadProGen tool [82] to build the total load profile of the community (shown in Figure 3.3a). The input data necessary to formulate the profile are contained in Table B.1 and their meaning is listed below:

(i) *Class type.* Type of user class, associated to a portfolio of appliances and a typical load profile.

(ii) N_{US}. Number of users within the class.

(iii) *App name.* Type of appliance.

(iv) *P [W].* Nominal power of the appliance.

(v) N_{App}. Number of appliances within a user class.

(vi) h_{funct}. Daily functioning time of the appliance.

(vii) W_f. Possible functioning windows of the appliance during the day (may exceed h_{funct}).

Table B.1: Load input data for Soroti community.

Class type	N_{US}	App name	P [W]	N_{App}	h_{funct}	W_{f1}		W_{f2}		W_{f3}		Tot_W
						h_{start}	h_{stop}	h_{start}	h_{stop}	h_{start}	h_{stop}	
Family 1	50	Lights	3	4	6	0	2	17	24	-	-	9
		Phone Charger	5	2	3	0	9	13	15	17	24	18
		Security Light	5	1	12	0	7	17	24	-	-	14
Family 2	15	Lights	3	4	6	0	2	17	24	-	-	9
		Phone Charger	5	2	3	0	9	13	15	17	24	18
		Security Light	5	1	12	0	7	17	24	-	-	14
		Radio	5	1	4	6	9	17	24	-	-	10
		AC-TV(small)	100	1	5	11	15	17	24	-	-	11
Family 3	15	Lights	3	8	6	0	2	17	24	-	-	9
		Phone Charger	5	2	3	0	9	13	15	17	24	18
		Security Light	5	2	12	0	7	17	24	-	-	14
		Radio	5	1	4	6	9	17	24	-	-	10
		AC-TV(small)	100	1	5	11	15	17	24	-	-	11
		Fridge (small)	250	1	5	0	24	-	-	-	-	24
Family 4	10	Lights	3	12	6	0	2	17	24	-	-	9
		Phone Charger	5	4	3	0	9	13	15	17	24	18
		Security Light	5	4	12	0	7	17	24	-	-	14
		Radio	5	1	4	6	9	17	24	-	-	10
		AC-TV(small)	100	1	5	11	15	17	24	-	-	11
		Fridge (small)	250	1	5	0	24	-	-	-	-	24
		Standing Fan	55	1	6	8	24	-	-	-	-	16
		Decoder	15	1	5	11	15	17	24	-	-	11
		Internet Router	20	1	6	0	24	-	-	-	-	24
		Laptop (small)	55	1	6	0	2	11	15	17	24	13
Family 5	5	Lights	3	16	6	0	2	17	24	-	-	9
		Phone Charger	5	4	3	0	9	13	15	17	24	18
		Security Light	5	6	12	0	7	17	24	-	-	14
		Radio	5	2	4	6	9	17	24	-	-	10

Table B.1: Load input data for Soroti community (continued).

Class type	N_{US}	App name	P [W]	N_{App}	h_{funct}	W_{f1}		W_{f2}		W_{f3}		Tot_W
						h_{start}	h_{stop}	h_{start}	h_{stop}	h_{start}	h_{stop}	
		AC-TV(big)	200	1	6	11	15	17	24	-	-	11
		Fridge (big)	400	1	5	0	24	-	-	-	-	24
		Standing Fan	55	2	6	8	24	-	-	-	-	16
		Decoder	15	1	6	11	15	17	24	-	-	11
		Internet Router	20	1	8	0	24	-	-	-	-	24
		Laptop (big)	80	2	8	0	2	11	15	17	24	13
Family 6	5	Lights	3	16	6	0	2	17	24	-	-	9
		Phone Charger	5	4	3	0	9	13	15	17	24	18
		Security Light	5	6	12	0	7	17	24	-	-	14
		Radio	5	2	4	6	9	17	24	-	-	10
		AC-TV(big)	200	1	6	11	15	17	24	-	-	11
		Fridge (big)	400	1	5	0	24	-	-	-	-	24
		Standing Fan	55	2	6	8	24	-	-	-	-	16
		Decoder	15	1	6	11	15	17	24	-	-	11
		Internet Router	20	1	8	0	24	-	-	-	-	24
		Laptop (big)	80	2	8	0	2	11	15	17	24	13
		Hair Dryer	1000	1	0.5	17	24	-	-	-	-	7
		Printer	50	1	0.5	17	24	-	-	-	-	7
		Stereo	100	1	3	17	24	-	-	-	-	7
		Water Heater	660	1	2	0	2	18	24	-	-	8
Enterprise 1	15	Fluor. Tube (small)	36	10	6	7	11	16	20	-	-	8
		Phone Charger	5	4	3	7	13	15	20	-	-	11
		Security Light	5	4	12	0	7	17	24	-	-	14
		Internet Router	20	1	10	7	20	-	-	-	-	13
		Laptop (big)	80	1	8	7	13	15	20	-	-	11
		Laptop (small)	55	5	8	7	13	15	20	-	-	11
		Printer	50	2	2	7	13	15	20	-	-	11
		Standing Fan	55	2	8	7	13	15	20	-	-	11

Table B.1: Load input data for Soroti community (continued).

Class type	N_{US}	App name	P [W]	N_{App}	h_{funct}	W_{f1}		W_{f2}		W_{f3}		Tot_W
						h_{start}	h_{stop}	h_{start}	h_{stop}	h_{start}	h_{stop}	
Enterprise 2	5	Fluor. Tube (big)	47	20	6	7	11	16	20	-	-	8
		Phone Charger	5	15	3	7	13	15	20	-	-	11
		Security Light	5	10	12	0	7	17	24	-	-	13
		Internet Router	20	1	10	7	20	-	-	-	-	13
		Laptop (big)	80	5	8	7	13	15	20	-	-	11
		Laptop (small)	55	10	8	7	13	15	20	-	-	11
		Standing Fan	55	5	8	7	13	15	20	-	-	11
		Water Dispenser	550	1	3	7	13	15	20	-	-	11
		Photocopier	750	1	1	7	13	15	20	-	-	11
		Ceiling Fan	75	5	8	7	13	15	20	-	-	11
		PC	400	1	10	7	20	-	-	-	-	13
Mobile Money	5	Lights	3	2	3	8	11	16	20	-	-	7
		Phone Carger	5	3	3	8	18	-	-	-	-	10
		Standing Fan	55	1	6	10	18	-	-	-	-	8
Kiosk	10	Lights	3	2	3	8	11	16	20	-	-	7
		Phone Carger	5	1	3	8	18	-	-	-	-	10
		Standing Fan	55	1	6	10	18	-	-	-	-	8
		Fridge (small)	300	1	8	0	24	-	-	-	-	24
		Fridge (big)	500	1	8	0	24	-	-	-	-	24
Barber	2	Lights	3	5	8	8	13	15	20	-	-	10
		12V Shaver	10	5	6	8	13	15	20	-	-	10
		Ceiling Fan	75	3	8	8	13	15	20	-	-	10
		UV Sterylizer	50	1	2	8	13	15	20	-	-	10
Tailor	3	Lights	5	3	8	8	13	15	20	-	-	10
		Sewing Machine	50	1	3	8	13	15	20	-	-	10
		Ceiling Fan	75	1	8	8	13	15	20	-	-	10
Market Place	1	Lights	3	25	3	8	11	16	20	-	-	7
		Security Light	5	25	12	0	7	17	24	-	-	14

Table B.1: Load input data for Soroti community (continued).

Class type	N_{US}	App name	P [W]	N_{App}	h_{funct}	W_{f1}		W_{f2}		W_{f3}		Tot_W
						h_{start}	h_{stop}	h_{start}	h_{stop}	h_{start}	h_{stop}	
		Fridge (small)	300	3	8	0	24	-	-	-	-	24
		Fridge (big)	500	3	8	0	24	-	-	-	-	24
		Standing Fan	55	10	8	8	13	15	20	-	-	10
		Radio	5	10	4	10	13	15	18	-	-	6
Club	3	Fluor. Tube (small)	36	10	8	0	4	17	24	-	-	11
		Fluor. Tube (big)	47	5	8	0	4	17	24	-	-	11
		Security Light	5	5	12	0	7	17	24	-	-	14
		Phone Charger	5	10	8	15	24	-	-	-	-	9
		AC-TV (small)	130	2	9	0	4	15	24	-	-	13
		AC-TV (big)	200	1	9	0	4	15	24	-	-	13
		PC	400	1	9	0	4	15	24	-	-	13
		Laptop (big)	80	10	6	15	24	-	-	-	-	9
		Printer	50	1	1	15	20	-	-	-	-	5
		PicoProjector	18	1	4	0	2	20	24	-	-	6
		Amplyfier	6	1	4	0	2	20	24	-	-	6
		Ceiling Fan	75	3	8	0	4	15	24	-	-	13
		Music System	178	1	8	0	4	15	24	-	-	13
		Internet Router	20	1	9	0	4	15	24	-	-	13
		Fridge (small)	300	2	8	0	24	-	-	-	-	24
		Fridge (big)	500	1	8	0	24	-	-	-	-	24
Street Lights	1	Lights (Street)	50	100	12	0	7	17	24	-	-	14
		Led Strips	8	100	12	0	7	17	24	-	-	14
Primary School	1	Fluor. Tube (small)	36	10	4	8	17	-	-	-	-	9
		Phone Charger	5	7	3	8	17	-	-	-	-	9
		Security Light	5	4	12	0	7	17	24	-	-	14
Pharmacy	1	Lights	3	10	3	8	11	16	20	-	-	7
		Security Light	5	4	12	0	7	17	24	-	-	14
		Fridge (small)	300	3	8	0	24	-	-	-	-	24

Table B.1: Load input data for Soroti community (continued).

Class type	N_{US}	App name	P [W]	N_{App}	h_{funct}	W_{f1}		W_{f2}		W_{f3}		Tot_W
						h_{start}	h_{stop}	h_{start}	h_{stop}	h_{start}	h_{stop}	
		Fridge (big)	500	2	8	0	24	-	-	-	-	24
		Standing Fan	55	3	8	8	13	15	20	-	-	10

Appendix C

IMY validation

The Iterative Multi-Year (IMY) procedure presented in Chapter 3 has been validated in Section 3.5 by discussing the numerical application on an isolated system in Uganda. This section aims at strengthening the validity of the results by testing the model on two further case studies. To guarantee the convergence of the traditional approach and provide a comparison of the computational burden of the two methodologies, representative days are used.

C.1 Case study 1: Lacor Hospital

St. Mary's Lacor hospital is sited near the city of Gulu, in Northern Uganda, and it is one of the largest private and non-profit hospitals in Equatorial Africa. A measured daily profile in shown in Figure C.1.
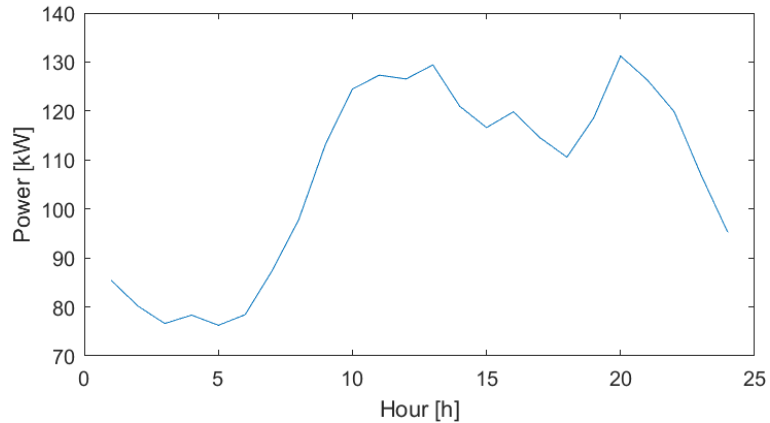
Figure C.1: Measured load profile of St. Mary's Lacor hospital.

The possible assets to be installed are DG units, PV panels and BESS. The techno-

economic specifications of the components are described in Section 3.4. The demand is supposed to be growing by 20% every year.

C.2 Case study 2: Ngarenanyuki secondary school

The school is located in a rural area in the Arusha region, Tanzania, and hosts around 500 students. A measured daily profile in shown in Figure C.2.
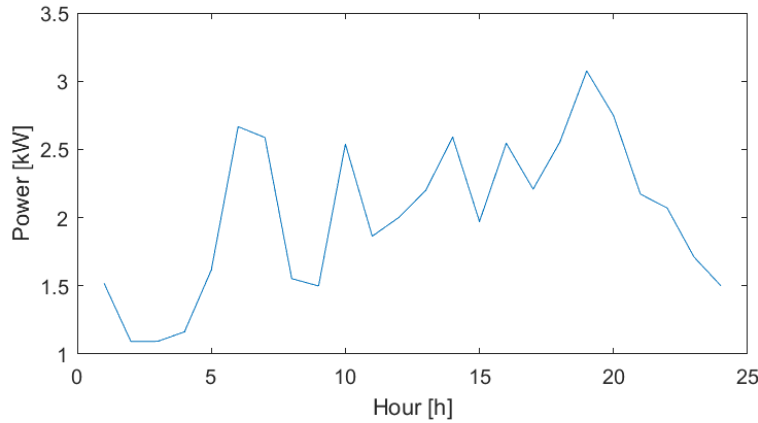
Figure C.2: Measured load profile of Ngarenanyuki secondary school.

The possible assets to be installed are PV panels and BESS. The techno-economic specifications of the components are described in Section 3.4. The demand is supposed to be growing by 20% every year.

C.3 Numerical results

The results obtained by testing IMYrd and OSMYrd on the two case studies are presented in Tables C.1 and C.2.

Table C.1: Optimization outputs (I)

		Time	NPC	IC	O&M	RC	RV
		[s]	[k€]	[k€]	[k€]	[k€]	[k€]
Lacor	IMYrd	2	2910	1915	1175	182	362
	OSMYrd	55140	2894	2011	1112	166	395
Ngarenanyuki	IMYrd	3	69	78	8	/	17
	OSMYrd	249	68	78	8	/	18

Table C.2: Optimization outputs (II)

		PV	DG	BESS	Y_b^{repl}	$\alpha_{\overline{H},b}$
		[kW]	[kW]	[kW]	[y]	[%]
Lacor	IMYrd	883	176	1258	/	83
	OSMYrd	905	176	1411	/	84
Ngarenanyuki	IMYrd	30	/	84	/	87
	OSMYrd	30	/	83	/	88

It is worth noticing that also in these instances the IMY procedure enables a significant reduction of the computational burden. In particular, the Lacor case sees a dramatic decrease from more than 15 hours down to 2 seconds. The architecture considered for Ngarenanyuki only admits the installation of solar panels and batteries, facilitating the definition of the optimal operating strategy, which involves more complex dynamics when fuel-fired generators are present; hence, OSMYrd only takes about 4 minutes to converge, but IMYrd still allows to significantly reduce the total time, which reaches 3 seconds.

The NPC difference does not exceed 1.5%, which is even below the expectations, given the 3% mipgap [78]. Limited variations on the assets installed can be identified, with an almost equal final relative BESS capacity $\alpha_{\overline{H},b}$.

These results confirm the findings of Chapter 3, conferring universal value upon the proposed approach, highlighting the quality of the results and the relevant advantages in terms of computational times.

Moreover, since the approach presented in Chapter 3 constitutes the core of the optimizations carried out in subsequent developments (Chapters 4 and 5), the presence of Appendix C guarantees the robustness of the results of the whole work with respect to the variation of the case study and input profiles.

Appendix D

A-AUGMECON2 source code

For the sake of clarity, the GAMS source code of A-AUGMECON2 is here applied to a test knapsack problem and it is publicly available on the GitHub platform at the following link: `https://github.com/marinapet/multi-objective`.

```
1    $title A-AUGMECON2:Advanced version of AUGMECON2 for Multiobjective
        Optimization
2    $ontext
3    The advanced version of AUGMECON2, denoted as A-AUGMECON2, is provided
        with
4    a novel pruning algorithm that avoids solving redundant optimizations,
5    leading to a significant reduction of the computational burden.
6
7    The algorithm has been developed starting from the AUGMECON2 code
8    available in GAMS Model Library at the following link:
9    https://www.gams.com/latest/gamslib_ml/libhtml/gamslib_epscmmip.html
10
11   For the sake of simplicity, A-AUGMECON2 is here applied to a trivial
12   Multi-Objective Integer Programming problem(specifically a Multi-Objective
13   Multi-Dimensional Knapsack Problem) with 50 binary variables X, 2
        objective
14   functions and 2 constraints. The higher the complexity of the problem to
        be
15   optimized in terms of number of objective functions and density of the
        Pareto
16   frontier, the more the novel A-AUGMECON2 outperforms the standard
        AUGMECON2.
17
18
19   Additional information can be found at:
20   https://doi.org/10.1016/j.apenergy.2021.117283
21
22   Marina Petrelli, Davide Fioriti, Alberto Berizzi, Cristian Bovo, Davide
        Poli,
23   "A novel multi-objective method with online Pareto pruning for multi-year
24   optimization of rural microgrids", Applied Energy, Volume 299, 2021,
        117283.
25
26
```

```
27   The paper compares the results of the novel A-AUGMECON2 with AUGMECON2
       applied
28   to a rural microgrid planning problem, evaluating costs, emissions, land
29   use, job creation and public lighting coverage. A-AUGMECON2 allows to
       reduce
30   the computational burden by 48% and the number of points in the Pareto
       frontier
31   by 42%, removing redundant simulations and improving the quality and
       readibility
32   of the results.
33
34
35   INSTRUCTIONS FOR REPLICATION:
36   In order to apply A-AUGMECON2 to a different model, it is enough to
       substitute
37   the Knapsack Problem (whose description finishes at line 98) with the
       desired
38   optimization problem. It is necessary to specify the set of objective
       functions
39   K, the related variable z(K) and direction of optimization dir(K). The
       desired
40   density of the Pareto curve should be set at line 198.
41   $offtext
42
43
44   $eolcom //
45   $STitle Example model definitions
46
47   Sets
48   I       constraints        /  i1* i2 /
49   J       decision variables /  j1*j50 /
50   K       objective functions /  k1* k2 /
51
52   $set min -1
53   $set max +1
54   Parameter
55   dir(K) direction of the objective functions / k1 %max%, k2 %max% /
56   b(I)    RHS of the constraints / i1 1445, i2 1502.5 /
57
58   Table c(K,J) matrix of objective function coefficients C
59   j1   j2   j3   j4   j5   j6   j7   j8   j9 j10 j11 j12 j13 j14 j15 j16 j17
60   k1   21   69   26   92   77   30   96   80   60   61   52   92   19   10   63   34 100
61   k2   24   92   53   25   10   31   83   34   64   69   95   40   59   87   13   94   53
62   +
63   j18 j19 j20 j21 j22 j23 j24 j25 j26 j27 j28 j29 j30 j31 j32 j33 j34
64   k1   60   11   12   37 100   74   17   60   69   49   69   49   59   17   21   74   85
65   k2   52   61   53   78   34   89   32   28   56   52   40   41   59   35   96   72   55
66   +
67   j35 j36 j37 j38 j39 j40 j41 j42 j43 j44 j45 j46 j47 j48 j49 j50
68   k1   83   41   29   63   56   38   66   92   25   84   89   21   46   94   96   92
69   k2 100   44   90   66   59   22   72   25   36   16   56   91   61   56   66   53
70   ;
71
72   Table a(I,J) matrix of technological coefficients A
73   j1   j2   j3   j4   j5   j6   j7   j8   j9 j10 j11 j12 j13 j14 j15 j16 j17
74   i1   84   49   68   20   97   74   60   30   13   95   19   41   17   95   73   12   66
75   i2   19   96   93   64   72   91   32   96   44   76   69   82   51   38   52   22   83
```

114

```
76    +
77    j18 j19 j20 j21 j22 j23 j24 j25 j26 j27 j28 j29 j30 j31 j32 j33 j34
78    i1  55  75  20  56  80  59  66  25  70  95  96  62  74  31  59  21  85
79    i2  27  70  56  29  89  86  48  13  95  66  94  16  44  67  90  48  29
80    +
81    j35 j36 j37 j38 j39 j40 j41 j42 j43 j44 j45 j46 j47 j48 j49 j50
82    i1  45  97  23  53  51  95  58  68  62  45  83  82  47  15  52  72
83    i2  90  54  77  28 100  86  51  62  40  54  21  55  50  62  51  77
84    ;
85
86    Variables
87    Z(K)      objective function variables
88    X(J)      decision variables
89    Binary Variables X;
90
91    Equations
92    objfun(K) objective functions
93    con(I)    constraints;
94
95    objfun(K)..   sum(J, c(K,J)*X(J)) =e= Z(K);
96    con(I)..      sum(J, a(I,J)*X(J)) =l= b(I);
97
98    Model example / all /;
99
100   $STitle eps-constraint method
101
102   Set k1(k)  the first element of k
103   km1(k) all but the first elements of k
104   kk(k)  active objective function in constraint allobj;
105
106   k1(k)$(ord(k)=1) = yes; km1(k)=yes; km1(k1) = no;
107
108   Parameter
109   rhs(k)    right hand side of the constrained obj functions in eps-
          constraint
110   maxobj(k) maximum value from the payoff table
111   minobj(k) minimum value from the payoff table
112   numk(k)   ordinal value of k starting with 1
113   val(k)    desired value of objective function in payoff table
114   price(k)  penalty for difference from desired value in payoff table;
115
116   val(k)=0; price(k)=0;
117
118   Scalar
119   iter         total number of iterations
120   elapsed_time elapsed time for eps-constraint
121   start        start time
122   finish       finish time
123
124   Variables
125   a_objval   auxiliary variable for the objective function
126   obj        auxiliary variable during the construction of the payoff table
127
128   Positive Variables
129   s(k)       slack or surplus variables for the eps-constraints
130   s1(k)      slack or surplus variables for the payoff table
131   s2(k)      slack or surplus variables for the payoff table
```

```
132
133   Equations
134   allobj     all the objective functions in one expression
135   con_payoff(k) constraint on desired value of objective function in payoff
        table
136   con_obj(k) constrained objective functions
137   augm_obj   augmented objective function to avoid weakly efficient
        solutions;
138
139   con_obj(km1)..   z(km1) - dir(km1)*s(km1) =e= rhs(km1);
140
141   * We optimize the first objective function and put the others as
        constraints
142   * the second term is for avoiding weakly efficient points
143
144   augm_obj.. a_objval =e= sum(k1,dir(k1)*z(k1)/(maxobj(k1)-minobj(k1)))
145   + 1e-3*sum(km1,power(10,-(numk(km1)-1))*s(km1)/(maxobj(km1)-minobj(km1)));
146
147   allobj.. sum(kk, dir(kk) * z(kk)) - sum(k, price(k) * (s1(k) + s2(k))) =e=
        obj ;
148
149   con_payoff(k).. z(k) + s1(k) - s2(k) =E= val(k) ;
150
151   Model mod_payoff    / example, allobj, con_payoff / ;
152   Model mod_epsmethod / example, con_obj, augm_obj / ;
153
154   Parameter
155   payoff(k,k)  payoff tables entries;
156   Alias(k,kp);
157   Alias(k,k2);
158
159   option optcr=0, limrow=0, limcol=0, solprint=off, solvelink=%Solvelink.
        LoadLibrary%;
160
161   * Generate payoff table applying lexicographic optimization
162   loop(kp,
163   * Modify the priority order to exploit these results as Pareto points,
        removing redundant simulations
164   loop(k2,
165   if (ord(k2) = 1,
166   kk(kp) = yes;
167   elseif ord(k2) <= ord(kp),
168   kk(k2-1) = yes;
169   else
170   kk(k2) = yes;
171   );
172   solve mod_payoff using mip maximizing obj;
173   val(kk) = z.l(kk); // desired value of the objective function
174   price(kk) = 1e5 ; // big constant to penalize distance from desired value
175   kk(k) = no;
176   );
177   payoff(kp,k) = z.l(k);
178   kk(k) = no;
179   * release the desired values of the objective functions for the new
        iteration
180   val(k) = 0; price(k) = 0;
181   );
```

116

```
182
183
184    if (mod_payoff.modelstat <>%ModelStat.Optimal% and
185    mod_payoff.modelstat <>%ModelStat.Integer Solution%,
186    abort 'no optimal solution for mod_payoff');
187
188    file fx  / 2kp50_augmecon2_results.txt /;
189    put fx ' PAYOFF TABLE'/   ;
190    loop (kp,
191    loop(k, put payoff(kp,k):12:2);
192    put /);
193
194    minobj(k)=smin(kp,payoff(kp,k));
195    maxobj(k)=smax(kp,payoff(kp,k));
196
197
198    $if not set gridpoints $set gridpoints 491
199    *$if not set gridpointsred $set gridpointsred 200
200    * gridpointsred coould be used to set reduced densities for some
         objectives
201    Set g            grid points /g0*g%gridpoints%/
202    *    gr_red(gr) reduced grid points /gr0*gr%gridpointsred%/
203    grid(k,g)       grid
204    Parameter
205    gridrhs(k,g) rhs of eps-constraint at grid point
206    maxg(k)        maximum point in grid for objective
207    posg(k)        grid position of objective
208    firstOffMax, lastZero, payoffSol some counters
209    numg(g)        ordinal value of g starting with 0
210    step(k)        step of grid points in objective functions
211    jump(k)        jumps in the grid points traversing;
212
213    lastZero=1; loop(km1, numk(km1)=lastZero; lastZero=lastZero+1); numg(g) =
         ord(g)-1;
214
215    * Here we could define different grid intervals for different objectives
216    * using set gr_red
217    grid(km1,g) = yes;
218    maxg(km1)   = smax(grid(km1,g), numg(g));
219    step(km1)   = (maxobj(km1)- minobj(km1))/maxg(km1);
220    gridrhs(grid(km1,g))$(dir(km1)=-1) = maxobj(km1) - numg(g)/maxg(km1)*(
         maxobj(km1)- minobj(km1));
221    gridrhs(grid(km1,g))$(dir(km1)= 1) = minobj(km1) + numg(g)/maxg(km1)*(
         maxobj(km1)- minobj(km1));
222
223    put / ' Grid points' /;
224    loop (g,
225    loop(km1, put gridrhs(km1,g):12:2);
226    put /);
227    put / 'Efficient solutions' /;
228
229    * Walk the grid points and take shortcuts if the model becomes infeasible
         or
230    * if the calculated slack variables are greater than the step size
231
232    $eval vNTOT power(%gridpoints% + 1, card(K)-1)
233
```

```
234   set         num      /1*%vNTOT%/
235   n(num) ;
236   parameter  numn(num)  ordinal value of num starting with 1
237   numord     ordinal number of the gridpoint examined
238   v(num)      vector of points to be examined; //v(n)=1 if point to be solved
         , v(n)=0 if point to be skipped
239   parameter  Nc          number of combinations to be excluded from
        examination because redundant
240   comb        counter of combinations
241   combb       scalar for computing combinations
242   deltav(k)   identifier of solutions to be excluded
243   posg_v(k)   position to be excluded
244   numordp(k)  ordinal number of payoff table points
245   posgp(k)    grid positions of payoff table points
246   numordPre
247   numordPost;
248
249   alias(km1,kmm1); alias (km1,kkm1);
250
251   n(num) = yes;
252   lastZero=1; loop(n, numn(n)=lastZero; lastZero=lastZero+1);
253   v(n)=1; // initialize all as 1
254
255   * this loop computes gridpoints corresponding to payoff table points
256   loop(km1,  posg(km1)=maxg(km1); posg(kmm1)$(numk(kmm1) NE numk(km1))=0;
257   numordp(km1)= sum(kkm1$(numk(kkm1)>1), posg(kkm1)* prod(kmm1$(numk(kmm1)
        LE numk(kkm1)-1), maxg(kmm1)+1 ))
258   + sum(kkm1$(numk(kkm1)=1), posg(kkm1)) + 1;
259   );
260
261   posg(km1) = 0; iter=0; start=jnow;
262
263   repeat
264
265   numord = sum(km1$(numk(km1)>1), posg(km1)* prod(kmm1$(numk(kmm1) LE numk(
        km1)-1), maxg(kmm1)+1 ))
266   + sum(km1$(numk(km1)=1), posg(km1)) + 1;
267
268   payoffSol=0;
269
270   if(sum(n$(numn(n)=numord), v(n)) = 1,
271
272   * the following two loops verify if the current gridpoint corresponds to a
         point of the payofftable
273   * if so, the optimization is skipped and the solution of the payofftable
        is directly included
274   loop(k1$(sum(km1, posg(km1)) = 0),
275   z.l(k) = payoff(k1,k);
276   payoffSol=1;
277   iter=iter+1;
278   put iter:5:0;
279   loop(k, put z.l(k):12:2);
280   put /;
281   jump(km1)$(%min%=dir(km1))=1+floor( (maxobj(km1) - z.l(km1)) / step(km1) )
        ; // posg(km1)=0
282   jump(km1)$(%max%=dir(km1))=1+floor( (z.l(km1) - minobj(km1)) / step(km1) )
        ;
```

118

```
283   );
284
285   loop(km1$(posg(km1)=maxg(km1) and sum(kmm1$(numk(kmm1) NE numk(km1)), posg
        (kmm1))=0),
286   z.l(k) = payoff(km1,k);
287   payoffSol=1;
288   iter=iter+1;
289   put iter:5:0;
290   loop(k, put z.l(k):12:2);
291   put /;
292   jump(km1)$(%min%=dir(km1))=1+floor( (minobj(km1) - z.l(km1)) / step(km1) )
        ; // posg(km1)=maxg(km1)
293   jump(km1)$(%max%=dir(km1))=1+floor( (z.l(km1) - maxobj(km1)) / step(km1) )
        ;
294   jump(kmm1)$(%min%=dir(kmm1) and (numk(kmm1) NE numk(km1)))=1+floor( (
        maxobj(kmm1) - z.l(kmm1)) / step(kmm1) ); // posg(kmm1)=0
295   jump(kmm1)$(%max%=dir(kmm1) and (numk(kmm1) NE numk(km1)))=1+floor( (z.l(
        kmm1) - minobj(kmm1)) / step(kmm1) );
296   );
297
298   if(payoffSol=1,
299   Nc = prod(km1, jump(km1));
300   for( comb = 0 to Nc-1 by 1, // find the positions of the points to be
        skipped
301   combb = comb ;
302   loop(km1, deltav(km1) = mod(combb,jump(km1));
303   combb = floor(combb/jump(km1));
304   posg_v(km1) = posg(km1) + deltav(km1);
305   );
306   numord = sum(km1$(numk(km1)>1), posg_v(km1)* prod(kmm1$(numk(kmm1) LE numk
        (km1)-1), maxg(kmm1)+1 ))
307   + sum(km1$(numk(km1)=1), posg_v(km1)) + 1;
308   v(n)$(numn(n)=numord) = 0 ;
309   );
310   else
311   rhs(km1) = sum(grid(km1,g)$(numg(g)=posg(km1)), gridrhs(km1,g));
312   solve mod_epsmethod maximizing a_objval using mip;
313   if (mod_epsmethod.modelstat<>%ModelStat.Optimal% and
314   mod_epsmethod.modelstat<>%ModelStat.Integer Solution%,
315   lastZero = 0; loop(km1$(posg(km1)>0 and lastZero=0), lastZero=numk(km1));
316   numordPre = sum(km1$(numk(km1)>1), posg(km1)* prod(kmm1$(numk(kmm1) LE
        numk(km1)-1), maxg(kmm1)+1 ))
317   + sum(km1$(numk(km1)=1), posg(km1)) + 1;
318   posg(km1)$(numk(km1)<=lastZero) = maxg(km1); // skip all solves for more
        demanding values of rhs(km1)
319   numordPost = sum(km1$(numk(km1)>1), posg(km1)* prod(kmm1$(numk(kmm1) LE
        numk(km1)-1), maxg(kmm1)+1 ))
320   + sum(km1$(numk(km1)=1), posg(km1)) + 1;
321   loop(km1$((numordPre<numordp(km1))and (numordPost>=numordp(km1))), //
        include points of the payofftable even if the counter would go beyond
322   z.l(k) = payoff(km1,k);
323   payoffSol=1;
324   iter=iter+1;
325   put iter:5:0 ,';';
326   loop(k, put z.l(k):18:5 ,';');
327   put /;
```

```
328    jump(km1)$(%min%=dir(km1))=1+floor( (minobj(km1) - z.l(km1)) / step(km1) )
          ; // posg(km1)=maxg(km1)
329    jump(km1)$(%max%=dir(km1))=1+floor( (z.l(km1) - maxobj(km1)) / step(km1) )
          ;
330    jump(kmm1)$(%min%=dir(kmm1) and (numk(kmm1) NE numk(km1)))=1+floor( (
          maxobj(kmm1) - z.l(kmm1)) / step(kmm1) ); // posg(kmm1)=0
331    jump(kmm1)$(%max%=dir(kmm1) and (numk(kmm1) NE numk(km1)))=1+floor( (z.l(
          kmm1) - minobj(kmm1)) / step(kmm1) );
332    );
333    if(payoffSol=1,
334    Nc = prod(km1, jump(km1)); display jump, Nc;
335    for( comb = 0 to Nc-1 by 1, // find the positions of the points to be
          skipped
336    combb = comb ;
337    loop(km1, deltav(km1) = mod(combb,jump(km1)));
338    combb = floor(combb/jump(km1));
339    posg_v(km1) = posg(km1) + deltav(km1);
340    );
341    numord = sum(km1$(numk(km1)>1), posg_v(km1)* prod(kmm1$(numk(kmm1) LE numk
          (km1)-1), maxg(kmm1)+1 ))
342    + sum(km1$(numk(km1)=1), posg_v(km1)) + 1;
343    v(n)$(numn(n)=numord) = 0 ;
344    );
345    );
346    else
347    iter=iter+1;
348    put iter:5:0;
349    loop(k, put z.l(k):12:2);
350    put /;
351    jump(km1)=1+floor(s.L(km1)/step(km1));
352    Nc = prod(km1, jump(km1));
353    for ( comb = 0 to Nc-1 by 1, // find the positions of the points to be
          skipped
354    combb = comb ;
355    loop(km1, deltav(km1) = mod(combb,jump(km1)));
356    combb = floor(combb/jump(km1));
357    posg_v(km1) = posg(km1) + deltav(km1);
358    );
359    numord = sum(km1$(numk(km1)>1), posg_v(km1)* prod(kmm1$(numk(kmm1) LE numk
          (km1)-1), maxg(kmm1)+1 ))
360    + sum(km1$(numk(km1)=1), posg_v(km1)) + 1;
361    v(n)$(numn(n)=numord) = 0 ;
362    );
363    );  // end of if on modelstat
364
365    ); // end of if on payoffSol
366
367    );  // end of if on v(n)
368
369
370    * Proceed forward in the grid
371    firstOffMax = 0;
372    loop(km1$(posg(km1)<maxg(km1) and firstOffMax=0),
373    posg(km1)=posg(km1)+1; firstOffMax=numk(km1));
374    posg(km1)$(numk(km1)<firstOffMax) = 0;
375    until sum(km1$(posg(km1)=maxg(km1)),1)= card(km1) and firstOffMax=0;
376
```

```
377
378    finish=jnow; elapsed_time=(finish-start)*60*60*24;
379
380    put /;
381    put 'Elapsed time: ',elapsed_time:10:2, ' seconds' / ;
382
```

Appendix E

Electrification planning through shadow cost analysis

E.1 Selecting the electrification strategy

Among the technologies adopted for rural electrification [126], stand-alone home-based systems, usually in the form of a diesel generator or a Solar Home System (SHS), are widely adopted, particularly in contexts with low population density and low expected electricity demand, as these two factors do not justify the expense for a more complex off-grid system, such as a microgrid, or the extension of the national grid [15]. The SHS technology consists of a PV panel, usually well below 1kW of power, and an associated battery, to allow energy shifting and use of electricity during the evening hours. However, those systems present several limits, and in particular they have a minimal capability of guaranteeing development possibilities to the beneficiaries, since the technology is usually sufficient to power very small appliances such as lightbulbs and phone chargers for a single household, completely leaving out the possibility for more complex appliances or productive uses of electricity, fundamental for unleashing development in rural areas [65].

When regional electrification planning tools are adopted to define which communities of the analysed area to be connected to the national grid and which to be powered with off-grid systems, the ideal mix of technologies for granting access to energy services is provided [13, 14, 23]. However, given the different opportunities for development provided by the technologies, the comparison is not always straightforward. Some works do not consider SHS systems in the optimization, defining a priori some outlier points, too sparse to be electrified with the national grid and hence suitable to be provided with home-based technologies [14, 121, 127], others tend to have solutions biased towards SHS, given their much lower cost when compared to grid extension and microgrids [12].

A novel method to account for the different development opportunities provided by the different electrification strategies is here proposed. This approach aims at overcoming, within a techno-economic model, the vision of access to energy as a binary variable, as if any availability of electricity was equivalent. As discussed in Section 1.3, access levels are defined by a wide variety of attributes and a mere traditional cost minimization is not able

to capture such characteristics. According to this rationale, the approach makes the grid connection and off-grid technologies comparable in a least-cost framework by associating a penalty to the installation of standalone systems, aimed at taking into account the different opportunities of socio-economic growth provided by the national grid, considered as potential supplier of infinite power, and SHS, suitable for covering only basic household needs and limiting the development of productive activities. Such penalty, in order to be translated into economic form, is designed as a shadow cost based on two parameters: the amount of electricity demand unmet by the standalone system and the different lifetime of the two technologies, that entails more frequent replacements of the SHS with respect to the grid infrastructure.

E.2 Methodology

The method aims at providing decision makers with a fair electrification strategy, ensuring equitable energy access to all households involved. The procedure is composed by the following steps:

(i) Formulating long-term demand curves using RAMP [122], a stochastic bottom-up open-source tool.

(ii) Sizing a "grid equivalent" standalone system, i.e. an SHS able to completely satisfy the demand of the user over the project lifetime. The size of the PV and storage components is designed in MicroGridsPy [37,128], an open-source linear programming tool for microgrid sizing.

(iii) Computing the shadow cost C_{SC} associated to standalone systems. This cost is related to two phenomena, firstly the unmet load which the actual SHS cannot satisfy, secondly the limited lifetime of such device with respect to the grid connection. It is computed as the difference between the cost of the "grid-equivalent" SHS C_{geSHS} (accounting for actualized replacement costs) and the cost of SHS C_{SHS}. The number of replacements n corresponds to the number of times the user is supposed to substitute the SHS in order to make up for a time equivalent to the grid lifetime.

$$C_{SC} = \left(C_{geSHS} + \sum_{rep=1}^{n} \frac{C_{geSHS}}{(1+i)^{rep \cdot lifetime_{SHS}}} \right) - C_{SHS} \qquad \text{(E.1a)}$$

$$n = \left[ceiling \left(\frac{lifetime_{grid}}{lifetime_{SHS}} \right) \right] - 1 \qquad \text{(E.1b)}$$

(iv) Identifying the optimal electrification strategy by including the shadow costs in the economic objective function, i.e., updating the cost of the standalone system with the cost of the "grid-equivalent" SHS, so as to account the poorer performances of the SHS in terms of availability and durability of the service in comparison to the national grid. A MILP algorithm selects which grid connection to keep and which to drop in favour of standalone systems, in compliance with power balances and technical constraints.

The output of the procedure is a detailed plan to provide fair and equitable energy access to the area under study, with georeferenced information on the grid infrastructure to be extended and on the households to be powered by standalone systems.

E.3 Case study

The method was tested on the case study of the municipality of Omereque, Bolivia, distributed over an area of 800 km^2, consisting of 11 scattered communities without access to electricity, 137 households in total. The area is crossed by a MV transmission line (see Figure E.1).
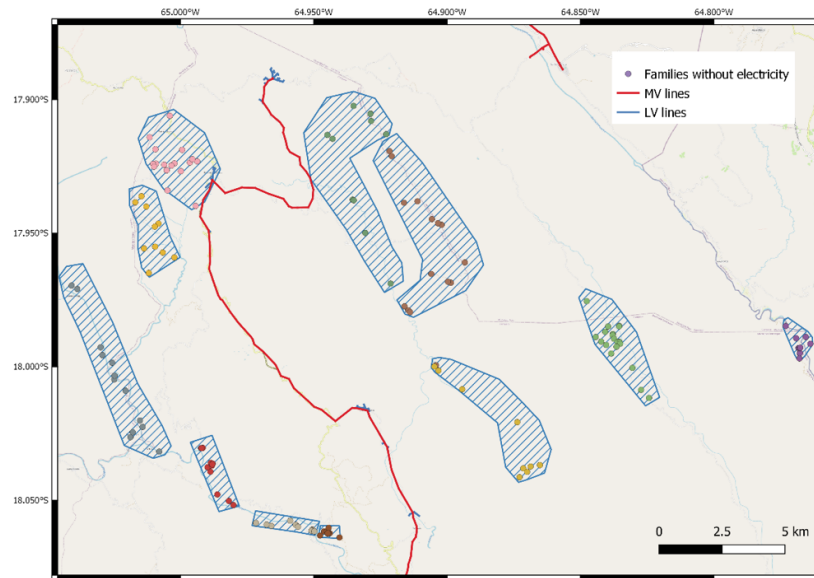

Figure E.1: Municipality of Omereque.

The SHS considered for the analysis is composed by a standalone PV (50 W) and Li-Ion Battery (10 A, 12 V) resulting into a 50W-120Wh system, produced by local providers. Cost and lifetime parameters are resumed in Table E.1.

Table E.1: Costs and lifetimes of components.

Component	Cost	Lifetime
MV feeder	10 k$/km	30 y
LV feeder	6 k$/km	30 y
MV/LV transformer	3500 $	30 y
SHS	500 ÷ 800 $	10 y

125

E.4   Results and discussion

Following the novel modelling approach, the optimization has been run minimizing the total investment cost, with the cost of the SHS increased by the defined penalty. The benchmark to assess the impact of shadow costs accounting is a mere techno-economic optimization. As the two electrification options are not economically comparable, a traditional cost evaluation would lead to a full electrification of the area by means of standalone systems. Hence, this approach, well-established among practitioners, requires either a priori evaluations, or the use of more complex tools, i.e., multi-objective optimization, or preliminary knowledge, hardly available, to establish a minimum grid connection rate or maximum budget.

Figure E.2 shows the resulting grid extensions and the households powered by standalone devices. The inclusion of the shadow cost makes the different technologies comparable within a simple least-cost framework and guides the solution towards a higher grid connection rate, ranging from 13% (see Figure E.2a) up to 37% (see Figure E.2b), according to the SHS cost range declared in Table E.1. These results suggest how the inclusion of the development constraints in the process influences the optimal strategy selection towards different shares of technologies.

Having the same budget resources at disposal, traditional methods would lead to much higher connection rates, at the price of an uneven distribution of development opportunities, which may bring about inequalities and conflicts. Hence, given a predefined budget, two alternatives are available to the decision maker. In the case of traditional optimization using actual components costs, a larger amount of population can get access to the grid with the development opportunities thereby associated, at the price of leaving the remaining population with limited chances to improve their living conditions. In case a penalty is applied to standalone systems, indeed, a smaller portion of the population is granted the connection to the grid, but the total shadow cost accounting for all the connections by SHS can be devoted to a variety of possible complementary activities aimed at improving community conditions, by either providing the off-grid users with standalone systems that can cover the full forecasted load, or considering interventions like cooperatives for food processing, community solar kiosks with refrigerators, solar pumps for agriculture, leading to a more equitable solution for all.

The key takeaway to practitioners is that the standard least-cost approach based on technology costs may suggest electrification strategies that provide inhabitants of the same area with very different means. The evaluation of the shadow cost allows identifying the budget portion to be invested in actions aimed at empowering the beneficiaries with equal development opportunities.

Therefore, the proposed approach can be used by decision makers to evaluate a fair and thorough electrification strategy. Such results should be a flag for stakeholders involved in the process of electrification strategy development, on the relevance that should be given to the needs of the population, over the technical aspect alone, and how this leads to different outputs in the optimization phase.

Moreover, this novel approach allows, through the evaluation of shadow costs, to make the two electrification strategies economically comparable by means of a general procedure which may be applied to any other technological option. Hence, the proposed methodology broadens the use of powerful and straightforward cost-minimization tools to applications

evaluating any set of electrification alternatives and where no preliminary information is available.
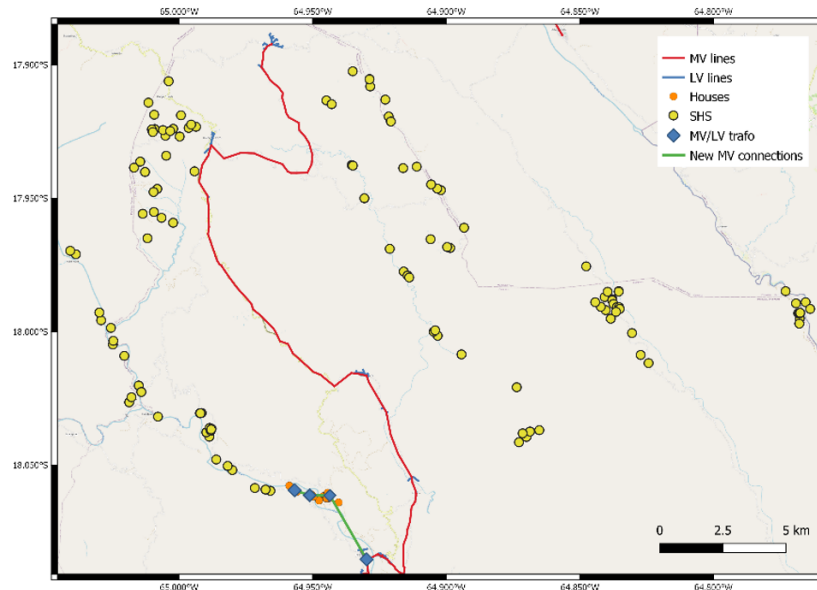
(a) C$_{\text{SHS}}$=500$
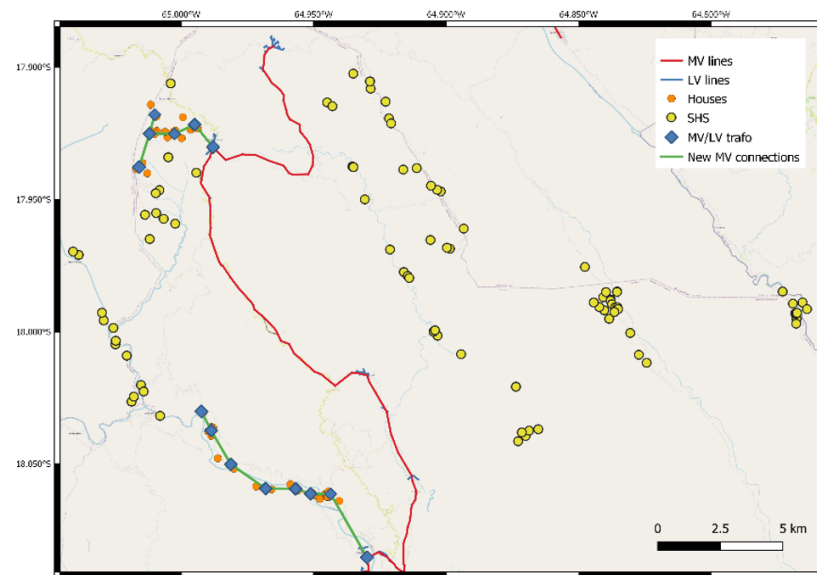
(b) C$_{\text{SHS}}$=800$

Figure E.2: Optimal electrification strategy with shadow costs accounting.

127

Bibliography

[1] United Nations, "Sustainable Development Goals." [Online]. Available: https://sdgs.un.org/goals

[2] IEA, "World Energy Outlook 2020," Tech. Rep., 2020. [Online]. Available: https://www.iea.org/reports/world-energy-outlook-2020

[3] United Nations, "The Sustainable Development Goals Report," 2020. [Online]. Available: https://unstats.un.org/sdgs/report/2020/

[4] ESMAP, "Tracking SDG7: The Energy Progress Report," 2020. [Online]. Available: https://openknowledge.worldbank.org/handle/10986/33822

[5] R. Jiménez, "Development Effects of Rural Electrification," *IDB Policy Brief*, no. January, 2017.

[6] Y. Malakar, "Evaluating the role of rural electrification in expanding people's capabilities in India," *Energy Policy*, vol. 114, no. January 2018, pp. 492–498, 2018.

[7] "Human Development Data Center." [Online]. Available: http://hdr.undp.org/en/data

[8] World Resources Institute, "Strategies for expanding universal access to electricity services for development," 2017. [Online]. Available: https://files.wri.org/d8/s3fs-public/Strategies_for_Expanding_Universal_Access_to_Electricity_Services_for_Development.pdf

[9] IRENA, "Off-grid renewable energy solutions to expand electricity access : An opportunity not to be missed," *International Renewable Energy Agency, Abu Dhabi*, p. 144, 2019.

[10] S. S. Rathi and C. Vermaak, "Rural electrification, gender and the labor market: A cross-country study of India and South Africa," *World Development*, vol. 109, pp. 346–359, 2018.

[11] ESMAP, "Beyond Connections Energy Access Redefined," 2015. [Online]. Available: https://openknowledge.worldbank.org/handle/10986/24368

[12] D. Mentis, M. Howells, H. Rogner, A. Korkovelos, C. Arderne, E. Zepeda, S. Siyal, C. Taliotis, M. Bazilian, A. De Roo, Y. Tanvez, A. Oudalov, and E. Scholtz, "Lighting the World: the first application of an open source, spatial electrification tool (OnSSET) on Sub-Saharan Africa," *Environmental Research Letters*, vol. 12, no. 8, 2017.

[13] P. Ciller, D. Ellman, C. Vergara, A. Gonzalez-Garcia, S. J. Lee, C. Drouin, M. Brusnahan, Y. Borofsky, C. Mateo, R. Amatya, R. Palacios, R. Stoner, F. De Cuadra, and I. Perez-Arriaga, "Optimal Electrification Planning Incorporating On- And Off-Grid Technologies- And Reference Electrification Model (REM)," *Proceedings of the IEEE*, vol. 107, no. 9, pp. 1872–1905, 2019.

[14] P. Blechinger, C. Cader, and P. Bertheau, "Least-Cost Electrification Modeling and Planning - A Case Study for Five Nigerian Federal States," *Proceedings of the IEEE*, vol. 107, no. 9, pp. 1923–1940, 2019.

[15] F. F. Nerini, O. Broad, D. Mentis, M. Welsch, M. Bazilian, and M. Howells, "A cost comparison of technology approaches for improving access to electricity services," *Energy*, vol. 95, pp. 255–265, 2016.

[16] Mini-Grids Partnership, "State of the Global Mini-grids Market," 2020. [Online]. Available: https://www.seforall.org/system/files/2020-06/MGP-2020-SEforALL.pdf

[17] ESMAP, "Mini Grids for Half a Billion People: Market Outlook and Handbook for Decision Makers," 2019. [Online]. Available: https://openknowledge.worldbank.org/handle/10986/31926

[18] M. P. Blimpo and M. Cosgrove-Davies, *Electricity Access in Sub-Saharan Africa: Uptake, Reliability, and Complementary Factors for Economic Impact*, 2019.

[19] IEA, "Africa energy outlook 2019," 2019. [Online]. Available: https://www.iea.org/reports/africa-energy-outlook-2019

[20] E. Colombo, S. Bologna, and D. Masera, *Renewable Energy for Unleashing Sustainable Development*, 2013.

[21] A. Eales, S. Strachan, D. Frame, and S. Galloway, "Assessing the Feasibility of Solar Microgrid Social Enterprises as an Appropriate Delivery Model for Achieving SDG7," *Proceedings of the International Conference on Energising the SDGs through Appropriate Technology and Governance*, 2019.

[22] A. Chaurey and T. C. Kandpal, "A techno-economic comparison of rural electrification based on solar home systems and PV microgrids," *Energy Policy*, vol. 38, no. 6, pp. 3118–3129, 2010.

[23] P. Ciller and S. Lumbreras, "Electricity for all: The contribution of large-scale planning tools to the energy-access problem," *Renewable and Sustainable Energy Reviews*, vol. 120, no. November 2019, p. 109624, 2020.

[24] B. Zhao, X. Zhang, P. Li, K. Wang, M. Xue, and C. Wang, "Optimal sizing, operating strategy and operational experience of a stand-alone microgrid on Dongfushan Island," *Applied Energy*, vol. 113, pp. 1656–1666, 2014.

[25] C. Brivio, M. Moncecchi, S. Mandelli, and M. Merlo, "A novel software package for the robust design of off-grid power systems," *Journal of Cleaner Production*, vol. 166, pp. 668–679, 2017.

[26] L. Moretti, M. Astolfi, C. Vergara, E. Macchi, J. I. Pérez-Arriaga, and G. Manzolini, "A design and dispatch optimization algorithm based on mixed integer linear programming for rural electrification," *Applied Energy*, vol. 233-234, pp. 1104–1121, 2019.

[27] W. Cai, X. Li, A. Maleki, F. Pourfayaz, M. A. Rosen, M. Alhuyi Nazari, and D. T. Bui, "Optimal sizing and location based on economic parameters for an off-grid application of a hybrid system with photovoltaic, battery and diesel technology," *Energy*, vol. 201, p. 117480, 2020.

[28] A. Kamjoo, A. Maheri, A. M. Dizqah, and G. A. Putrus, "Multi-objective design under uncertainties of hybrid renewable energy system using NSGA-II and chance constrained programming," *International Journal of Electrical Power and Energy Systems*, vol. 74, pp. 187–194, 2016.

[29] L. Guo, W. Liu, J. Cai, B. Hong, and C. Wang, "A two-stage optimal planning and design method for combined cooling, heat and power microgrid system," *Energy Conversion and Management*, vol. 74, pp. 433–445, 2013.

[30] J. Zhang, K. J. Li, M. Wang, W. J. Lee, and H. Gao, "A bi-level program for the planning of an islanded microgrid including CAES," *IEEE Industry Application Society - 51st Annual Meeting, IAS 2015, Conference Record*, pp. 1–8, 2015.

[31] D. R. Prathapaneni and K. P. Detroja, "An integrated framework for optimal planning and operation schedule of microgrid under uncertainty," *Sustainable Energy, Grids and Networks*, vol. 19, p. 100232, 2019.

[32] D. Fioriti, R. Giglioli, D. Poli, G. Lutzemberger, A. Micangeli, R. Del Citto, I. Perez-Arriaga, and P. Duenas-Martinez, "Stochastic sizing of isolated rural mini-grids, including effects of fuel procurement and operational strategies," *Electric Power Systems Research*, vol. 160, pp. 419–428, 2018.

[33] B. Li, R. Roche, and A. Miraoui, "Microgrid sizing with combined evolutionary algorithm and MILP unit commitment," *Applied Energy*, vol. 188, pp. 547–562, 2017.

[34] N. E. Koltsaklis, M. Giannakakis, and M. C. Georgiadis, "Optimal energy planning and scheduling of microgrids," *Chemical Engineering Research and Design*, vol. 131, pp. 318–332, 2018.

[35] S. Mashayekh, M. Stadler, G. Cardoso, M. Heleno, S. C. Madathil, H. Nagarajan, R. Bent, M. Mueller-Stoffels, X. Lu, and J. Wang, "Security-Constrained Design of Isolated Multi-Energy Microgrids," *IEEE Transactions on Power Systems*, vol. 33, no. 3, pp. 2452–2462, 2018.

[36] Z. K. Pecenak, M. Stadler, and K. Fahy, "Efficient multi-year economic energy planning in microgrids," *Applied Energy*, vol. 255, no. April 2019, p. 113771, 2019.

[37] S. Balderrama, F. Lombardi, F. Riva, W. Canedo, E. Colombo, and S. Quoilin, "A two-stage linear programming optimization framework for isolated hybrid microgrids in a rural context: The case study of the "El Espino" community," *Energy*, vol. 188, p. 116073, 2019.

[38] "HOMER Pro 3.14," 2021. [Online]. Available: https://www.homerenergy.com/products/pro/docs/latest/index.html

[39] R. Dufo-López, "iHOGA 3.0 User's Manual," 2021.

[40] F. Riva, F. Gardumi, A. Tognollo, and E. Colombo, "Soft-linking energy demand and optimisation models for local long-term electricity planning: An application to rural India," *Energy*, vol. 166, pp. 32–46, 2019.

[41] N. Nguyen-Hong, H. Nguyen-Duc, and Y. Nakanishi, "Optimal Sizing of Energy Storage Devices in Isolated Wind-Diesel Systems Considering Load Growth Uncertainty," *IEEE Transactions on Industry Applications*, vol. 54, no. 3, pp. 1983–1991, 2018.

[42] Y. Zhang, J. Wang, A. Berizzi, and X. Cao, "Life cycle planning of battery energy storage system in off-grid wind-solar-diesel microgrid," *IET Generation, Transmission and Distribution*, vol. 12, no. 20, pp. 4451–4461, 2018.

[43] A. S. Aziz, M. F. N. Tajuddin, M. R. Adzman, A. Azmi, and M. A. Ramli, "Optimization and sensitivity analysis of standalone hybrid energy systems for rural electrification: A case study of Iraq," *Renewable Energy*, vol. 138, pp. 775–792, 2019.

[44] A. Azizi, P. O. Logerais, A. Omeiri, A. Amiar, A. Charki, O. Riou, F. Delaleux, and J. F. Durastanti, "Impact of the aging of a photovoltaic module on the performance of a grid-connected system," *Solar Energy*, vol. 174, no. August, pp. 445–454, 2018.

[45] S. D. Hamilton, D. Millstein, M. Bolinger, R. Wiser, and S. Jeong, "How Does Wind Project Performance Change with Age in the United States?" *Joule*, vol. 4, no. 5, pp. 1004–1020, 2020.

[46] R. Guerrero and M. A. Pedrasa, "Component degradation and battery replacement in energy resource sizing for autonomous systems," *2018 IEEE Asia-Pacific Power and Energy Engineering Conference, APPEEC*, pp. 106–111, 2018.

[47] D. Fioriti, D. Poli, P. Duenas-Martinez, and I. Perez-Arriaga, "Multi-year stochastic planning of off-grid microgrids subject to significant load growth uncertainty: overcoming single-year methodologies," *Electric Power Systems Research*, vol. 194, no. February, p. 107053, 2021.

[48] H. Bindner, T. Cronin, P. Lundsager, J. F. Manwell, U. Abdulwahid, and I. Baring-gould, *Lifetime Modelling of Lead Acid Batteries*, 2005, vol. 1515, no. April. [Online]. Available: https://www.researchgate.net/publication/246687286_Lifetime_Modelling_of_Lead_Acid_Batteries

[49] N. Diorio, A. Dobos, S. Janzou, A. Nelson, and B. Lundstrom, "Technoeconomic Modeling of Battery Energy Storage in SAM," *NREL Technical Report NREL/TP-6A20-64641*, no. September, 2015.

[50] A. Perez, R. Moreno, R. Moreira, M. Orchard, and G. Strbac, "Effect of Battery Degradation on Multi-Service Portfolios of Energy Storage," *IEEE Transactions on Sustainable Energy*, vol. 7, no. 4, pp. 1718–1729, 2016.

[51] D. Jimenez, D. Ortiz-Villalba, A. Perez, and M. E. Orchard, "Lithium-ion battery degradation assessment in microgrids," *2018 IEEE International Autumn Meeting on Power, Electronics and Computing, ROPEC 2018*, 2019.

[52] A. Pérez, V. Quintero, H. Rozas, F. Jaramillo, R. Moreno, and M. Orchard, "Modelling the degradation process of lithium-ion batteries when operating at erratic state-of-charge swing ranges," *2017 4th International Conference on Control, Decision and Information Technologies, CoDIT 2017*, pp. 860–865, 2017.

[53] Y. Cheng and Y. Tai, "A MILP Model for Optimizing Distributed Resource System with Energy Storage and PV Considering Energy Storage Life Loss," *2nd IEEE Conference on Energy Internet and Energy System Integration, EI2 2018 - Proceedings*, pp. 1–6, 2018.

[54] G. Cardoso, T. Brouhard, N. DeForest, D. Wang, M. Heleno, and L. Kotzur, "Battery aging in multi-energy microgrid design using mixed integer linear programming," *Applied Energy*, vol. 231, no. May, pp. 1059–1069, 2018.

[55] L. H. Macedo, J. F. Franco, R. Romero, and M. J. Rider, "An MILP model for the analysis of operation of energy storage devices in distribution systems," *2016 IEEE PES Transmission and Distribution Conference and Exposition-Latin America, PES T and D-LA 2016*, pp. 1–6, 2017.

[56] F. K. Abo-Elyousr and A. Elnozahy, "Bi-objective economic feasibility of hybrid micro-grid systems with multiple fuel options for islanded areas in Egypt," *Renewable Energy*, vol. 128, pp. 37–56, 2018.

[57] M. Kharrich, O. H. Mohammed, N. Alshammari, and M. Akherraz, "Multi-objective optimization and the effect of the economic factors on the design of the microgrid hybrid system," *Sustainable Cities and Society*, vol. 65, no. October 2020, p. 102646, 2021.

[58] D. Silva and T. Nakata, "Multi-objective assessment of rural electrification in remote areas with poverty considerations," *Energy Policy*, vol. 37, no. 8, pp. 3096–3108, 2009.

[59] R. B. Hiremath, B. Kumar, P. Balachandra, and N. H. Ravindranath, "Bottom-up approach for decentralised energy planning: Case study of Tumkur district in India," *Energy Policy*, vol. 38, no. 2, pp. 862–874, 2010.

[60] M. A. Cuesta, T. Castillo-Calzadilla, and C. E. Borges, "A critical analysis on hybrid renewable energy modeling tools: An emerging opportunity to include social indicators to optimise systems in small communities," 2020.

[61] F. Fuso Nerini, M. Howells, M. Bazilian, and M. F. Gomez, "Rural electrification options in the Brazilian Amazon. A multi-criteria analysis," *Energy for Sustainable Development*, vol. 20, no. 1, pp. 36–48, 2014.

[62] B. Mainali and S. Silveira, "Using a sustainability index to assess energy technologies for rural electrification," *Renewable and Sustainable Energy Reviews*, vol. 41, pp. 1351–1365, 2015.

[63] A. Kumar, A. R. Singh, Y. Deng, X. He, P. Kumar, and R. C. Bansal, "Integrated assessment of a sustainable microgrid for a remote village in hilly region," *Energy Conversion and Management*, vol. 180, pp. 442–472, 2019.

[64] M. Juanpera, P. Blechinger, L. Ferrer-Martí, M. M. Hoffmann, and R. Pastor, "Multicriteria-based methodology for the design of rural electrification systems. A case study in Nigeria," *Renewable and Sustainable Energy Reviews*, vol. 133, p. 110243, 2020.

[65] F. Riva, H. Ahlborg, E. Hartvigsson, S. Pachauri, and E. Colombo, "Electricity access and rural development: Review of complex socio-economic dynamics and causal diagrams for more appropriate energy modelling," *Energy for Sustainable Development*, vol. 43, pp. 203–223, 2018.

[66] F. Riva, A. Tognollo, F. Gardumi, and E. Colombo, "Long-term energy planning and demand forecast in remote areas of developing countries: Classification of case studies and insights from a modelling perspective," *Energy Strategy Reviews*, vol. 20, pp. 71–89, 2018.

[67] L. Lorenzoni, P. Cherubini, D. Fioriti, D. Poli, A. Micangeli, and R. Giglioli, "Classification and modeling of load profiles of isolated mini-grids in developing countries: A data-driven approach," *Energy for Sustainable Development*, vol. 59, pp. 208–225, 2020.

[68] S. M. Mustonen, "Rural energy survey and scenario analysis of village energy consumption: A case study in Lao People's Democratic Republic," *Energy Policy*, vol. 38, no. 2, pp. 1040–1048, 2010.

[69] N. Stevanato, F. Lombardi, G. Guidicini, L. Rinaldi, S. L. Balderrama, M. Pavičević, S. Quoilin, and E. Colombo, "Long-term sizing of rural microgrids: Accounting for load evolution through multi-step investment plan and stochastic optimization," *Energy for Sustainable Development*, vol. 58, pp. 16–29, 2020.

[70] K. B. Debnath, M. Mourshed, and S. P. K. Chew, "Modelling and Forecasting Energy Demand in Rural Households of Bangladesh," *Energy Procedia*, vol. 75, pp. 2731–2737, 2015.

[71] E. Hajipour, M. Bozorg, and M. Fotuhi-Firuzabad, "Stochastic Capacity Expansion Planning of Remote Microgrids with Wind Farms and Energy Storage," *IEEE Transactions on Sustainable Energy*, vol. 6, no. 2, pp. 491–498, 2015.

[72] E. Hartvigsson, M. Stadler, and G. Cardoso, "Rural electrification and capacity expansion with an integrated modeling approach," *Renewable Energy*, vol. 115, no. 2018, pp. 509–520, 2018.

[73] D. Fioriti, D. Poli, P. Cherubini, G. Lutzemberger, A. Micangeli, and P. Duenas-Martinez, "Comparison among deterministic methods to design rural mini-grids: Effect of operating strategies," *2019 IEEE Milan PowerTech, PowerTech 2019*, 2019.

[74] W. X. Shen, "Optimally sizing of solar array and battery in a standalone photovoltaic system in Malaysia," *Renewable Energy*, vol. 34, no. 1, pp. 348–352, 2009.

[75] C. Zhang, Y. Xu, and Z. Y. Dong, "Probability-weighted robust optimization for distributed generation planning in microgrids," *IEEE Transactions on Power Systems*, vol. 33, no. 6, pp. 7042–7051, 2018.

[76] G. G. Moshi, C. Bovo, A. Berizzi, and L. Taccari, "Optimization of integrated design and operation of microgrids under uncertainty," *19th Power Systems Computation Conference, PSCC 2016*, 2016.

[77] A. Vaccaro, M. Petrelli, and A. Berizzi, "Robust Optimization and Affine Arithmetic for Microgrid Scheduling under Uncertainty," *Proceedings - 2019 IEEE International Conference on Environment and Electrical Engineering and 2019 IEEE Industrial and Commercial Power Systems Europe, EEEIC/I and CPS Europe 2019*, pp. 1–6, 2019.

[78] IBM, "CPLEX User Manual," pp. 227–228, 2016.

[79] S. Mandelli, C. Brivio, E. Colombo, and M. Merlo, "A sizing methodology based on Levelized Cost of Supplied and Lost Energy for off-grid rural electrification systems," *Renewable Energy*, vol. 89, pp. 475–488, 2016.

[80] S. Pfenninger and I. Staffell, "Long-term patterns of European PV output using 30 years of validated hourly reanalysis and satellite data," *Energy*, vol. 114, pp. 1251–1265, 2016.

[81] I. Staffell and S. Pfenninger, "Using bias-corrected reanalysis to simulate current and future wind power output," *Energy*, vol. 114, pp. 1224–1239, 2016.

[82] S. Mandelli, M. Merlo, and E. Colombo, "Novel procedure to formulate load profiles for off-grid rural areas," *Energy for Sustainable Development*, vol. 31, pp. 130–142, 2016.

[83] S. Ssewanyana and I. Kasirye, "Poverty and inequality dynamics in Uganda: Insights from the Uganda national Panel Surveys 2005/6 and 2009/10," *Research Series*, no. 94, 2012.

[84] X. Luo, J. Wang, M. Dooner, and J. Clarke, "Overview of current development in electrical energy storage technologies and the application potential in power system operation," *Applied Energy*, vol. 137, pp. 511–536, 2015.

[85] P. Haidl, A. Buchroithner, B. Schweighofer, M. Bader, and H. Wegleiter, "Lifetime analysis of energy storage systems for sustainable transportation," *Sustainability*, vol. 11, no. 23, 2019.

[86] M. Moncecchi, C. Brivio, S. Mandelli, and M. Merlo, "Battery energy storage systems in microgrids: Modeling and design criteria," *Energies*, vol. 13, no. 8, pp. 1–18, 2020.

[87] A. Malheiro, P. M. Castro, R. M. Lima, and A. Estanqueiro, "Integrated sizing and scheduling of wind/PV/diesel/battery isolated systems," *Renewable Energy*, vol. 83, pp. 646–657, 2015.

[88] A. Berizzi, C. Bovo, M. Innorta, and P. Marannino, "Multiobjective optimization techniques applied to modern power systems," in *2001 IEEE Power Engineering Society Winter Meeting*, 2002, pp. 1503–1508.

[89] G. Chiandussi, M. Codegone, S. Ferrero, and F. E. Varesio, "Comparison of multi-objective optimization methodologies for engineering applications," *Computers and Mathematics with Applications*, vol. 63, no. 5, pp. 912–942, 2012.

[90] L. Li, H. Mu, N. Li, and M. Li, "Economic and environmental optimization for distributed energy resource systems coupled with district energy networks," *Energy*, vol. 109, pp. 947–960, 2016.

[91] J. Martínez-Gomez, J. Peña-Lamas, M. Martín, and J. M. Ponce-Ortega, "A multi-objective optimization approach for the selection of working fluids of geothermal facilities: Economic, environmental and social aspects," *Journal of Environmental Management*, vol. 203, pp. 962–972, 2017.

[92] D. Zhang, S. Evangelisti, P. Lettieri, and L. G. Papageorgiou, "Optimal design of CHP-based microgrids: Multiobjective optimisation and life cycle assessment," *Energy*, vol. 85, pp. 181–193, 2015.

[93] C. Cambero and T. Sowlati, "Incorporating social benefits in multi-objective optimization of forest-based bioenergy and biofuel supply chains," *Applied Energy*, vol. 178, pp. 721–735, 2016.

[94] J. Zhong, T. E. Yu, C. D. Clark, B. C. English, J. A. Larson, and C. L. Cheng, "Effect of land use change for bioenergy production on feedstock cost and water quality," *Applied Energy*, vol. 210, pp. 580–590, 2018.

[95] G. Mavrotas, "Effective implementation of the ϵ-constraint method in Multi-Objective Mathematical Programming problems," *Applied Mathematics and Computation*, vol. 213, no. 2, pp. 455–465, 2009.

[96] G. Mavrotas and K. Florios, "An improved version of the augmented ε-constraint method (AUGMECON2) for finding the exact pareto set in multi-objective integer programming problems," *Applied Mathematics and Computation*, vol. 219, no. 18, pp. 9652–9669, 2013.

[97] A. Jabbarzadeh, B. Fahimnia, and S. Rastegar, "Green and Resilient Design of Electricity Supply Chain Networks: A Multiobjective Robust Optimization Approach," *IEEE Transactions on Engineering Management*, vol. 66, no. 1, pp. 52–72, 2019.

[98] M. Wang, H. Yu, R. Jing, H. Liu, P. Chen, and C. Li, "Combined multi-objective optimization and robustness analysis framework for building integrated energy system under uncertainty," *Energy Conversion and Management*, vol. 208, no. February, p. 112589, 2020.

[99] S. Sudeng and N. Wattanapongsakorn, "Post Pareto-optimal pruning algorithm for multiple objective optimization using specific extended angle dominance," *Engineering Applications of Artificial Intelligence*, vol. 38, pp. 221–236, 2015.

[100] L. Yan'Gang and Q. Zheng, "A decision support system for satellite layout integrating multi-objective optimization and multi-attribute decision making," *Journal of Systems Engineering and Electronics*, vol. 30, no. 3, pp. 535–544, 2019.

[101] M. J. Brusco, "Partitioning methods for pruning the Pareto set with application to multiobjective allocation of a cross-trained workforce," *Computers and Industrial Engineering*, vol. 111, pp. 29–38, 2017.

[102] Z. Wang and G. P. Rangaiah, "Application and Analysis of Methods for Selecting an Optimal Solution from the Pareto-Optimal Front obtained by Multiobjective Optimization," *Industrial and Engineering Chemistry Research*, vol. 56, no. 2, pp. 560–574, 2017.

[103] J. M. Sanchez-Gomez, M. A. Vega-Rodríguez, and C. J. Pérez, "Comparison of automatic methods for reducing the Pareto front to a single solution applied to multi-document text summarization," *Knowledge-Based Systems*, vol. 174, pp. 123–136, 2019.

[104] Y. Z. Mehrjerdi and M. Shafiee, "A resilient and sustainable closed-loop supply chain using multiple sourcing and information sharing strategies," *Journal of Cleaner Production*, vol. 289, 2020.

[105] N. Caglayan and S. I. Satoglu, "Multi-Objective Two-Stage Stochastic Programming Model for a Proposed Casualty Transportation System in Large-Scale Disasters: A Case Study," *Mathematics*, vol. 9, no. 4, p. 316, 2021.

[106] A. Nikas, A. Fountoulakis, A. Forouli, and H. Doukas, "A robust augmented ε-constraint method (AUGMECON-R) for finding exact solutions of multi-objective linear programming problems," *Operational Research*, no. 0123456789, 2020.

[107] Y. Cui, Z. Geng, Q. Zhu, and Y. Han, "Review: Multi-objective optimization methods and application in energy saving," *Energy*, vol. 125, pp. 681–704, 2017.

[108] R. Dufo-López, I. R. Cristóbal-Monreal, and J. M. Yusta, "Optimisation of PV-wind-diesel-battery stand-alone systems to minimise cost and maximise human development index and job creation," *Renewable Energy*, vol. 94, pp. 280–293, 2016.

[109] J. C. Rojas-Zerpa and J. M. Yusta, "Application of multicriteria decision methods for electric supply planning in rural and remote areas," *Renewable and Sustainable Energy Reviews*, vol. 52, pp. 557–571, 2015.

[110] N. Martín-Chivelet, "Photovoltaic potential and land-use estimation methodology," *Energy*, vol. 94, pp. 233–242, 2016.

[111] J. J. Cartelle Barros, M. Lara Coira, M. P. de la Cruz López, and A. del Caño Gochi, "Comparative analysis of direct employment generated by renewable and non-renewable power plants," *Energy*, vol. 139, pp. 542–554, 2017.

[112] C. O. Henriques, D. H. Coelho, and N. L. Cassidy, "Employment impact assessment of renewable energy targets for electricity generation by 2020—An IO LCA approach," *Sustainable Cities and Society*, vol. 26, no. 2016, pp. 519–530, 2016.

[113] Institute for Sustainable Futures, "Calculating global energy sector jobs 2015 methodology update," pp. 1–48, 2015.

[114] A. Okunlola, O. Evbuomwan, H. Zaheer, and J. Winklmaier, "Assessment of Decentralized Hybrid Mini-grids in Sub-Saharan Africa: Market Analysis, Least-Cost Modelling, and Job Creation Analysis," in *Africa-EU Renewable Energy Research and Innovation Symposium 2018*, 2018, pp. 21–34. [Online]. Available: https://www.springer.com/gp/book/9783319934372

[115] J. Jithendranath and D. Das, "Stochastic planning of islanded microgrids with uncertain multi-energy demands and renewable generations," *IET Renewable Power Generation*, vol. 14, no. 19, pp. 4179–4192, 2020.

[116] H. Alharbi and K. Bhattacharya, "Stochastic optimal planning of battery energy storage systems for isolated microgrids," *IEEE Transactions on Sustainable Energy*, vol. 9, no. 1, pp. 211–227, 2018.

[117] R. Jabbari-Sabet, S. M. Moghaddas-Tafreshi, and S. S. Mirhoseini, "Microgrid operation and management using probabilistic reconfiguration and unit commitment," *International Journal of Electrical Power and Energy Systems*, vol. 75, pp. 328–336, 2016.

[118] N. Nikmehr, S. Najafi-Ravadanegh, and A. Khodaei, "Probabilistic optimal scheduling of networked microgrids considering time-based demand response programs under uncertainty," *Applied Energy*, vol. 198, pp. 267–279, 2017.

[119] D. Fioriti and D. Poli, "A novel stochastic method to dispatch microgrids using Monte Carlo scenarios," *Electric Power Systems Research*, vol. 175, p. 105896, 2019.

[120] CIGRE, *Active Distributed Systems and Distributed Energy Resources*, 2021, no. Technical Brochure 835.

[121] S. Corigliano, T. Carnovali, D. Edeme, and M. Merlo, "Holistic geospatial data-based procedure for electric network design and least-cost energy strategy," *Energy for Sustainable Development*, vol. 58, pp. 1–15, 2020.

[122] F. Lombardi, S. Balderrama, S. Quoilin, and E. Colombo, "Generating high-resolution multi-energy load profiles for remote areas with an open-source stochastic model," *Energy*, vol. 177, pp. 433–444, 2019.

[123] "GISEle - ENERGY4GROWING." [Online]. Available: http://www.e4g.polimi.it/ ?page_id=524

[124] S. Cavallini, R. Soldi, J. Friedl, and M. Volpe, "Using the Quadruple Helix Approach to Accelerate the Transfer of Research and Innovation Results to Regional Growth," 2016.

[125] F. Riva and E. Colombo, "System-dynamics modelling of the electricity-development nexus in rural electrification based on a Tanzanian case study," *Energy for Sustainable Development*, vol. 56, pp. 128–143, 2020.

[126] S. Mandelli, J. Barbieri, R. Mereu, and E. Colombo, "Off-grid systems for rural electrification in developing countries: Definitions, classification and a comprehensive literature review," pp. 1621–1646, 2016.

[127] C. Krüger, F. Castellani, J. Geldermann, and A. Schöbel, "Peat and pots: An application of robust multiobjective optimization to a mixing problem in agriculture," *Computers and Electronics in Agriculture*, vol. 154, no. June, pp. 265–275, 2018.

[128] N. Stevanato, F. Lombardi, E. Colombo, S. Balderrama, and S. Quoilin, "Two-stage stochastic sizing of a rural micro-grid based on stochastic load generation," *2019 IEEE Milan PowerTech, PowerTech 2019*, 2019.